FACULTY OF SCIENCE
UNIVERSITY OF COPENHAGEN

PhD thesis

Kristine Skovgaard Madsen

Recent and future climatic changes in temperature, salinity, and sea level of the North Sea and the Baltic Sea

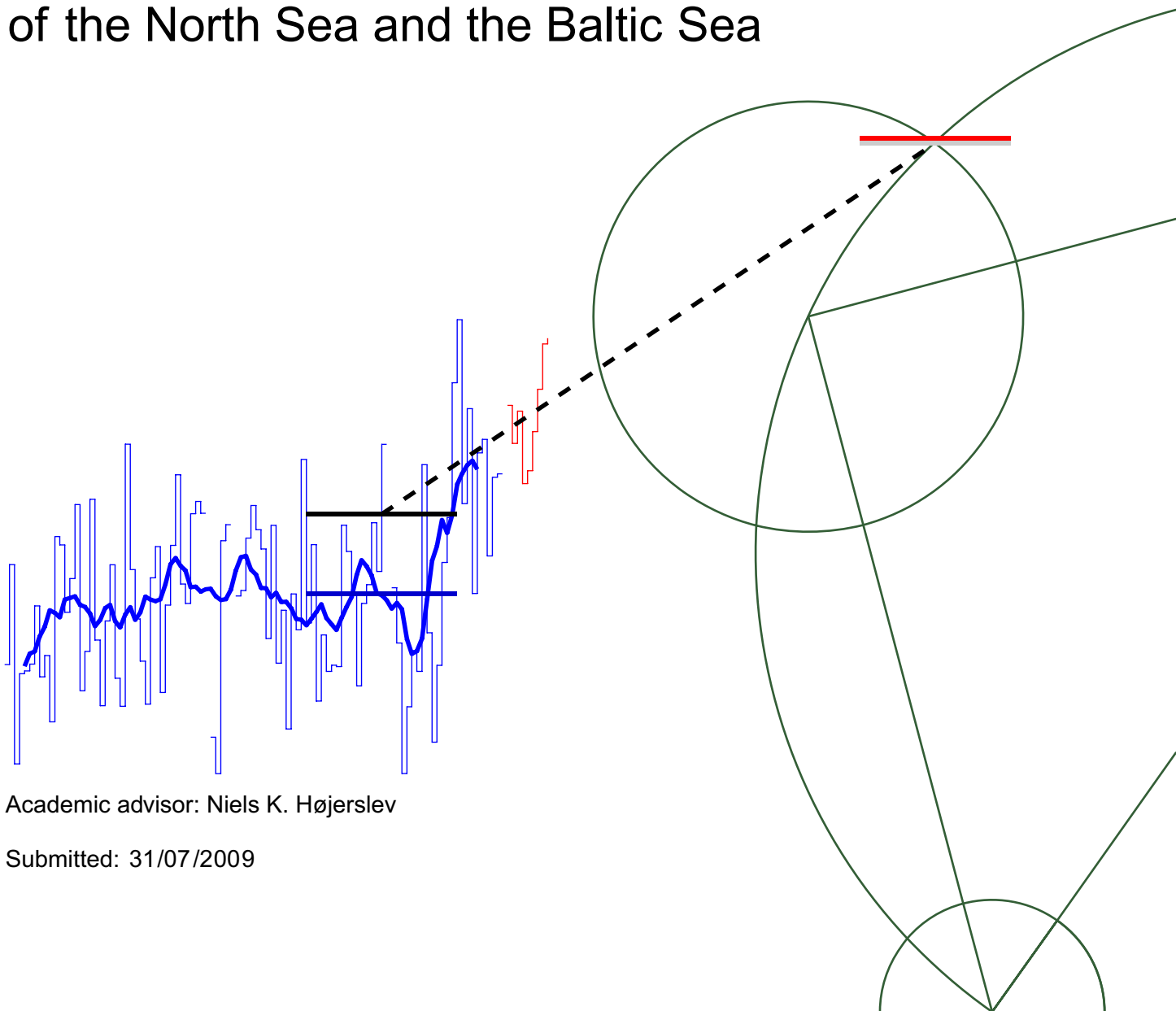

Academic advisor: Niels K. Højerslev

Submitted: 31/07/2009

Preface and acknowledgments

This thesis is submitted in partial fulfillment of the requirements for the PhD degree at the Graduate School of Science, Faculty of Science, University of Copenhagen, Denmark. The project was funded by the COGCI PhD School, University of Copenhagen, and the Danish Meteorological Institute (DMI). It was carried out at DMI and at the Niels Bohr Institute, University of Copenhagen.

The project was supervised by Associate Professor Niels Kristian Højerslev and Deputy Director and PhD, Centre for Ocean and Ice, DMI, Jun She, whose advice and friendly conversations during the project I greatly appreciate.

I would like to extend my gratitude to Abbas S. Khan, Bjørn Ådlandsvik, Corinna Schrum, Katja Woth, Lonny Hansen, Markus Meier, Ole B. Christensen, Per Knudsen, Phil Graham, Ralf Weisse, and Stephan Dick for providing me with data and kind advice. Data was also obtained from ECMWF, PSMSL, the SMHI SHARK database, ICES, CICL Research Data Archive, and CCAR (University of Colorado), but the main source has been DMI's data archive.

I would like to thank my colleagues in Centre for Ocean and Ice, DMI for help and advice, especially on the challenges of setting up the DMI-BSHcmod model for climate simulations and retrieving the observational data, and John Wilkin and the Ocean Modeling Group at Rutgers University for a memorable 5 months visit.

Last but not least, I would like to thank friends and family for continuous encouragement and support. My very special thanks go to my husband Anders Søndergaard.

The front page illustration show the observed and projected temperature development at the Drogden Station (free after Fig. 56, page 102).

Abstract

The North Sea and the Baltic Sea are undergoing climatic changes. In this thesis, long time series of direct observations from lightships and coastal stations are combined with regional ocean modeling. This contributes with new information about the changes in sea temperature, salinity, and sea level of the 20th century, and a scenario for the 21st century. Focus is on the spatial differences of climate signals, especially for the North Sea – Baltic Sea transition zone.

The observed sea surface temperature at the Drogden Station in the transition zone had 10-year running mean temperatures ranging from 8.2 to 9.1°C during 1904–1985. By 1992, it had increased to 9.8°C, and it has kept that level since. The temperature increase is statistically significant and supported by other observations in the area. The model scenario shows larger warming in the Baltic Sea than in the North Sea, and larger warming of the atmosphere than of the sea for the 21st century. The projected warming at the Drogden Station was 2.9°C from 1960–1990 to 2070–2100, based on one realization of the IPCC A2 scenario. This indicates that the rate of warming observed since the 1980s may continue.

Salinity observations from the transition zone show Baltic Sea inflow events and the vertical stratification in high detail. No significant long-term trends were detected. The combined temperature and salinity data also provide the basis for a detailed climatology for the locations of the lightships. Model results indicate that future changes in salinity in the transition zone depend on changes in the Baltic Sea salinity and the wind. These effects may counteract each other, so the sign of the salinity changes in transition zone is uncertain, but the magnitude in the presented scenarios is smaller than the natural variability.

The increase in mean sea level in the study area is mainly projected to originate from outside the North Sea – Baltic Sea area. In Denmark, the changes will be partly compensated by isostatic land uplift. The mean observed sea level rise measured by 8 Danish tide gauges between 1901 and 2000 and corrected for land uplift was 1.5 $\pm$ 0.5 mm/year (90% confidence interval) with the largest part of the uncertainty originating from a preliminary determination of the land uplift. The model scenario indicates increased westerly winds and increased storm surge heights on the German, Danish, and Norwegian North Sea coasts, as well as in the far ends of the Gulf of Finland and Bothnian Bay. The lower estimate of the increase at Esbjerg on the Danish North Sea coast for the IPCC A2 emission scenario was 19–37 cm for a 10 year event, additionally to the changes in mean sea level. No significant wind induced storm surge height increase was seen in the transition zone.

The lightship and tide gauge observations from the transition zone have proven to be of sufficient quality for climate studies, and the digitized data has allowed for multi-station and long-term studies. This first use of the DMI-BSHcmod model for long simulations has shown that the model is suited for detailed climate simulations.

Contents

1 Introduction

The Earth is experiencing climate change, and it is expected that even larger changes will occur in the next 100 years (Solomon et al., 2007). The oceans play an important role in the climate system, and a major question is how they react and contribute to climate changes. 10% of the world's population live less than 10 m above sea level, and thus the coastal regions of the ocean are of special concern (McGranahan, Balk, & Anderson, 2007). One such heavily populated coastal region is the North Sea – Baltic Sea area (Roode, Baarse, Ash, & Salado, 2008; The BACC Author Team, 2008). In this thesis I will investigate climate change in this area, focusing on:

- Sea level and storm surges
- Temperature and salinity, including stratification and inflows to the Baltic Sea

Special attention will be paid to the transition zone between the North Sea and the Baltic Sea.

To understand the future climate changes, it is important to investigate the characteristics of the climate system in the past. For the transition zone, a unique dataset is available, consisting of long records of sea level observations from tide gauges and temperature and salinity observations from lightships[1] and coastal stations. These data are investigated in Chapter 2–4.

The future changes are investigated with a dynamical downscaling experiment with a slightly modified version of DMI-BSHcmod (hereafter denoted cmod), the regional ocean model currently used at the Danish Meteorological Institute, DMI. The cmod model is a 3D primitive equation physical ocean model developed for regional modeling, especially of the North Sea – Baltic Sea area (Kleine, 1994; Dick, Kleine, Mueller-Navarra, Kleine, & Komo, 2001, further development at DMI). It is used operationally for storm surge warnings and other ocean forecasts, and in various research projects. The simulations presented here are the first long-term simulations with the model. The model was run for two time slices, year 1960–1990 and 2070–2100, to investigate the projected changes in the future physical state of the ocean, see Chapter 5–7.

Discussion of and conclusions on the overall implications for the North Sea – Baltic Sea area are given in Chapter 8 and 9. The electronic supplement referred to throughout the thesis is found on the attached cd-rom and online on `www.gfy.ku.dk/~kristine/thesis` .

[1] The lightships have also measured meteorological parameters and currents.

1.1 Study area

This thesis focuses on the open sea in the North Sea – Baltic Sea area (Fig. 1). The Baltic Sea is semi-enclosed with a bathymetry characterized by the division into several basins separated by sills. The hydrography is dominated by a large freshwater surplus and limited water exchange with the North Sea, which results in low salinities and strong stratification (Chapter 4). The lowest salinity is found in the surface waters of the Bothnian Bay and Sea to the north, and the Gulf of Finland to the east. In the central parts, the Baltic Proper, there is a permanent halocline with relatively salty deep water from earlier inflows (Leppäranta & Myrberg, 2009).

The transition zone is the Baltic Sea's only open boundary to the open ocean and consists of the Kattegat and the Danish Straits (the Great Belt, the Little Belt and the Sound). In this thesis, the Arkona Basin will also be considered a part of the transition zone, and I have defined the boundaries to run along 14.5°E (just west of the island of Bornholm) and 57.5°N, a bit south of the Skagen–Marstrand transect.[2] The bathymetry is characterized by narrow straits and shallow sill depths (8 m at Drogden Sill and 18 m at Darss Sill, see Fig. 1), and the water exchange to the Baltic Sea is limited by the transition zone bathymetry and the sea level difference between the Kattegat and the Arkona Basin. On average a two layer system is seen, stratified with brackish water from the Baltic Sea flowing out in the surface and a compensating, high salinity bottom current. The inflow of high saline water is especially limited by the topography, and only at special events will large amounts of high saline water cross the sills and flow into the Baltic Sea (Kullenberg, 1983; Rodhe, 1998, Chapter 4.7 and 7.7).

The North Sea is a marginal sea with a large open boundary to the North East Atlantic towards north and a smaller opening through the English Channel to the south west. Also, it is connected to the Baltic Sea through the Skagerrak and the transition zone. The southern part up to the Dogger Bank is shallow (less than 50 m), further north it gradually becomes deeper down to about 150 m. In contrast to this, the Norwegian Trench is up to 700 m deep, with a sill depth of 270 m, and extends along the Norwegian coast into the Skagerrak. The North Sea is dominated by tides, especially in the southern and eastern parts, where the water column is permanently mixed (Pugh, 1987). Both the tidal and the averaged residual current are counter-clockwise; the residual current is strongest in the Norwegian Trench area, with inflow in the western and deeper parts and outflow in the Norwegian Coastal Current to the east (Otto et al., 1990; Rodhe, 1998; OSPAR Commission, 2000).

[2]The transition zone area was defined to coincide with the inner part of the cmod fine grid area (see Chapter 5)

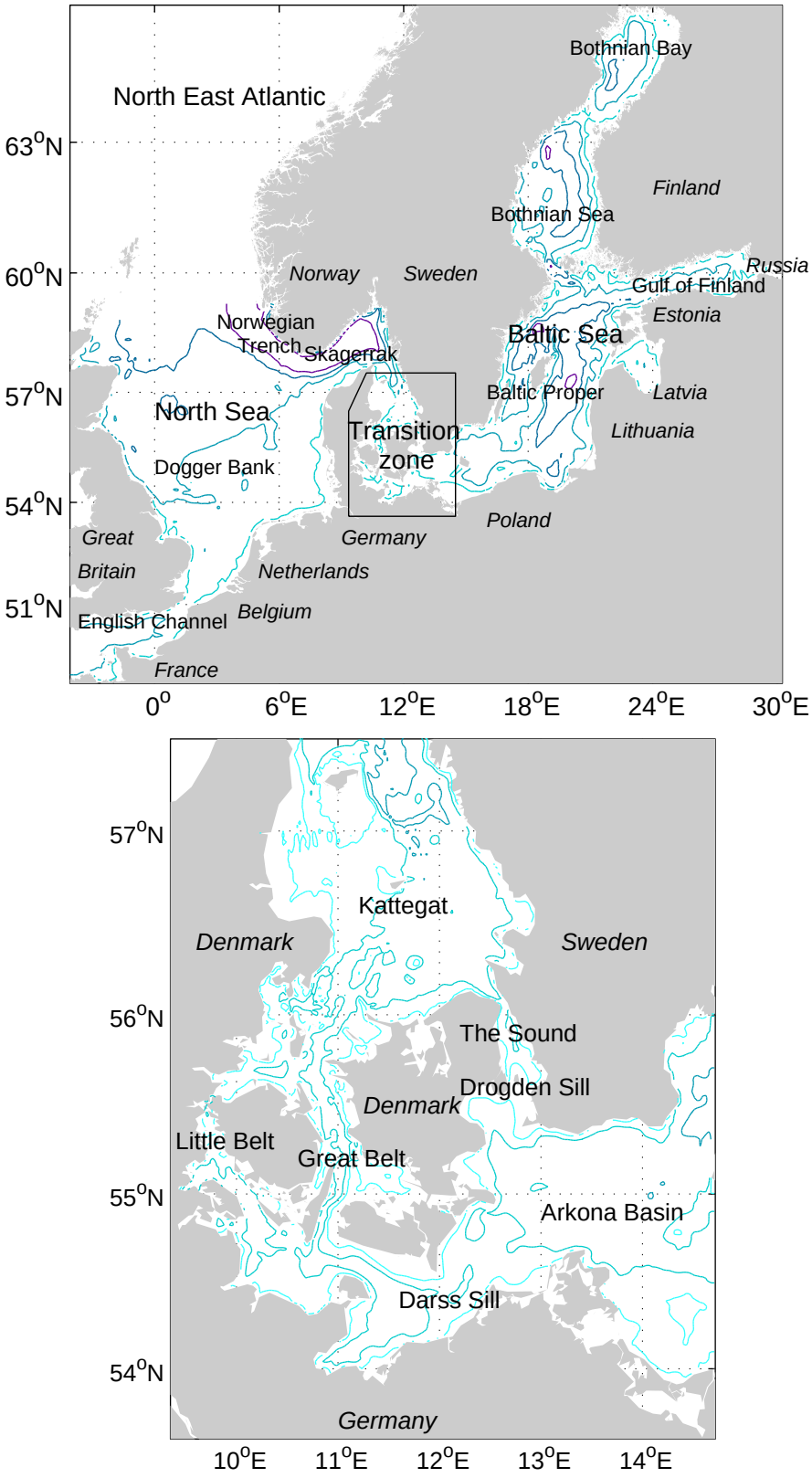

Figure 1: Top: Study area with model bathymetry, 20-, 50-, 100-, and 200 m contours. Bottom: zoom of the transition zone with model bathymetry, 10-, 20-, and 50 m contours.

1.2 Modeling approach

To investigate future climate change, several different approaches are used in the scientific community today. Models can be ordered by the level of complexity, from simple relations, often statistically based, over models of the atmosphere and ocean based on the governing physical equations, to full-blown earth system models that incorporate as many elements as possible, including the ocean, atmosphere, biosphere and cryosphere and includes both physics and bio-geo-chemistry. The modeling approach of the second part of this thesis belongs to the middle category.

Another separation can be made for regional studies, depending on how a global climate signal is transformed into regional values. One approach is to make a sensitivity study with a regional model, e.g., if an ocean simulation for the North Sea, forced with an atmospheric reanalysis of the last 30 years, has already been made, what changes are seen in the ocean if the simulations are run again with the atmospheric temperature increased by 2°C or the wind increased by 10%?

Alternatively, the result of a global circulation model (GCM) scenario run can be downscaled to the region of interest, either through some statistical relationship (statistical downscaling), or by using the GCM data as boundary conditions for a regional climate model (RCM, dynamical downscaling). In this way it is possible to make time slice experiments, for instance running the GCM–RCM system for 30 years in the past (control run) and 30 years in the future (scenario run) and compare, or to make transient runs, where the model system is run for a continuous period from the past and into the future.

For dynamical downscale and sensitivity experiments, the regional ocean model can either be integrated (coupled) with the regional atmospheric model or the atmospheric data can be used to force the ocean model. Common for both is that they require large computational resources. The results presented here were made by a dynamical downscaling experiment using two time slices, and the ocean model was run separately from the RCM.

The main advantage of using the dynamical downscaling approach over the sensitivity approach is that the model system calculates a full climate change scenario from a few fundamental data. For the current simulations input to the GCM was the observed atmospheric greenhouse gas and aerosol contents and a scenario for the future changes in these (an IPCC SRES scenario), as well as the observed ocean sea surface temperature and sea ice extent. From this, the model system generates a complete climate change scenario, where all processes and feedback mechanisms included in the model are taken into account. However, the model system is not perfect, and the model output will contain errors. The errors can be assessed by validating the model results of the control run against observations. In a time slice experiment, it is also common to focus on the changes between the control- and scenario runs, with the expectation that model errors cancel out.

On the other hand, the sensitivity study approach has the advantage of more realistic forcing of the ocean model. The dynamical downscaling method is not made to reproduce the full observed variability of the past except in a statistical sense, whereas the assimilated observations in the reanalysis largely secure this. Also, in the downscaling experiment, the model is so complex that it can be difficult to determine cause and effect relations in the climate change signal; this may be easier in a sensitivity study.

Thus, the best choice of approach depends on the application, and in many situations the sensitivity and dynamical downscaling experiments can compliment each other. Here, the dynamical downscaling approach was chosen in order to give the most comprehensive picture of possible future changes.

2 Observed mean sea level changes

2.1 Introduction

Changes in the mean sea level around Denmark influence coastal erosion, the risk of flooding in storm surge situations (see Chapter 3), the fresh water supply through sea water intrusion to the ground water, and the near-shore eco system, including breeding grounds for many birds (Fenger, 2000; Fenger, Buch, Jakobsen, & Vestergaard, 2008).

When discussing sea level changes, it is very often the global mean sea level that is discussed. However, sea level changes are not uniform over the globe, and it is the local, coastal sea level changes that impact the human population (S. J. Holgate & Woodworth, 2004; Milne, Gehrels, Hughes, & Tamisiea, 2009). Here, the changes in sea level are seen as the sum of global, regional, and local effects.

In the following, I will give a brief review of the current published knowledge on sea level change, and then go into more details of what we can learn about regional and local variations in the Danish sea level from satellite altimetry and tide gauges. Satellite altimetry is very suitable for studying the regional fields, because the method gives open ocean values free of land uplift effects, and allows for easy comparison with global results. But we only have high quality data since the end of 1992 (16 years), and the presented data product can only be used away from the coast. The tide gauge records are more than 110 years long and with a good coverage in the Danish area, making it a highly valuable source of information on local effects.

2.2 Review

The current global sea level rise has been extensively studied, and observations by tide gauges and satellite altimetry shows a mean increase of 1.7 ± 0.3 mm/year for the 20th century and 3.1 ± 0.1 mm/year for 1993–2008 (Church & White, 2006; Cazenave, Lombard, & Llovel, 2008). The increased sea level rise in recent years is primarily due to increased thermal expansion (mainly during the 1990s) and increased melting of ice sheets (increasing the latest years).

Future global mean sea level rise is an area of intense investigation. The fourth IPCC report largely represents the consensus view in the scientific community as of 2007, and reports a best estimated rise of 18–59 cm during the 21st century (95% confidence intervals for different SRES scenarios), with a possible addition of up to 17 cm from increasing ice sheet discharge (Meehl et al., 2007). The future global changes will be dominated by thermal expansion (thermosteric effects) and land ice melt. The thermosteric sea level rise for a given temperature rise is fairly well understood, whereas uncertainty remains about the melt rates of land ice, especially for the ice sheets on Greenland and West Antarctica. The IPCC results include the thermosteric effects calculated from GCMs and constant land ice melt rates referring

to observed values. The possible extra 0.17 m comes from linear extrapolation of the trends in observed melt rates. This approach was taken because ice sheet models are not yet reliable enough for climate simulations. One major reason for concern about the IPCC results is that the present day sea level rise as observed from satellite is underestimated (Rahmstorf et al., 2007). Therefore the scientific community has paid increasing attention to alternative methods for determining sea level rise. Newer studies based on statistical methods suggest that there is a strong sea level response to temperature increases, and that the sea level may rise by 1 meter or more by 2100 (Rahmstorf, 2007b; Grinsted, Moore, & Jevrejeva, 2009). Though these approaches are very simplified, and the method of Rahmstorf has been debated (Schmith, Johansen, & Thejll, 2007; S. Holgate, Jevrejeva, Woodworth, & Brewer, 2007; Storch, Zorita, & González-Rouco, 2008; Rahmstorf, 2007a), it is generally accepted that the IPCC reports do not provide a reasonable upper estimate on sea level rise. Studies of sea level rise from the Eemian period (last interglacial) and of the possible discharge rate of present day glaciers show that sea level rise rates of 1–2 meters per 100 years are possible (Rohling et al., 2008; Pfeffer, Harper, & O'Neel, 2008). To sum up, there is a consensus view that the global mean sea level will continue to rise with at least the same rates as seen in the 20th century, but higher rates are more likely. The Dutch Deltacommissie estimated reasonable upper limits based on present day knowledge to be 0.55–1.2 m by year 2100 and 1.5–3 m by year 2200 (Veerman, 2008).

Regional effects include thermo- and halosteric effects, effects of general changes in wind, surface pressure and ocean currents, and gravitational effects. For the North Sea – Baltic Sea area the gravitational effects are important, since the region is located within about 30 degrees of the Greenland Ice Sheet and within limited distance of many of the small glaciers. According to Mitrovica, Tamisiea, Davis, and Milne (2001) and Farrell and Clark (1976), the North Sea – Baltic Sea area will experience less than 20% of the global mean for melting from Greenland and 60–80% of the global mean for melting from small glaciers on a 100-year time scale. The effect from a melting at Antarctica is 100–110% of the global mean. However, these studies assume all other sea level effects to be uniform over the globe and independent of the melting ice.

On a global scale, the steric effects can be assumed to be dominated by thermal expansion, since the total salt content is almost constant. At basin-scales the halosteric effects can reach similar magnitude as thermosteric effects. The effects will often partly counteract each other, since motion beneath the thermocline in the open ocean is in general along isopycnals, and this dynamic constraint means that the salinity of moving water parcels must be higher if the temperature is higher, to retain density (Ivchenko et al., 2007). However, at some locations, *e.g.* the Arctic Ocean, both the thermosteric and halosteric effects will increase, when water becomes warmer and fresher (Landerer, Jungclaus, & Marotzke, 2007). For the North Atlantic, historic observations show a steric sea level trend close to the global mean the second half of the 20th century (Church, White, Coleman, Lambeck, & Mitrovica, 2004; Levitus,

Antonov, Boyer, Garcia, & Locarnini, 2005). This is also the case for more recent data for the North East Atlantic, but the uncertainty of regional values is larger than for the global mean (Ivchenko et al., 2007; Cazenave et al., 2008). As to 21st century changes, the IPCC report indicates a slightly higher increase in steric effect in the North East Atlantic than the global average, but the results vary between different models (Meehl et al., 2007). The detailed study by Landerer et al. (2007) indicates rather steep gradients in changes in steric height in the North East Atlantic, with negative relative changes south of Iceland but a 10 cm relative increase by the end of the 21st century at the North Sea entrance area for the MPI-OM model forced with a A1B emission scenario. Katsman, Hazeleger, Drijfhout, Oldenborgh, and Burgers (2007) has made a scenario study for the North East Atlantic ocean with all of these processes included, and found a mean sea level increase of 0.3–0.8 m for year 2100 and a temperature increase of 2–4°C.

One of the main indicators for sea level variability on regional scales in the North Sea – Baltic Sea area is the winter NAO index. The general North Atlantic pressure pattern and storm track varies on a decadal time scale, and influences the sea level both through direct pressure effects, the influence on the zonal wind, and through steric effects (Andersson, 2002; Wakelin, Woodworth, Flather, & Williams, 2003; Tsimplis, Shaw, Flather, & Woolf, 2006). The climate change impact on the NAO index is unfortunately not very well determined, as the GCMs have difficulties at modeling today's NAO variability. However, most models indicate a possible increase in the general pressure difference across Western Europe, and thus the NAO (Osborn, 2004; Meehl et al., 2007).

Local effects can include a wide spectrum of phenomena, depending on the point of interest. For the Danish area, I expect the most important local effects to be land uplift and wind effects. For the Baltic Sea, increased freshwater input and higher increase in temperatures than open ocean could also make a contribution.

The most-common picture of land uplift in Denmark is that the northern part of Denmark is experiencing land uplift due to isostatic rebound of Scandinavia after the last ice age, while the southern and western part may be sinking. This is based on local observations of long term relative sea level trends and an assumed absolute sea level rise of 0–1 mm/year (Duun-Christensen, 1990; Rossiter, 1967). However, according to the above, the global sea level rise has been larger, which opens up for the possibility that also the local, absolute rise has been larger, and thus that the land uplift has been underestimated.[3] Currently, this is studied in a cooperation, where Danish governmental institutions and universities work together to work out the best possible determination of land uplift. In Denmark, we have a network of 3 permanent GPS stations which are included in the EUREF system and additionally 3

[3]Relative sea level: sea level relative to a point on land, *e.g.* as measured by a tide gauge. Absolute sea level: sea level relative to the center of the Earth (free of land uplift effects).

stations with several years of measurements. By combining the information from all stations, as well as information from tide gauges, historic surveys of precise leveling, and glacial isostatic adjustment models, stable estimates of the land uplift rates may be obtained. Preliminary results of this study will be discussed below.

The North Sea – Baltic Sea area is located in an area with pronounced westerly winds, which, together with the freshwater surplus and the resulting low salinity of the Baltic Sea, creates a permanent sea level gradient of about 35 cm from the North Sea to the northern Baltic Sea, with a gradient of 10–15 cm through the transition zone (Ekman & Mäkinen, 1996). Changes in the mean wind may change this picture. Several studies have been made about wind effects on the sea level in the North Sea, but they focus on the extreme sea level in connection with storm surges (see Chapter 3 and 6).

Relative sea level trends in Denmark has previously been studied by Duun-Christensen (1990, 1992), who found that the long-term trend in sea level depends on location and measuring period, with the largest increases in southern Denmark (Year 1890–1989: 1.10 ± 0.19 m at Esbjerg and 0.96 ± 0.15 m at Gedser, vs. -0.42 ± 0.14 m at Hirtshals, for locations see page 11). Recent investigations in the Danish Wadden Sea showed that the sea level at Esbjerg has risen with up to 5 mm/year in recent years (Knudsen, Sørensen, & Sørensen, 2008). Quantile regression of monthly mean sea level in the Baltic Sea and the transition zone has shown that the 99th quantile has risen more than the mean sea level in the central, northern, and eastern Baltic Sea, while the difference is not significant for the transition zone stations (Barbosa, 2008).

2.3 Material and methods

2.3.1 In-situ observations

In Denmark, 10 tide gauges have records longer than 100 years (Fig. 2 and Table 1). All of them have continuous series of data with only small gaps, and their reference level have been calibrated with local bench mark stations on a regular basis. However, the Frederikshavn stations is suspected of local subduction problems, and was left out of the trend analysis, and the København Station may have been affected by local gate building until the 1930s, so for this station, only data after 1930 is used (Binderup & Frich, 1993).

All of the stations are available as monthly mean values from the GLOSS database through PSMSL (`www.pol.ac.uk/psmsl/psmsl_individual_stations.html` , `www.gloss-sealevel.org`), and the hourly time series from the Esbjerg, Hornbæk, and Gedser Stations are digitally available from DMI (Hansen, 2007, Esbjerg data available on request). From the 1970s onwards, data are available on sub-hourly basis

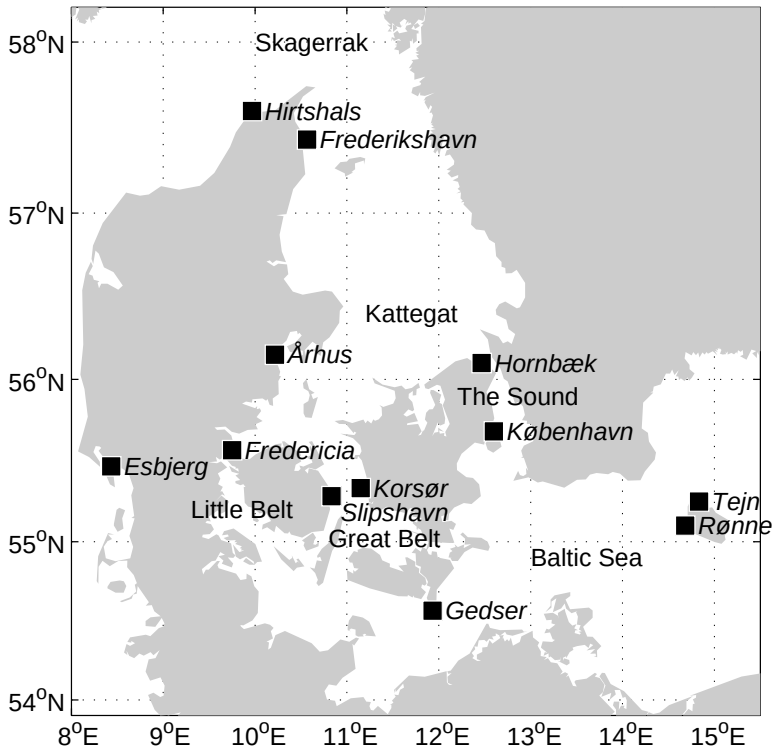

Figure 2: Map of Danish tide gauges with long data records (see also Table 1).

Table 1: Station list – Danish tide gauges with long data records (see also Figure 2). St. num. refers to the DMI station numbers. All measurements are continued till today. The KDI dataset is used in Chapter 3.

St. num.	Start date			Lat	Lon	Name
	GLOSS	DMI	KDI			
20047–20048	1892-01	1971-11-04	1966-01-01	57.600	9.967	Hirtshals
20098, 20101	1888-09	1970-01-14	1894-01-01	57.433	10.567	Frederikshavn
22331–22332	1888-09	1970-03-14	1888-01-01	56.150	10.217	Århus
23292–23293	1889-08	1972-06-07	1889-07-01	55.567	9.750	Fredericia
25148–25149	1889-03	1891-01-01	1874-01-01	55.467	8.433	Esbjerg
28232–28234	1896-01	1971-10-15	1890-01-01	55.283	10.833	Slipshavn
29392–29393	1897-01	1972-10-20	1890-01-01	55.333	11.150	Korsør
30017–30018	1898-01	1891-01-01	1891-01-01	56.100	12.467	Hornbæk
30336–30339	1889-01	1974-07-18	1888-07-01	55.683	12.600	København (Copenhagen)
31616–31618	1898-01	1891-09-01	1892-12-01	54.567	11.933	Gedser
Stations on Bornholm						
32048		1992-08-19		55.250	14.833	Tejn
32096			1987	55.100	14.683	Rønne

Table 2: Preliminary land uplift estimates [mm/year] at Danish EUREF GPS stations (Per Knudsen, pers. comm.).

Name	Lat	Lon	Abs. land uplift	DVR90−DNN	Difference
Smidstrup (SMID)	55.64	9.56	0.68 ± 0.5	-0.95	1.63 ± 0.5
Suldrup (SULD)	56.84	9.74	1.36 ± 0.5	-0.28	1.64 ± 0.5
Buddinge (BUDP)	55.74	12.50	0.67 ± 0.5	-0.13	0.80 ± 0.5
Mean value					1.4

from DMI. The highest recorded storm surges have been tabulated by the Danish Coastal Authority (KDI), see Chapter 3.

Three Danish permanent GPS stations are included in the EUREF network, Smidstrup, Suldrup, and Buddinge. These are all located inland and were set up during 1997–1999. Three other permanent GPS stations with shorter data records are located at Gedser, Hirtshals and Esbjerg, closer to tide gauges. The absolute land uplift relative to the ITRF2005 reference frame is currently being analyzed by Abbas Khan and Per Knudsen, DTU Space, and preliminary results are available for the EUREF stations (Table 2). The errors of the single station trends are around 0.5 mm/year. On top of this, there may be a bias in the reference frame realization of up to 0.5 mm/year, though no sign of this has been detected (Per Knudsen, pers. comm.).

To compare the results of the individual GPS stations, and to transfer the signal to the location of the tide gauges, the geographical pattern in the difference between the local reference systems based on the two leveling campaigns of Denmark, the DNN and the DVR90, has been used. First the mean offset of the GPS station locations was calculated (Table 2), and then this was added to the reference system difference at the tide gauge locations. This resulted in estimated absolute land level rates between 0.26 and 1.52 mm/year at the tide gauges with long data records (Table 3). This introduces an additional error of 0.2–0.3 mm/year (Per Knudsen, pers. comm.). Thus there are relatively large uncertainties connected to the determination of land uplift, and the estimate will be improved for the tide gauges that are close to the permanent GPS stations once the processing is finished. A basic assumption in this analysis is that the land uplift rates have been constant over the last century. This is valid within the uncertainty in case of isostatic land uplift after the last ice age, but not necessarily if other factors are involved (*e.g.* sediment compaction).

2.3.2 Satellite altimetry

Since 1992, satellite altimetry measurements with single point accuracy better than 4 cm have been available from the TOPEX/Poseidon, Jason 1–2, ERS, and Envisat missions. When the data are averaged over space and time, sea surface height information with sub-cm accuracy and almost global coverage is obtained, and therefore information about the global mean and regional variations in sea surface height trend

can be obtained (Cazenave et al., 2008). Special treatment of the satellite altimetry product and the applied corrections is needed in coastal regions, but until about 100 km from the coastline, the open ocean product is valid in most cases (Fu & Cazenave, 2001; Madsen, Høyer, & Tscherning, 2007). For the current study, data have been downloaded from `sealevel.colorado.edu/wizard.php`. This is a gridded, multi-satellite open ocean product with 1 degree, 10 day resolution.[4] Available data from the North Sea – Baltic Sea area with a minimum distance of 1 degree from the coast have been downloaded, together with global and Atlantic Ocean mean time series.

2.4 Results

2.4.1 Regional variations – Satellite altimetry

Figure 3 shows the 60-day running mean sea surface height measurements from 22 points in the North Sea and 7 points in the Baltic Sea, as well as similar mean values of tide gauge data from Hirtshals and Tejn tide gauges, respectively. It is seen that the satellite measurements within each sea area are very similar. In the Baltic Sea, the satellite time series have a correlation coefficient of 0.88 or more with each other, in the North Sea it varies between 0.54 and 0.99, with a separation between eastern, western and northern profiles with boundaries around 3 degrees east and 59 degrees north; within each of these groups, the correlation is 0.87 or more. There is a fairly good agreement between the open ocean measurements and the coastal tide gauges in Hirtshals and Tejn, with correlation coefficients between the tide gauges and the best fitting satellite data of 0.71 and 0.97 respectively. The higher correlation coefficient in the Baltic Sea is expected, since the correlation scales in the Baltic Sea are generally longer than in the North Sea. Figure 3 also show that the sea level variations at the Hirtshals tide gauge are larger than in the open North Sea, the standard deviation of the running mean tide gauges is 2.7 times higher than the open ocean value. This is expected, since short term sea level signals in the North Sea, such as storm surges, generally travel as Kelvin waves along the coast, with exponentially decreasing sea level away from the coast. In the Baltic Sea, the tide gauge standard deviation is 1.7 times larger than open water values.

From the satellite data, the linear trends for the time period December 1992 – December 2008 can be calculated (Fig. 4). The trend in each basin is quite uniform, and the best estimates for the North Sea is 1.9 mm/year, with a single point standard deviation of 0.6–1.1 mm/year, and accordingly for the Baltic Sea 5.8 mm/year and 1.4–1.6 mm/year. The single point standard deviation is used because data are spatially correlated. In the North Sea there are some indication of increasing trend towards west, but since the dataset is not suitable for the coastal regions. That will not be

[4] The product is based on data from TOPEX/Poseidon and Jason-1 GDR records, with radiometer wet tropospheric correction and GOT00.1 tidal correction applied.

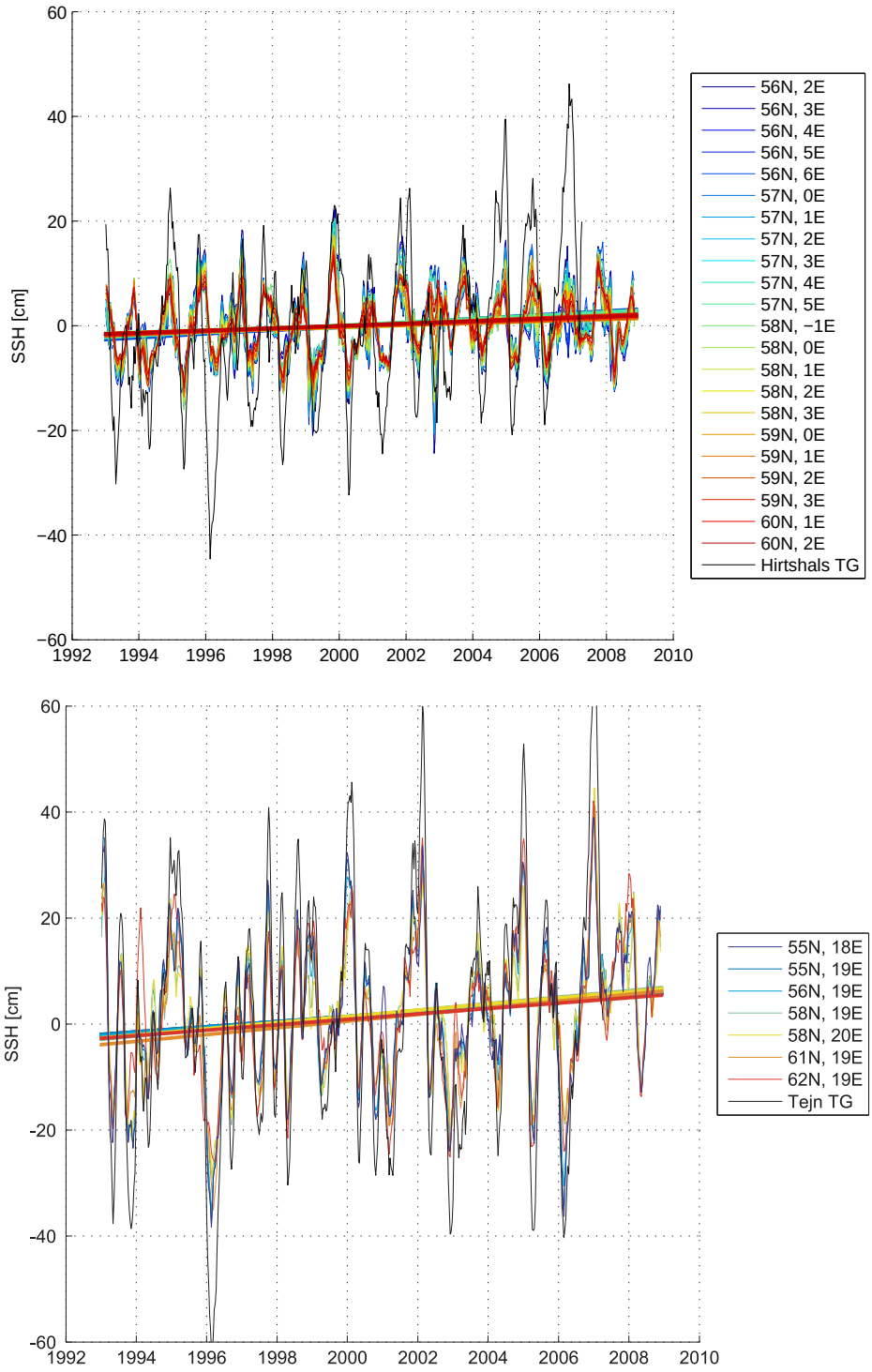

Figure 3: Time series of 60 day running mean sea surface height measured by satellite altimetry (colored lines) and selected tide gauges (black lines). Top: North Sea, bottom: Baltic Sea.

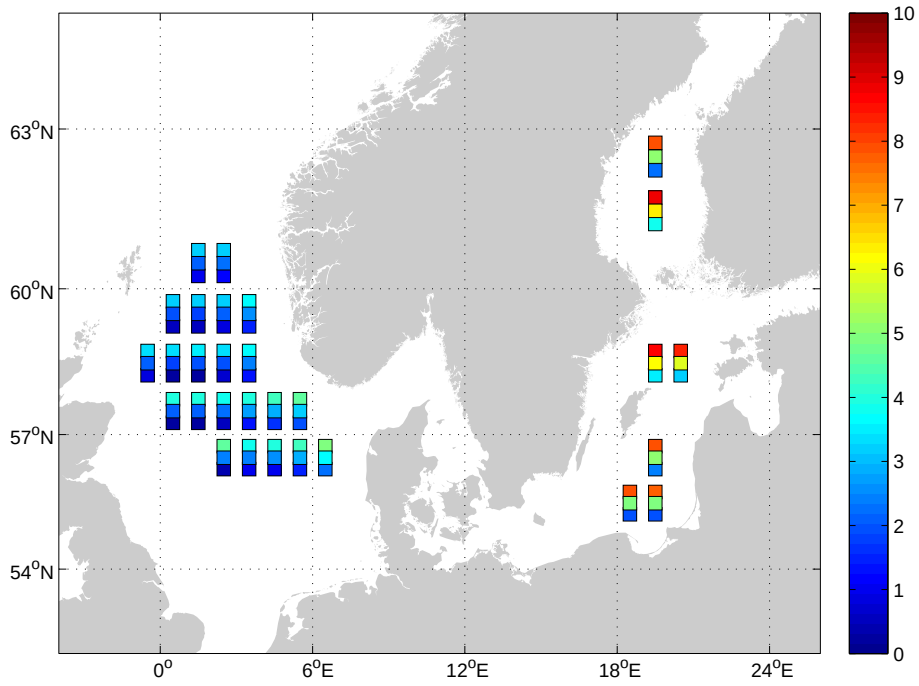

Figure 4: Linear trend in sea surface height (mm/year, center boxes) and 90% confidence intervals (upper and lower boxes) as calculated from satellite altimetry.

investigated further here. For comparison, the global mean value for the same data set and time period is 3.23 ± 0.04 mm/yr and the Atlantic mean is 3.3 ± 0.1 mm/yr. From this, it is clearly seen that the uncertainty in the trends are much larger for the regional determination, both because of the smaller number of samples, and, especially for the Baltic Sea, because of the large natural variability. This also means that the trends are sensible to the choice of time period. With these precautions, it is seen that the North Sea trend is likely to be lower than the global mean, and the Baltic Sea trend is very likely to be higher than the global mean, and perhaps just as interesting for the Danish area, higher than the North Sea trend.

It would be interesting to investigate the along-track satellite altimetry data of the coastal area, to link these trend values tighter to tide gauge data. This is left for future studies.

2.4.2 Local variations – In-situ observations

The analysis in this chapter was based on the monthly GLOSS data. The data were filtered with a 19 year running mean filter to remove any short term and most tidal variations, and the 1960–1990 mean was subtracted from each dataset to remove any

Table 3: 1901–2000 linear sea level trend at Danish tide gauges [mm/year]. Column 2–4: Measured relative sea level trend from tide gauges with 90% confidence interval and number of months with missing data. Column 5 and 6: The difference between the reference systems DVR90 and DNN, and the derived land uplift. Column 7–8: the absolute trend, calculated as the sum of the relative trend and the land uplift, with 90% confidence interval.

Station name	Relative trend	90% conf. int.	Missing data	DVR90 −DNN	Land uplift	Absolute trend	90% conf. int.
Gedser	1.04	0.15	13	-0.54	0.86	1.9	0.7
Fredericia	0.95	0.08	12	-0.93	0.47	1.4	0.7
Slipshavn	0.89	0.11	51	-0.63	0.77	1.7	0.7
Korsør	0.78	0.11	27	-0.74	0.66	1.4	0.7
Århus	0.42	0.10	36	-0.43	0.97	1.4	0.7
København*	0.69	0.25	20	-0.12	1.28	2.0	0.7
Hornbæk	0.12	0.16	27	-0.18	1.22	1.3	0.7
Hirtshals	-0.23	0.19	59	0.12	1.52	1.3	0.7
Esbjerg	1.15	0.26	24	-1.14	0.26	1.4	0.7

* København: only year 1930–2000.

permanent bias between the stations (Fig. 5 top). The 100 year relative sea level trend for year 1901–2000 was calculated from each time series (Table 3). This was done with a least squares fit to the linear function and the seasonal harmonics, to avoid any effects of seasonality of missing data.

The effect of land uplift is obvious. While the southern Danish stations have clear positive trends, with rising sea level at most times, the trend decreases further north, and at Hirtshals the trend is slightly negative and the relative sea level has been decreasing for long periods. When the estimated land uplift is taken into account, most of this variability is removed (Fig. 5 bottom), resulting in a mean trend of 1.5 $\pm$ 0.5 mm/year (90% confidence interval) for the stations with at least 100 years of data (Table 3). Thus, the best estimated value for the Danish sea level rise for year 1901–2000 is lower than the global mean, but the global mean is well within the error bounds, due to the relatively large uncertainty in the land uplift determination. The difference in trend value between the København and Hornbæk stations is partly due to the shorter record length at København; the trend at Hornbæk for the 1930–2000 period is 0.4 mm/year. It is reassuring to see the similarities of the Esbjerg and Hirtshals curves after the land uplift correction. Other issues remain to be clarified, especially the record from Gedser stands out with larger than average trend early in the 20th century (Fig. 5 bottom). Also, the difference between Slipshavn and Korsør is relatively large, considering that the stations are located only 21 km apart on each side of the Great Belt. When comparing with earlier estimates of relative sea level trend, the agreement is good, but the relatively large increase in the 1990s means that the trends calculated here are slightly higher than the values obtained by Duun-Christensen (1992).

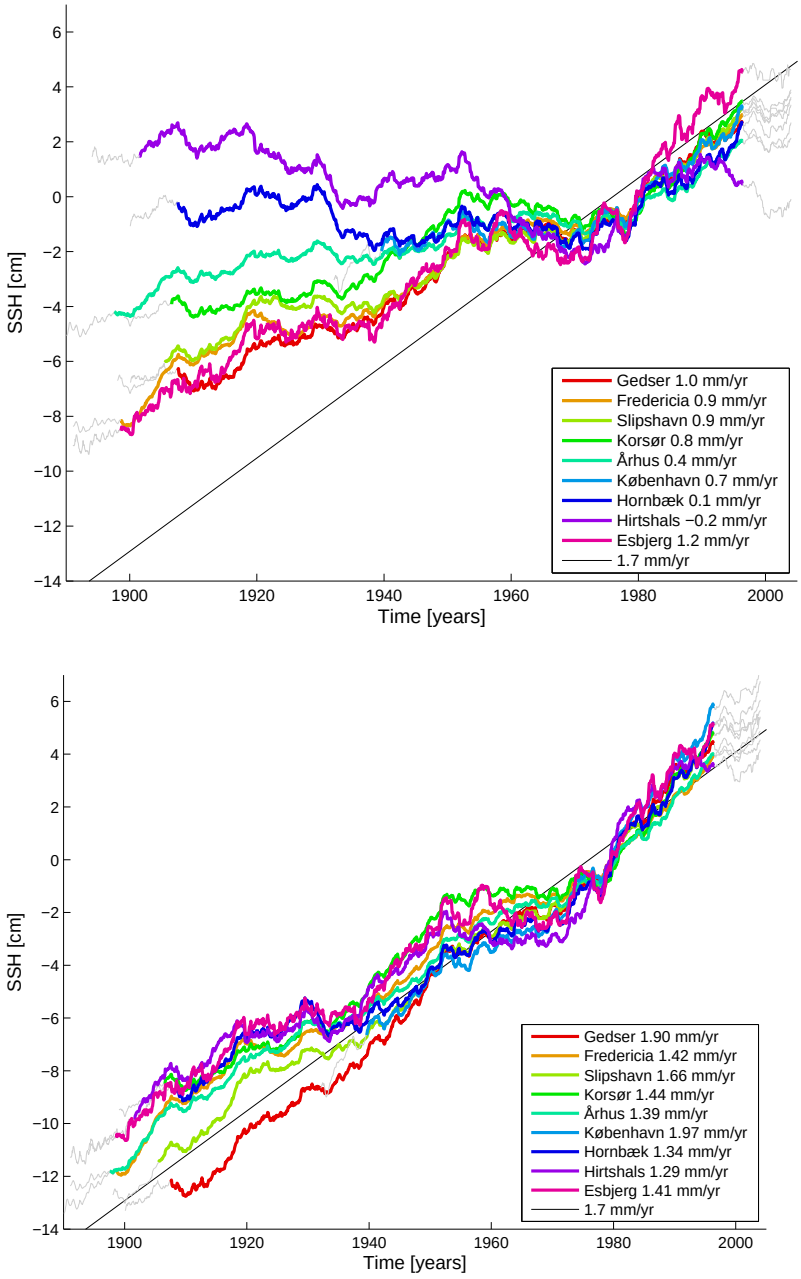

Figure 5: 19 year running mean sea surface height at Danish tide gauges [cm]. Top: the relative sea level as observed at tide gauges. Bottom: the estimated absolute sea level, calculated as the relative sea level plus the land uplift (see Table 3). The 1961–1990 mean value has been subtracted. For reference, the global mean sea level rise of 1.7 mm/year is also shown, and the 1901–2000 linear trend for each station is listed in the legend.

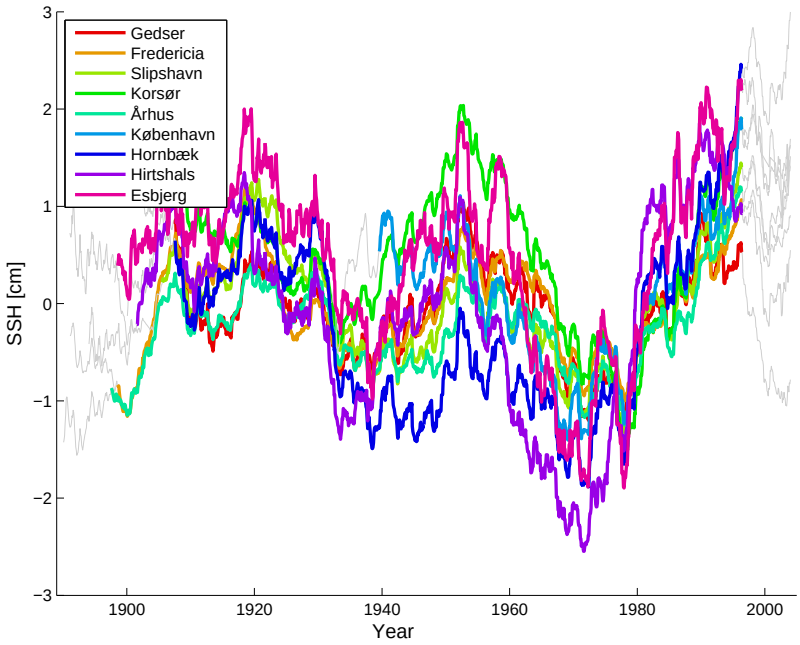

Figure 6: Detrended running mean sea level [cm]. As Figure 5, but with the linear trend for year 1901–2000 removed. Note the changed scale on the y-axis.

The data also show long-term variability. This becomes obvious when best estimate of the linear trend is removed from the data (Fig. 6). There was a general relative dip in the 1970s, and in the 1980s and early 1990s the relative sea level trend was larger than average. However, the most recent data do not show signs of increased trends.

The correlation between the detrended data and the 19 year running mean values of the NAO and AO indices (Hurrell, Kushnir, Ottersen, & Visbeck, 2003) is 0.8–0.9 at the Hirtshals and Hornbæk stations, and lower at the other stations. This geographical pattern seems reasonable, since the Hirtshals and Hornbæk stations are relatively exposed to the North Atlantic. The values of both the NAO and AO indices are increasing in the 1980 and 1990 like the sea level trend, but the indices do not explain the variability earlier in the century.

3 Observed storm surges

3.1 Introduction

Large parts of the North Sea and the Baltic Sea coasts are storm surge risk areas (Schmidt-Thomé et al., 2006). Through history, storm surges have taken many lives and caused large material damage along these coasts. Especially the large surges in 1872 in the southwestern Baltic Sea and in 1953 and 1962 in the North Sea have meant that there has been focus on coastal protection against and prediction of storm surges for many years (Colding, 1881; Heaps, 1967, 1983; Gram-Jensen, 1991; Feistel, Nausch, & Wasmund, 2008; Storch & Woth, 2008).

In the North Sea, surges are most often created by low pressure systems, and the southern and south-eastern coasts are most exposed. This area includes the southern Danish North Sea coast and the Esbjerg tide gauge (Fig. 2). The rest of the Danish North Sea coast is also exposed to frequent storm surges, and large parts of the coast are protected by dikes, groins, and beach nourishment, and have storm surge forecast and warning systems (J. W. Nielsen, 2001; Fenger et al., 2008).

In the Baltic Sea, storm surges occur as the result of wind stew, and often in connection with general high sea level. Thus the south-western parts are exposed to storms from the east and north. Storm surges on the south-western Baltic Sea coasts are not as frequent as on the Danish North Sea coast, but can be severe (Sztobryn et al., 2005).

The Danish coasts of the Kattegat and the Danish straits are better protected from storm surges because of the surrounding land masses. However, high water levels, especially in the southern part of the Kattegat, can occur in connection with storms over both the North Sea and the Baltic Sea. On special occasions, especially when water is pressed into the Danish straits from both the North Sea and the Baltic Sea, storm surges occur even in the Danish straits and cause damage to these less-protected areas. An example of this is the November 2006 storm surge (`ocean.dmi.dk/case_studies/surges/01nov06.php` [in Danish]).

Storm surge statistics can be made in different ways. When looking at "peaks over threshold", a statistical distribution is fitted to the N highest independent values in the data, either a few values per year or the highest values in the full record. This method is suitable for determining the return height of a 20- 50- or 100-year event, and thus for safety and insurance issues and design specifications for e.g. dikes and maritime constructions. The method is used by DMI and KDI. Alternatively, the "threshold" method is used. Here, the value of a specified percentile, often the 99 or 99.5 percentile, is used to characterize the highest observed values. This method is more statistically robust in the sense that it does not make assumptions about statistical distributions, but if the percentile becomes very high, the amount of included data can become low. The method is suitable for planning purposes, e.g. for determining how many days

a year high water levels are expected, and it has been used for earlier studies in the North Sea (Woth, Weisse, & Storch, 2006). In this thesis, the focus is on the peaks over threshold method.

3.2 Methods and material

For the peaks over threshold analysis, a truncated Weibull distribution was used, with cumulated probability distribution

$$F(x) = 1 - \exp\left(-\left(\frac{x-\gamma}{\beta-\gamma}\right)^{\alpha}\right), x > \gamma \tag{1}$$

where x is the water level, γ is a cut-off level selected to include only extreme events in the statistics, and $\alpha > 0$ and $\beta > \gamma$ are the shape and scale parameters, respectively, that are fitted using maximum likelihood (Tawn, 1988; Smith, 1986; Sørensen, Sørensen, Ingvardsen, Andersen, & Kloster, 2007). For $\alpha = 1$, the distribution reduces to a truncated exponential distribution.

The Weibull distribution is used by KDI for all stations treated here except Esbjerg. KDI chose it over exponential, Gumbel, Frechet, and log-normal distributions by testing how well the distributions fit the data (Sørensen et al., 2007). At Esbjerg, KDI used a log-normal distribution. However, the results for return heights can be reproduced by assuming a Weibull distribution, while I have not been able to reproduce them using a log-normal distribution. Therefore I have chosen to use the Weibull distribution for Esbjerg as well in this analysis.

The truncation is performed because the statistics of the extreme data is different from the average data and it is an alternative to using e.g. the highest annual value. It was preferred because it allows including more than one storm surge from a given year, and independence of the events was ensured by requiring a separation of at least 36 hours between events. The cut-off levels used by KDI were found through a trial-and-error procedure, focusing on stabilizing the statistics with regards to the number of points included in the analysis and minimizing the difference between observed and theoretical percentiles (Sørensen et al., 2007). Here, the KDI cut-off levels were tested using a Weibull distribution plot, made with the Matlab function wblplot(x), where data with a Weibull distribution will show up as a straight line (Fig. 7). The typical image is that the most extreme data form a more or less straight line, and then the data fall off. The ideal cut-off level is found where the data start to follow the straight line.

The return height (x) for a specific period (T) can be found from the inverse cumulated probability density as

$$x = F^{-1}(p) = (\beta-\gamma)\left(\ln\left(\frac{1}{1-p}\right)\right)^{\frac{1}{\alpha}} + \gamma \tag{2}$$

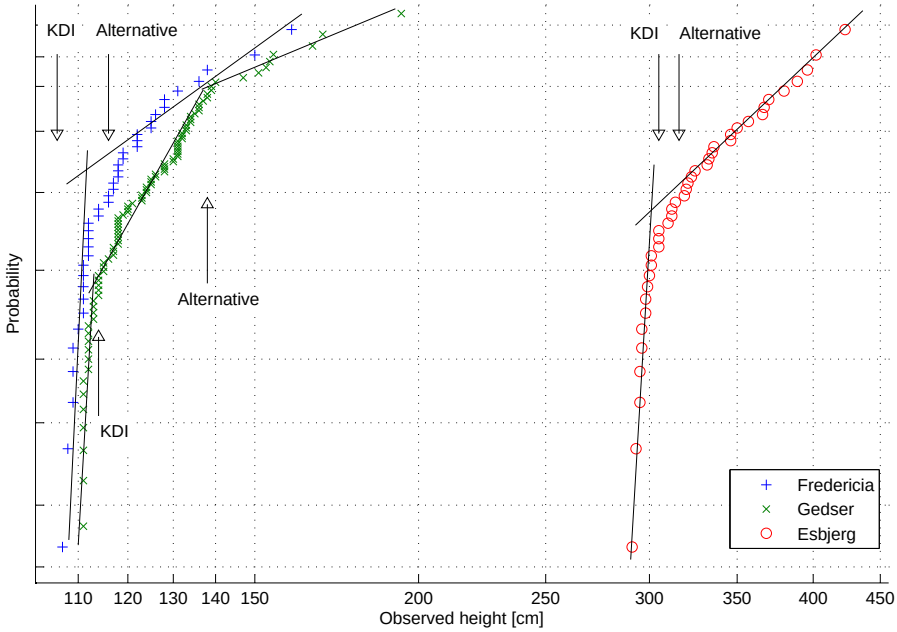

Figure 7: Weibull probability distribution plots of the most extreme sea level measurements from Fredericia, Gedser, and Esbjerg. Data that are well fitted by a Weibull estimation appear as a straight line in this type of plot, and the cut-off level can be determined by visually inspecting where this assumption breaks down.

where $p = 1 - \frac{1}{\lambda T}$ and λ is the average return frequency of extreme events, corresponding to γ.

This study was limited to the ten DMI tide gauge stations with long data records, supplemented with data from Rønne on Bornholm (Fig. 2). The peak records as presented in Sørensen et al. (2007) were used, since they include data from the entire observational records. For Esbjerg, an extra analysis was made for data after 1909, since it is suspected that extreme data prior to 1909 has not been recorded correctly (Jacob Woge Nielsen, pers. comm.). Similarly, an extra analysis was made for Copenhagen after 1930, because gate building may have changed the statistics (Binderup & Frich, 1993). For Gedser, the KDI data do not go all the way to the cut-off level (the cut-off level is 114 cm, while only events of 126 cm and up are included), so an extra analysis was made with the DMI data record, for peaks of more than 114 cm (72 events all in all).

Two shorter time periods have been analyzed, January 1, 1961 – December 30, 1990, which corresponds to the model hindcast simulation period, and December 1, 1976 – November 30, 2006, the newest 30 year time period available at all stations. The Hirtshals Station has been excluded from the first part of the analysis and the

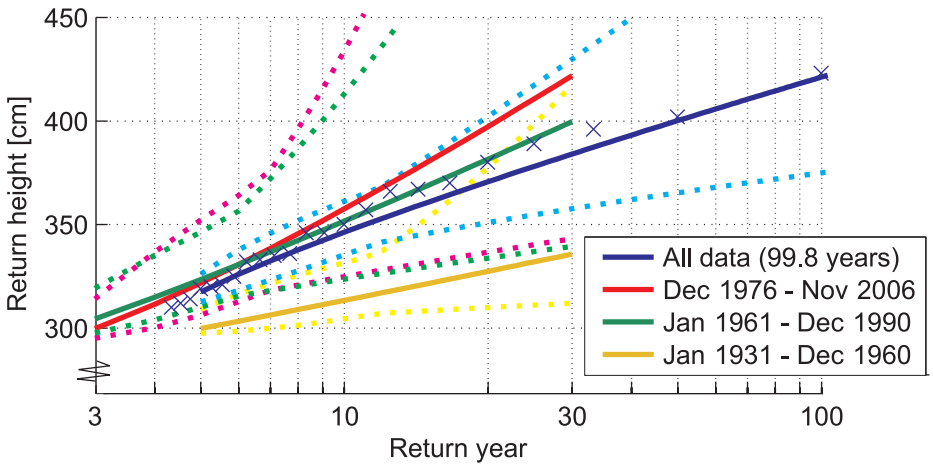

Figure 8: Return heights at Esbjerg when data prior to 1909 are excluded (solid lines). The dashed lines show the 90% confidence intervals. The blue line represents statistics with all data included; other curves are for selected 30 year periods.

Rønne Station from both parts, due to missing data. For the short time periods, only the 10- and 20-year return heights have been studied. For Esbjerg, the time period January 1, 1931 – December 30, 1960 was also analyzed.

3.3 Results and discussion

The cut-off levels for the peaks over threshold analysis can be estimated from a Weibull distribution plot, as exemplified for Fredericia, Gedser, and Esbjerg in Figure 7. This method gives a cut-off level which is equal to or up to 24 cm higher than the KDI levels. However, the corresponding changes in the extreme values are small (max 4 cm for a 100 year event, found at Hornbæk and Korsør), so KDI's original values have been kept here.

The return heights as obtained with the peaks over threshold analysis are presented in Table 4 and Figure 8. For the full time series, the KDI statistics were reproduced within 1–2 cm. The Esbjerg return heights were increased 8–14 cm, or about 3%, by excluding data prior to 1909, and the Copenhagen return heights were decreased 5–16 cm, or 4–10%, by excluding data prior to 1930. Using the alternative data source for Gedser gives a 0–2 cm (1%) decrease, most likely due to differences in reference level.

For the shorter time series, there are no statistically significant changes in recent years, if the alternative data series for Esbjerg, Copenhagen and Gedser are used. However, there are two cross station tendencies. First, the southern transition zone stations tend to have lower return heights 1961–1990, which can be explained by the lack of large storm surges in this period and area. At Gedser, there are no surges from this period in the top 17 of record storm surges. Second, all western stations have

Table 4: Return heights for 10-, 20-, 50-, and 100-year events in cm based on observations, with 90% confidence intervals given in parentheses. For the 30 year time intervals, only the 10- and 20 year events are given, since the uncertainty of longer return periods is large for the short records.

Station		10 year	20 year	50 year	100 year
Esbjerg	1874–2006	338 (328–351)	362 (347–383)	389 (362–434)	407 (371–471)
	1909–2006	346 (335–361)	371 (351–402)	400 (365–465)	421 (375–515)
	1976–2006	358	397		
	1961–1990	352	382		
Hirtshals	1966–2006	129 (120–141)	135 (124–154)	144 (129–170)	150 (132–182)
	1976–2006	131	140		
Frederikshavn	1894–2006	130 (126–135)	137 (130–146)	145 (135–160)	151 (138–171)
	1961–1990	133	140		
	1976–2006	135	142		
Århus	1888–2006	131 (126-137)	140 (132–154)	153 (138–178)	162 (143–196)
	1976–2006	138	151		
	1961–1990	133	144		
Fredericia	1889–2006	123 (120–128)	130 (124–140)	139 (129–154)	145 (132–165)
	1976–2006	126	134		
	1961–1990	118	121		
Slipshavn	1890–2006	121 (117–127)	129 (122–140)	139 (128–158)	147 (132–171)
	1976–2006	131	144		
	1961–1990	120	125		
Korsør	1890–2006	119 (116–124)	128 (122–139)	142 (128–171)	153 (132–200)
	1976–2006	125	140		
	1961–1990	116	120		
Hornbæk	1891–2006	141 (137–146)	148 (141–158)	157 (147–175)	164 (150–188)
	1976–2006	140	147		
	1961–1990	143	149		
København	1888–2006	123 (120–128)	131 (126–140)	143 (131–167)	152 (135–190)
	1930–2006	118 (117–122)	124 (120–130)	131 (123–152)	136 (124–174)
	1976–2006	118	121		
	1961–1990	118	120		
Gedser	1892–2006	141 (137–147)	149 (142–161)	160 (148–182)	168 (152–198)
	alternative	142 (137–150)	151 (142–162)	161 (149–178)	168 (154–190)
	1976–2006	142	150		
	1961–1990	133	137		
Rønne	1987–2006	103 (92.6–122)	110 (95.6–136)	117 (99.2–154)	123 (102–168)

increased return heights 1976–2006, which can be explained by the large storm surge November 1, 2006 in the western transition zone and a general tendency towards a more stormy climate in Denmark in resent years, with 14 heavy storms recorded by DMI 1971–2005, just as many as in the previous 80 years [5].

[5]Here, heavy storms were defined as storms of at least 26.5 m/s, covering at least 10% of Denmark. Figure available at www.dmi.dk/dmi/index/klima/klimaet_indtil_nu/vind_og_vandstand_i_danmark.htm, data available at www.dmi.dk/dmi/storme-2.pdf (John Cappelen, pers. comm.).

4 Observed temperature and salinity

4.1 Introduction

The North Sea is the only source of salinity and a main source of deep water oxygen to the Baltic Sea. Also, the Skagerrak and the Norwegian Coastal Current in the North Sea are greatly influenced by the low-saline outflow from the Baltic Sea. Any changes in these forcings will be reflected in the conditions in the transition zone, and the response is two-way – changes in the transition zone will also affect the North Sea and Baltic Sea.

The Baltic Sea is one of the most studied areas of the world's oceans (Fonselius, 2001), and a detailed literature review will not be given here. However, it should be mentioned that three books have come out recently. The physical oceanography is introduced in Leppäranta and Myrberg (2009), Feistel et al. (2008) give an in-depth description of Baltic Sea observational programs, and The BACC Author Team (2008) review recent climate studies for the region.

The Baltic Sea salinity is dominated by the freshwater surplus from river runoff, net precipitation, and the restricted inflow of high saline oceanic water (Omstedt, Meuller, & Nyberg, 1997; B. G. Gustafsson & Westman, 2002). This results in increasingly brackish water away from the Baltic Sea entrance and a permanent halocline (Rodhe, 1998; Stigebrandt, 2001). The temperature is dominated by the ocean–atmosphere heat exchange, with 14–16°C difference between summer and winter surface temperatures and extensive sea ice in winter (Jacob & Omstedt, 2005). On long time scales, the Baltic Sea is in balance with the World Ocean and the atmospheric forcing. The time scale for this is about one year for heat, and thus temperature, and 30 times longer for salinity (Stigebrandt & Gustafsson, 2003; Omstedt & Hansson, 2006). There are large natural interannual variations in temperature and salinity, which makes the detection of climatic trends difficult. The sea surface temperature was high in the 1940s and has been rising since the late 1980s, with an increase of 1°C from 1990 to 2005 and the largest increase in summertime (Feistel et al., 2008; Belkin, 2009). The salinity has been affected by two stagnation periods in the last century, in the 1920s–1930s and in the 1980s–1990s, both times resulting in long periods with decreased salinity (The BACC Author Team, 2008).

The North Sea can be split into 3 regions; the shallow, tidally mixed southern and eastern part, the central part with a summer thermocline and salinity above 34, and the Norwegian Trench including the Skagerrak with inflow of high-saline oceanic water and outflow of diluted Baltic Sea water (Dietrich, 1950; Rodhe, 1998; Otto et al., 1990; Janssen, Schrum, & Backhaus, 1999). When looking at long-term variations, the "Great Salinity Anomaly" in the late 1970s stands out with unusually low salinity (Danielssen, Svendsen, & Ostrowski, 1996). As for the Baltic Sea, a sea surface

temperature increase has been observed in recent years (Belkin, 2009; MacKenzie & Schiedek, 2007a; Wiltshire & Manly, 2004).

Thus the transition zone connects two very different oceanographic areas, creating a dynamic zone with large fluctuations in currents and salinity (Bendtsen, Gustafsson, Söderkvist, & Hansen, 2009). The average condition is a two layer system, with outflowing Baltic Sea water in the surface, inflowing oceanic water in the deeper layer, and dilution throughout the transition zone (Højerslev, 1989; Rodhe, 1998). The salinity changes are often concentrated in 1–2 fronts, one located around the Kattegat–Skagerrak boundary, and the other in the Danish straits. Also, a baroclinic eddy has been observed in the Kattegat (Jakobsen, 1997; M. H. Nielsen, 2005). The inflow of high salinity, oxygen-rich water to the deep parts of the Baltic Sea is limited by the topography of the Danish straits, and occurs in inflow events. The largest inflows are driven by wind and river runoff generated differences in sea level between the Skagerrak and the Arkona Basin. These occur in fall and winter, and are rated according to their strength and duration (*e.g.* Matthäus & Franck, 1992; Feistel et al., 2008). In recent years (2002, 2003), baroclinic summer inflows have also been detected. These are generated by a combination of the density driven currents and tides, and occur in connection with long periods of stabile weather. They can be detected as extended periods with high salinity at the Darss Sill and warm water in the deep parts of the Gotland Deep (Feistel et al., 2008). Monitoring data for the transition zone show rapidly increasing temperatures the last 10 years, and an increasing stratification, both because of larger differences between surface and bottom salinity and because of a larger warming in the surface than in the bottom layers (Ærtebjerg, 2007; Jensen et al., 2008).

Historic observations of sea temperature and salinity, made on a daily basis from a dense network of lightships and coastal hydrographic stations, give a detailed picture of the physical state of the transition zone. The lightship observational program ran from the 1890s to the withdrawal of the ships in the 1970s, and data have been digitized from 1931 onwards. The coastal stations also have data for recent years, with temperature measurements up to today, and the observations at Drogden, first from a lightship, later from a permanent, open water platform, have been digitized from 1900 to 1998. Data from individual stations have been investigated in numerous studies (*e.g.* Pettersson, 1931; Svansson, 1975; Stigebrandt, 1984), while long-term multi-station studies have been limited, most likely by the amount of work required to analyze paper records of data.

Here the cross-station mean and long-term and seasonal variability in temperature and salinity are investigated for climate signals and to allow for model validation. Special attention will be paid to the transition zone stratification, which is important for the bottom oxygen contents, and the visualization of inflows to the Baltic Sea. Parts of the materials in this Chapter have been published in Madsen and Højerslev (2009), which is available in Appendix B.

4.2 Material

The study area is heavily loaded with ship traffic, and the systematic use of light towers for navigational purposes was initiated in 1560. From 1829, this system was supplemented by semi-stationary lightships in places where light towers could not be established, and most of these anchored ships have made oceanographic observations from 1875 onwards. The ships were withdrawn in the 1970s and 1980s (Hahn-Pedersen, 2003).

The Danish lightship data, located at DMI, have been digitized from 1931 and onwards (Sparre, 1984), and are available for scientific use. Earlier data can be found in Nautical-Meteorological annuals of the Danish Meteorological Institute. The digital data includes vertical profiles of temperature and salinity, waves, and surface currents, all with daily resolution (measured at 7 or 8 a.m. local time), as well as synoptic observations[6] measured six times a day. Data from Swedish ships are currently being digitized by SMHI (Jan Szaron, pers. comm.). Vertical profiles of temperature and salinity, as well as currents at the surface and at one deep level, are available at variable temporal resolution (sub-daily to monthly), with some time series going back to 1924. Table 5 gives an overview of the available data.

Besides the lightships, temperature and salinity have also been measured daily at Danish coastal stations, but only at the surface. DMI has paper records of these data in the Nautical-Meteorological annuals back to 1873, and digitized data going back to 1931 (Table 6, Andersen, 1994). Before 2000, the stations were regularly maintained and both temperature and salinity measurements were of similar quality as the lightship data; hereafter the stations were replaced by automatic stations where only the temperature measurement is reliable.

Many temperature and salinity measurements have been made from scientific cruises, ships of opportunity and other non-permanent platforms. These data are collected at ICES (The International Council for Exploration of the Sea, `www.ices.dk`), and were compiled in a climatology by Janssen et al. (1999). Today, the open water observational network for temperature and salinity in the transition zone is made up of this type of data, as well as German moorings at Kiel, Fehmern Belt, Darßer Schwelle, and Arkona Becken (`www.bsh.de/de/Meeresdaten/Beobachtungen/MARNET-Messnetz`), a few buoys, satellite measurements of sea surface temperature, and ferrybox data.

The lightship-based observational network was dense in the transition zone (Fig. 9), with much fewer stations in the Skagerrak and the surrounding seas. The number of observing lightships with digitized data is maximal (12–14) in the 1930s, 1950s and 1960s, whereas the number of observing coastal stations remains between 9 and 14 from 1931 to 1999 (Fig. 10). Note that the Drogden Station started as a lightship, but was replaced by a permanent station in 1937. This record is digitized from 1900

[6] The synoptic observations include air temperature, wind speed and direction, cloudiness, precipitation type, and sight.

Table 5: Station list – Lightships. Station number 7–11 were Swedish, all other were Danish. See also Figure 9.

St. num.	Start date	End date	Lat.	Lon.	Name	Small moves
07	1923-09-01	1951-08-31	56.1167	16.5667	Ölands Rev	
08	1923-01-01	1972-11-30	55.3000	12.7833	Falsterbo Rev*	
09	1923-01-01	1961-12-12	55.5833	12.8500	Oskarsgrundet	
10	1923-01-01	1960-10-05	56.1667	12.5167	Svinbådan	
11	1948-01-01	1969-11-09	57.1667	11.6667	Fladen	
6037	1931-01-01	1977-09-02	57.7667	10.7333	Skagens Rev	1945-09-04, 1955-01-01
"	1977-09-03	1979-10-09	57.7833	10.7667	" *	
6047	1931-01-01	1943-04-13	57.4733	11.3350	Læsø Trindel*	
"	1943-04-14	1945-04-11	57.5150	11.2600	" *	
"	1945-08-23	1961-12-31	57.5333	11.3417	Læsø Nord	1949-01-01
"	1962-01-01	1975-09-03	57.5333	11.3417	"	
"	1975-10-05	1977-11-24	57.4667	11.4167	Læsø Trindel*	
6057	1931-01-01	1943-03-31	57.2133	10.6933	Læsø Rende	
"	1943-04-01	1962-02-06	57.2083	10.7333	"	1945-09-01, 1949-01-01, 1955-01-01
"	1962-02-07	1965-11-30	57.2000	10.7333	"	
6067	1931-01-01	1942-12-31	56.9733	10.8950	Østre Flak*	
"	1943-01-01	1973-02-28	56.8500	10.8000	Aalborg Bugt	1945-09-05, 1949-01-01, 1956-01-01, 1960-01-01
6077	1931-01-01	1944-12-31	56.1483	11.1867	Schultz's Grund	
"	1945-01-01	1971-09-03	56.1000	11.1500	Kattegat SW	1949-01-01, 1956-01-01, 1960-01-01
6087	1931-01-01	1945-04-22	56.7667	11.8633	Anholt Knob	
"	1945-09-01	1948-08-20	56.7500	11.9917	"	
"	19480821	1961-12-31	56.8500	11.8000	Anholt Nord	1949-01-01
"	1962-01-01	1975-03-09	56.8500	11.8000	"	
"	1975-03-10	1985-08-08	56.7500	11.8833	Anholt Knob	
6097	1961-01-01	1969-07-31	55.4000	6.9500	ER	1966
6107	1931-01-01	1939-12-31	55.3667	7.6833	Vyl	
"	1945-01-01	1948-12-31	55.4000	7.6167	" *	
"	1949-01-01	1975-03-06	55.4000	7.5667	"	1961
"	1975-03-07	1980-04-15	55.5667	7.3333	Horns Rev*	
6127	1931-01-01	1973-08-31	55.3367	11.0467	Halsskov Rev	1949-01-01, 1950-12-08, 1955-02-01
6147	1931-01-01	1939-12-31	54.4533	12.1833	Gedser Rev	
"	1945-01-01	1955-04-18	54.4200	12.1467	" *	
"	1955-04-19	1976-03-31	54.4533	12.1833	"	
"	1976-04-01	1979-01-24	54.7833	12.7500	Kadetrenden*	
"	1979-01-25	1988-12-12	54.8000	12.7833	Møn SE*	
6148	1987-07-01	1988-01-31	54.6167	11.0167	Femernbælt*	
6157	1966-01-01	1975-03-03	56.2500	12.2500	Kattegat Syd	
6167	1931-01-01	1969-06-30	56.0667	12.6333	Lappegrund	19390116, 19510421
6183	1900-01-01	1937-06-12	55.5333	12.7167	Drogden Fyrskib	
"	1937-06-13	1998-09-30	55.5333	12.7167	Drogden Fyr	

*Not used for isopleths

Table 6: Station list – Danish coastal based stations. See also Figure 9.

St. num.	Start date	End date	Lat.	Lon.	Name
Maintained stations (temperature and salinity)					
20098	1939-01-01	1990-03-27	57.4333	10.5667	Frederikshavn
20108	1990-04-01	1995-08-31	57.4833	10.5667	Hirsholm
22160	1931-01-01	1985-04-30	56.1000	10.5167	Sletterhage
26458	1931-01-01	1967-05-31	54.9333	10.0500	Mommark
26478	1931-01-01	1999-04-30	54.9167	9.7833	Sønderborg
27022	1990-10-01	1999-02-28	56.7167	11.5167	Anholt
28118	1931-01-01	1999-04-29	55.5167	9.7333	Middelfart
28548	1931-01-01	1952-10-22	54.7333	10.7167	Keldsnor
"	1952-10-23	1999-04-15	54.7500	10.6667	Bagenkop
29007	1991-02-01	1999-03-27	56.0000	11.2833	Gniben
29008	1931-01-01	1942-01-03	55.9667	11.8500	Hundested
"	1942-04-06	1999-04-30	55.9500	11.7667	Rørvig
29118	1931-01-01	1983-12-31	55.7000	11.0333	Refsnæs
30332	1936-01-01	1983-03-29	55.7000	12.6000	Langelinie
30342	1931-01-01	1999-03-31	55.7167	12.6667	Middelgrundsfortet
31062	1931-01-01	1999-04-30	55.2500	12.3833	Rødvig
31248	1931-01-01	1990-01-31	54.9500	12.4667	Klintholm
31308	1931-01-01	1937-09-26	55.0000	11.8833	Masnedø
"	1939-01-21	1988-09-26	54.9667	11.8833	Storstrøm
"	1988-12-01	1998-09-30	54.9500	11.9833	Farø
31572	1931-01-01	1999-12-31	54.6500	11.3500	Rødbyhavn
32002	1931-01-01	1998-05-31	55.3167	15.1833	Christiansø
Automatic stations (temperature)					
21009	1999-01-21	-	57.1167	8.6000	Hanstholm
23293	2002-08-28	-	55.5667	9.7500	Fredericia
25149	1999-11-16	-	55.4667	8.4333	Esbjerg
26457	2002-10-01	-	55.0000	9.9833	Fynshav
28234	1999-12-01	-	55.2833	10.8333	Slipshavn
29393	2000-10-12	-	55.3333	11.1500	Korsør
30017	2000-06-21	-	56.1000	12.4667	Hornbæk
30336	1999-06-24	-	55.7000	12.6000	København*
31573	1999-11-30	-	54.6500	11.3500	Rødby*
31616	2001-11-23	-	54.5667	11.9333	Gedser
32048	2001-06-20	-	55.2500	14.8333	Tejn

*Continuation of maintained station

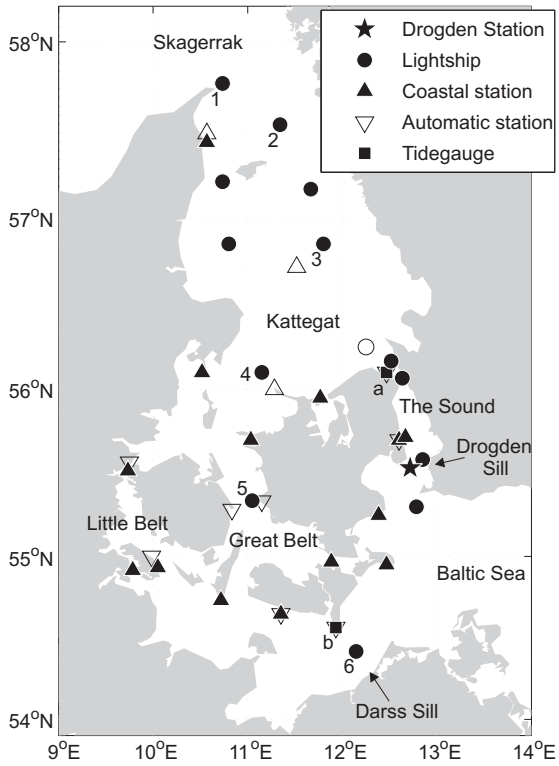

Figure 9: Map of lightships and coastal stations in the transition zone. See also Table 5 and 6. Stations with data available during the 1951 inflow, described in Chapter 4.7, are marked with filled marks, other stations have open marks. The lightships used in Fig. 20 are marked with numbers: 1) l/s Skagens Rev, 2) l/s Læsø N, 3) l/s Anholt, 4) l/s Kattegat SW, 5) l/s Halsskov Rev, 6) l/s Gedser Rev. The tide gauges are a) Hornbæk and b) Gedser. The Drogden Station consisted of a lightship until 1937, where it was replaced by a permanent station.

to 1998, thus making it the longest digitally available high resolution sea temperature and salinity record in the area.

The lightships were withdrawn in case of sea ice. Therefore many of the records lack data in cold winters. However, this is not the case for Drogden, since this station was maintained even in icy conditions (Sparre, 1984).

The measurements are generally expected to have accuracies of 0.2°C and 0.1 for temperature and salinity, respectively (Andersen, 1994). However, errors and complications are introduced, most importantly because of uncertainties in the depth determination for below-surface data (especially in case of strong currents), changes in instrumentation and personnel, and re-deployment of the lightships at new sites. Also, the coastal stations have mostly been placed in harbors. The monthly mean surface temperature and salinity records were compared with data from neighboring

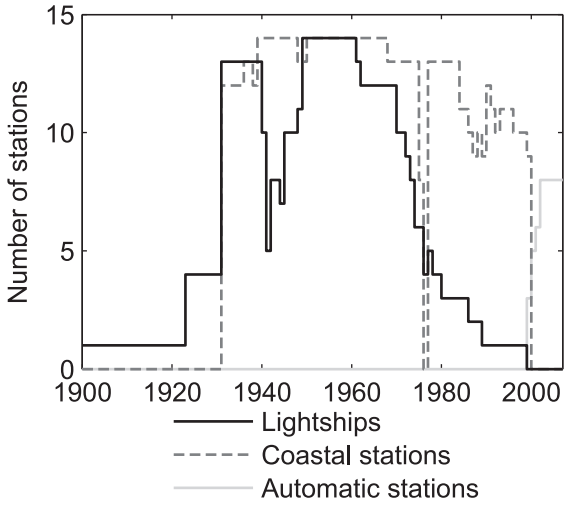

Figure 10: Number of lightships, coastal stations, and automatic stations per year. Note that the Drogden Station is counted as a lightship.

stations and with data available from ICES (`www.ices.dk/ocean`), and it was found that the salinity values agree very well, while some of the coastal data show a larger seasonal cycle in temperature than off-coast measurements.

4.3 Spatial patterns

To investigate the geographical distribution of temperature and salinity and compare the lightship data with the climatology of Janssen et al. (1999, hereafter denoted the Janssen climatology), the monthly mean lightship data at 5 and 25 m, averaged over the whole observational record, was calculated for each ship. The depths were chosen to match the climatology, and they represent the surface and bottom water, respectively, in the transition zone. In the Janssen climatology, the 5 m data represents data measured at 0–10 m depth, and the 25 m data represents data measured at 20–30 m depth. In the following, the mean values, as well as the months with minimum and maximum values, are compared. When examining the minimum and maximum values, it should be noted that especially the transition zone, salinity is much more variable than what is reflected in a climatology, see Chapters 4.6 and 4.7.

The mean 5 m temperature in the whole transition zone is close to 9°C; at 25 m it increases from 7 to 9°C from the Baltic Sea to the North Sea (Fig. 11). Many of the lightships show surface temperatures that are 0.2–0.3°C cooler than the Janssen climatology; this may be due to differences in the sampling period. The 25 m tem-

perature shows 0.4°C lower temperatures at lightships in southern Kattegat than the climatology, but better agreement in the rest of the area.

The minimum temperature at 5 m increases from 2°C around Bornholm to 4°C in the western Skagerrak. In the transition zone, the minimum is seen in February, whereas March is the coldest month in surrounding parts of both the North Sea and the Baltic Sea. The lightship data are in general 0.5–1°C colder than the Janssen climatology. At 25 m the Janssen climatology shows a clear separation of the Baltic Sea water, which has almost the same minimum temperature as the surface water, and the Skagerrak and the Kattegat, where the minimum is 4–5°C. That is, the relatively warm North Sea water is dominant in the deep Kattegat. Again, the lightships show cooler temperatures than the climatology. The minimum 25 m temperature occurs in March except in the coastal regions close to the Danish straits, where it is in February. At l/s Kattegat Syd, a cold finger reaches deep water in May (see isopleth in electronic supplement).

The maximum temperature at 5 m is higher in the transition zone than in the surrounding seas, with temperatures up to 17–18°C in August. A gradient is seen across the Kattegat, with slightly colder maximum temperature in the western part than in the eastern and southern part, corresponding to the difference between inflowing Skagerrak water and outflowing water from the Danish straits. The east–west difference is about 0.6°C for the lightships, the gradient is slightly less steep in the Janssen climatology. The 25 m maximum temperature is 13–14°C in the Kattegat. At l/s Skagens Rev and l/s Læsø Nord, this is reached in August; in the more wind protected southern Kattegat it is not reached until October.

The mean, minimum, and maximum salinity as calculated from the monthly climatology are shown in Figure 12. The field is dominated by the strong salinity gradient from the Baltic Sea to the North Sea. At 5 m, the 8-isohaline contour runs through the Arkona Basin, close to 13.0°E, 13.7°E, and 14.0°E for the minimum, mean, and maximum climatological salinity respectively, and the 24-isohaline moves from the northern to the central Kattegat. Thus, there is a mean change in salinity of 16 through the transition zone. In the Kattegat, the isohalines are tilted towards northeast, indicating how the outflowing Baltic Sea water tends to stay along the Swedish coast, and the water running through Øresund is on average fresher than through the Great Belt. The overall agreement between the Janssen climatology and lightship observations is fairly good, but the tilt in the Kattegat is steeper in the climatology than in the lightship observations. At 25 m's depth, the Arkona Basin and the Kattegat salinities are very different, with 8–10 in Arkona Basin and 30–33 in the Kattegat. Whereas the surface water shows a gradual change, the subsurface water is fairly uniform in each basin, except that there are signs of inflowing high salinity in the very western part of the Arkona Basin in mean and maximum salinity situations.

The timing of minimum and maximum salinity (electronic supplement) is more patchy than for temperature. In the 5 m layer, the lowest salinity is seen in May and

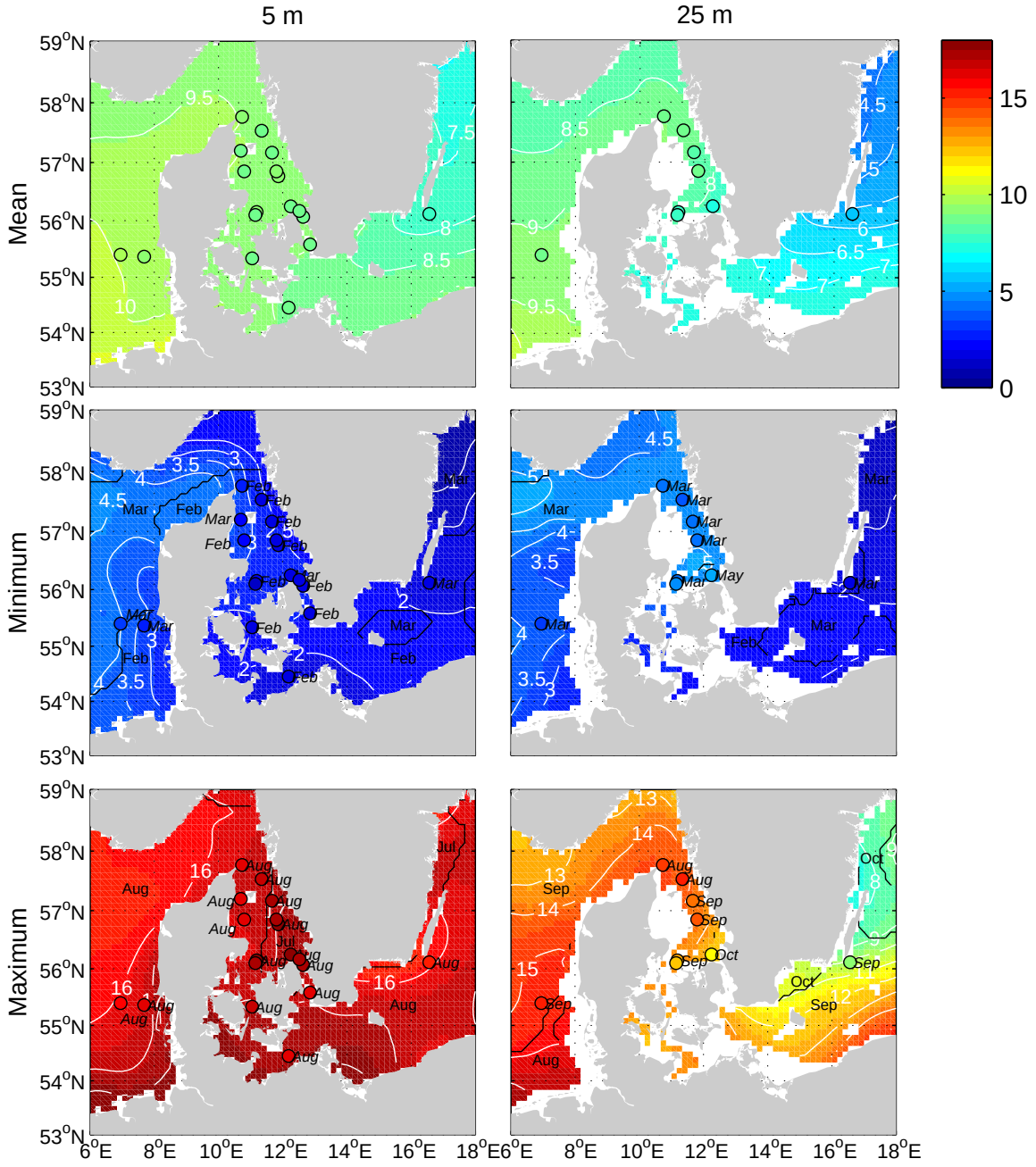

Figure 11: Climatological temperature and monthly mean lightship temperatures (colored dots). Top is mean, middle is minimum and bottom is maximum. Left is 5 m, right is 25 m. The black curves in the minimum and maximum plots show the month of the extremum, and the italic month names indicate the month of extremum in the lightship observations.

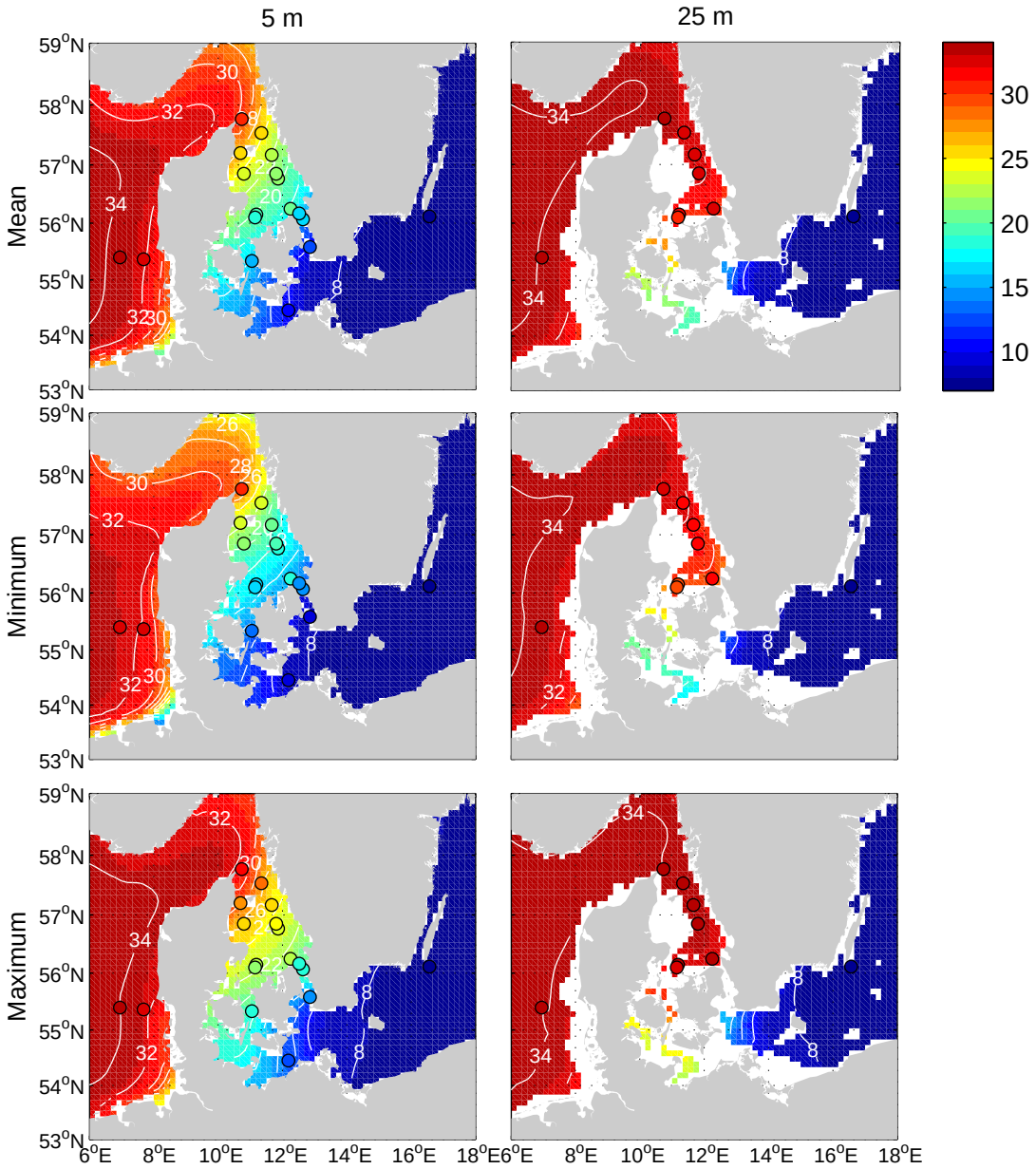

Figure 12: Climatological salinity and monthly mean lightship salinities (colored dots). Top is mean, middle is minimum and bottom is maximum. Left is 5 m, right is 25 m.

June in the transition zone and the Skagerrak, but in late summer both in the North Sea and the Baltic Sea. At l/s Skagens Rev, the seasonal variability in salinity at 5 m is close to zero, and the minimum in March and maximum in April is considered noise, see isopleth in the electronic supplement. The surface measurements have a minimum in May and maximum in fall and winter. At 25 m, the month of minimum salinity is not well-defined, but there is a tendency for maximum salinity in April around l/s Skagens Rev, in May in central Kattegat, and in June in the southern Kattegat and the Great Belt (see also Chapter 4.5).

Overall the agreement between lightship data and the climatology is good, and most differences can be explained by different sampling periods. However, the 5 m salinity was found to be too smooth in the climatology, especially in the Kattegat. Thus, the lightship salinity data underlines the findings of M. H. Nielsen (2005) that there is an anticyclonic circulation in the Kattegat. The lightships also give a more detailed picture of the vertical structure of the water column than the climatology, see Chapter 4.5.

4.4 Long-term variability

The Drogden Station measurements constitute an almost continuous 98 year long time series of daily direct surface temperature and salinity measurements at a fixed location. The only major change was the shift from lightship to permanent station in 1937, and the only large data gaps were during the second world war and in 1976. From these data, the annual mean values were calculated, requiring at least 250 measurements per year (Fig. 13). To investigate the long-term development, the 10 year centered running mean surface temperature and salinity were calculated from the annual mean data. The 10 year average length was chosen to filter out short-term variability while maintaining as narrow filtering window as possible; a 15 year filter was tested with much the same results but less information in the ends of the time series. In the calculation, single missing years were allowed. The 10 year running mean temperature from the Langelinie coastal station in the northern harbor of Copenhagen follows the Drogden data closely, with a warm bias of 0.4°C (Fig. 13). The modern automatic station Copenhagen is located at the same location as the Langelinie station, and it has monitored the temperature the last 10 years. These data, corrected for the 0.4°C bias, are used to extend the mean temperature curve to the present. The salinity (Fig. 14b) and seasonal temperature (Fig. 14c) records have not been extended in this way. To support the analysis of the observations from Drogden Station, similar calculations were made for all other stations (Figs. 14a and b), and for air temperature measurements from the station at Landbohøjskolen, Copenhagen, Denmark (55.6°N, 12.7°E, Fig. 14a). Similarly to the temperature time series extension in the Copenhagen area, there is a continuous series of data from the coastal station in Rødby, and a time series has been constructed from coastal Great Belt stations (Keldsnor,

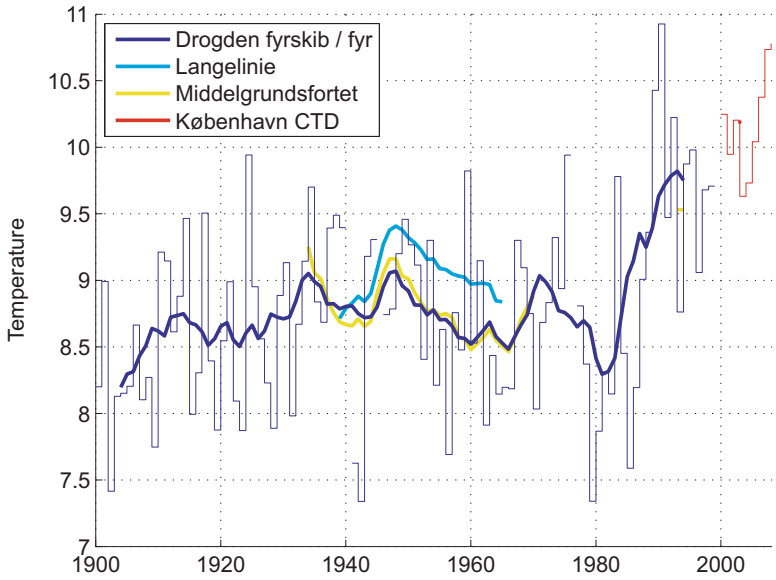

Figure 13: Annual mean (staircase) and 10 year running mean (solid curves) surface temperature from stations in the Copenhagen area.

Bagenkop, and Slipshavn). The Great Belt series has a greater uncertainty than the two other series since it is combined from stations with different locations and no overlapping measurements. The extensions have not been made for salinity or for the seasonal temperature records.

Many stations have experienced moves on the order of a few kilometers. To compensate for this effect, and allow for comparison between stations, the climatological mean value (Janssen et al., 1999) was subtracted from the salinity data, but not from the temperature data, where the spatial variation in this area is much smaller. In Figure 14c, the mean value for each season has been subtracted to allow comparison.

The running mean temperature at the Drogden Station varied between 8.2 and 9.1°C during 1905–1985 with no significant trend, then rising to 9.8°C in 1992 (Fig. 14a). The change between the 1950–1985 mean temperature and the 1988–1997 mean temperature is statistically significant at the 99.5% level. With the extension with data from the Copenhagen station, it is seen that this high level has been kept since. The large increase is also seen in reconstructed time series from Rødby and the Great Belt, though the timing varies with a few years. The overall temperature signal is also seen in data from the other stations during the time they have data, and is thus assumed representative for the transition zone. The running mean air temperature shows a trend of 1.0°C per century for the time period 1904–1985, while only 0.1°C per century for the Drogden Station record. Despite of this, the correlation coefficient between the two records is 0.80.

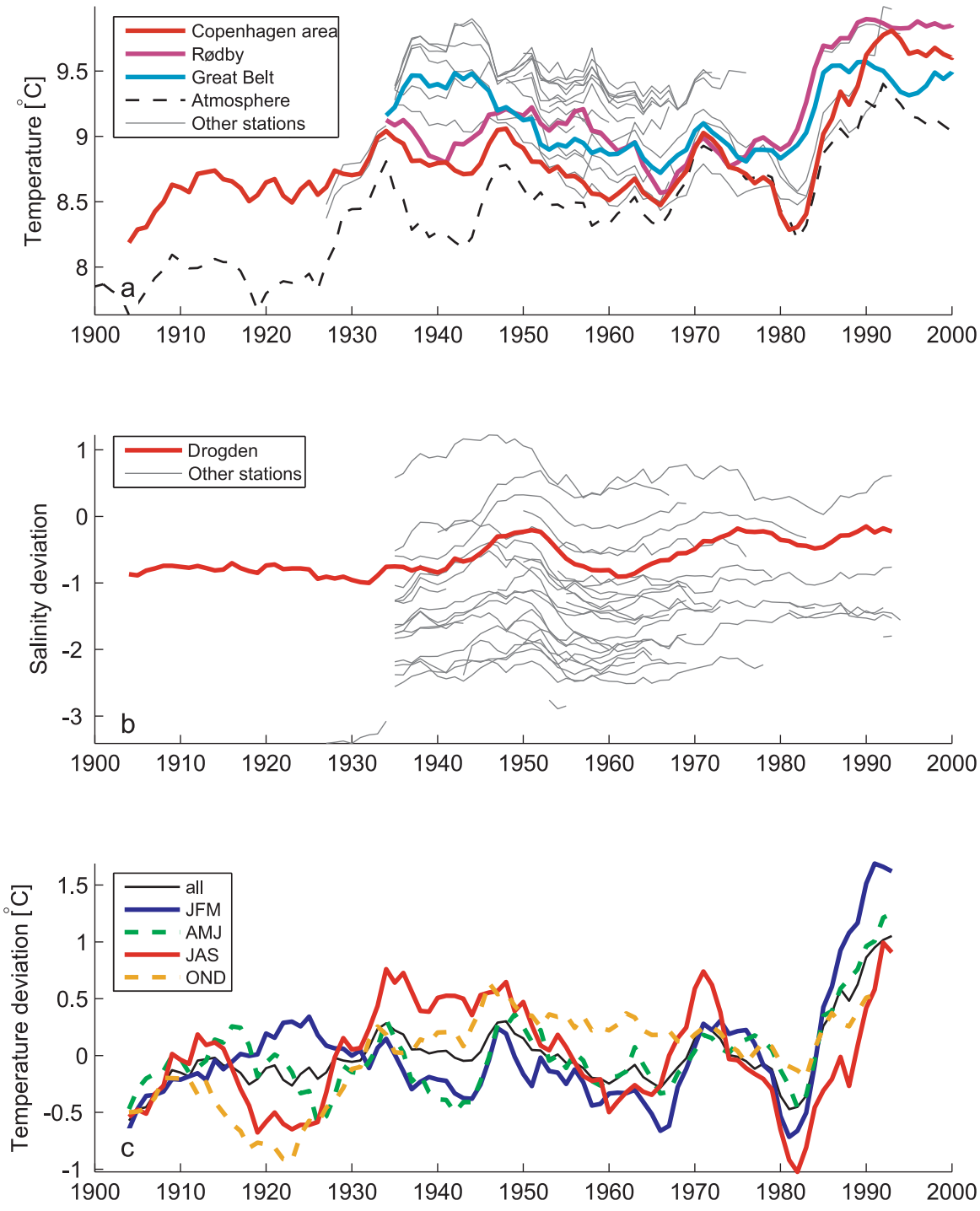

Figure 14: 10 year running mean surface data. a: temperature. b: salinity deviations from climatology. c: seasonal temperatures at the Drogden Station (January–March, April–June, July–September, and October–December), deviations from seasonal mean.

The change in temperature towards the end of the 20th century is largest in the winter and spring, whereas the summer and fall signals only are slightly larger than variations earlier in the century (Fig. 14c).

The Drogden Station running mean salinity record varies within 0.85 throughout the century (Fig. 14b). The salinity is generally high around 1950 and from 1975 onwards, but with no large change towards the end of the time period. Again, data from the other stations support this.

The temperature increase detected here agrees with the findings from the Baltic Sea and the Danish monitoring network (Feistel et al., 2008; Jensen et al., 2008; Belkin, 2009), and the long data records show how large and unusual this warming signal is. The differences in the timing of the warming at Drogden, Rødby and in the Great Belt will not be speculated here, but it should be noted that the monitoring data from the Danish straits also show low temperatures in the 1980s and rapid warming in the early 1990s, while coastal stations in the same study only show the 1990s warming (Ærtebjerg, 2007).

4.5 Seasonal variability – a lightship climatology

The seasonal variations at each lightship were investigated through the 10 day running climatological mean[7] of temperature, salinity and density, and the corresponding standard deviation. The density was calculated with Rich Pawlowicz's Oceans Toolbox for Matlab (`ftp://acoustics.whoi.edu/ pub/Matlab/oceans/`) from the equation of state (UNESCO, 1981). Data records were split when ships were renamed or otherwise moved significantly, and short time series were discarded. However the following moves have been ignored: l/s Læsø Rende, 2.6 km in 1943/1962; l/s Anholt Knob, 8.0 km in 1945; l/s Vyl, 8.8 km reallocation after World War 2. The station positions and data periods are shown in Table 5.

There is a strong seasonal variation in temperature at all lightship locations, with surface summer maximum in the transition zone of 16–18°C and winter minimum of 2°C.[8] Examples of isopleths for l/s Gedser Rev, l/s Halsskov Rev, and l/s Fladen are seen in Figure 15, isopleths from other stations are available in the electronic supplement. The warm summer temperatures extend to the bottom at all stations with a small dampening. The deepest measurements in the transition zone are made at l/s Kattegat SW, l/s Fladen, l/s Læsø Nord and l/s Skagens Rev (38–40 m), and here the bottom temperatures reach 12–14°C, with a surface to bottom delay of 1–2.5 months, increasing towards south. Similarly, the winter minimum is transferred downwards, this process is somewhat faster. The standard deviation shows that the

[7]The climatological mean is here defined as the average over years for the same time of year.

[8]The winter minimum may have a small warm bias due to the withdrawal of ships in icy conditions.

main variation is in the depth of the summertime halocline. At l/s Gedser Rev, the standard deviation shows that the thermocline does not always exist.

If this propagation of heat from surface to the deep layers could be seen as a case of one-dimensional heat diffusion, the vertical turbulent mixing coefficient could be calculated as (Aas, 1986):

$$T(z,t) = T_0 + \frac{T_H - T_0}{H} z + T_1 \exp(-\alpha z) \cos(\sigma t - \beta z - \varphi)$$

where T_0 and T_H are the mean surface and bottom temperatures, H is the depth, T_1 and φ are the amplitude and phase of the surface seasonal cycle, $\sigma = 2\pi/\text{one year}$, and $\alpha \approx \beta$ are linked to the diffusion coefficient A through the relations

$$A = \frac{\sigma}{2\alpha^2} \text{ and } A = \frac{\sigma}{2\beta^2} \quad .$$

However, several issues complicate the calculations. The surface water down to about 10 m is wind mixed, so these data should be disregarded. Also, a strong halocline may hinter the turbulent heat diffusion. By using data from 20 m and below (the typical halocline depth is 10–15 m), values of $10^{-3} - 10^{-4}$ m^2/s were obtained through a least square fit to the lightship data. These simple calculations do not take the strong advection in the transition zone into account, and are thus only valid if the rough assumption is made that the advected water column is horizontally uniform on the time scale of the calculation.

For salinity, the dominant feature is the increasing salinity from the Baltic Sea to the Skagerrak and from surface to bottom. The temporal variability in salinity in the transition zone is large, with a standard deviation of up to 6 at l/s Halsskov Rev and the stations in the Sound, but when looking at the climatological mean, some distinct seasonal patterns are seen (Fig. 16). The Baltic Sea river runoff peaks in late spring (Chapter 5.4), and the outflowing fresh water creates a minimum in the summer time, peaking in early May at l/s Gedser Rev and late May at l/s Fladen, and staying low over the summer. The low summertime salinity is mainly seen in the top 10 m of the water column, and here the standard deviation is relatively low, so this is a persistent phenomenon. In deeper parts, a peak in salinity is seen in May–June in the Kattegat, and around July 1 at l/s Halsskov Rev. The occurrence of the high salinity water is very likely (low standard deviation), but the depth of the halocline, especially in May and June, shows a large variability. A bottom layer maximum of 20 is seen at l/s Gedser Rev in August. This also shows a large variability, so that bottom water salinities of 24 are within one standard deviation of the mean in July and August.

Observations show that baroclinic summer inflows have not occurred during the lightship observational period, except for year 1959 and maybe 1947 (Feistel et al., 2008). However, the lightship observations show that the bottom summer water at

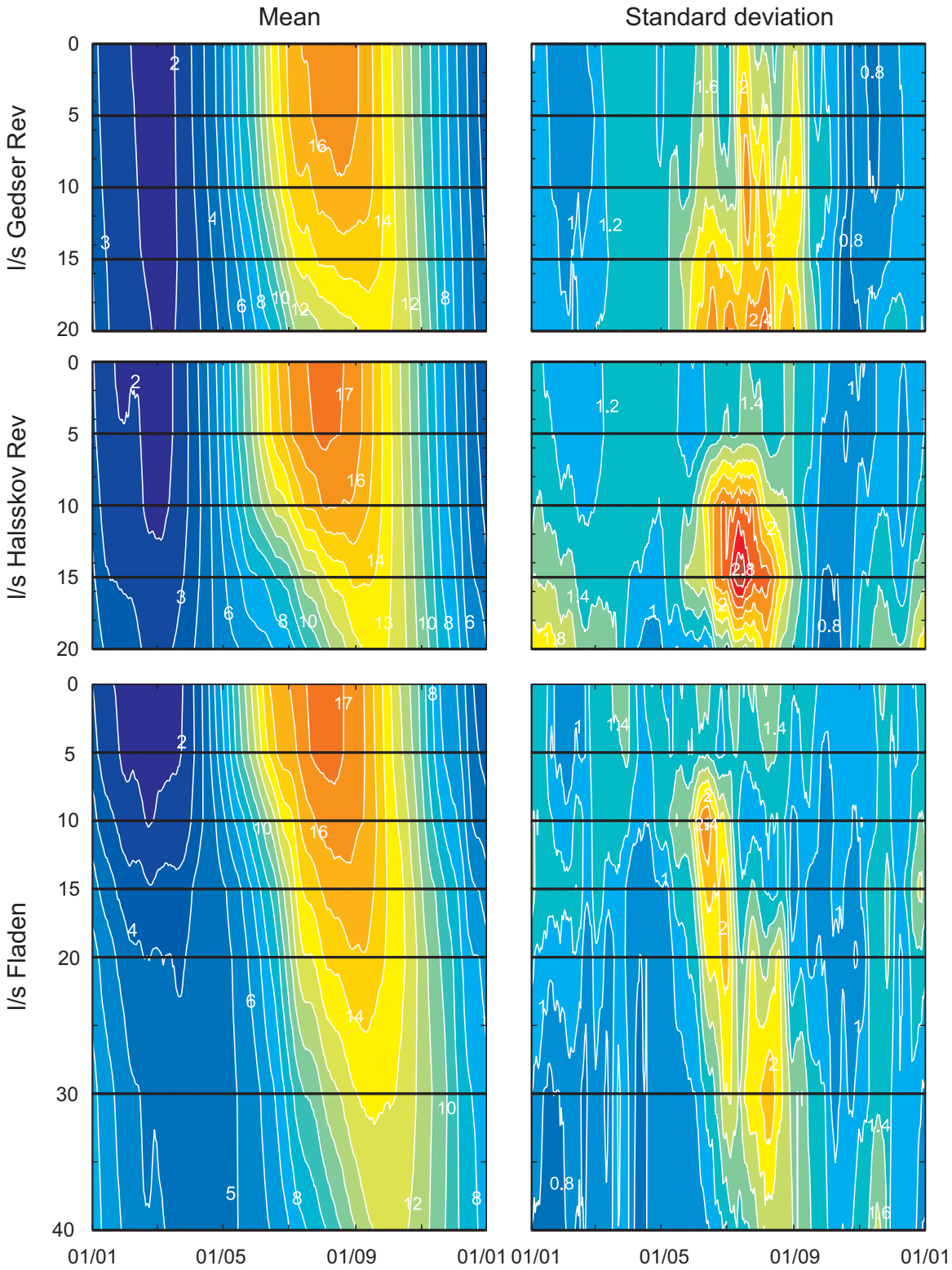

Figure 15: Isopleths of observed seasonal temperature variations (°C as a function of the time of year and depth [m], 10 day running mean) from l/s Gedser Rev (top), l/s Halsskov Rev (middle), and l/s Fladen (bottom). Mean values left and standard deviations right.

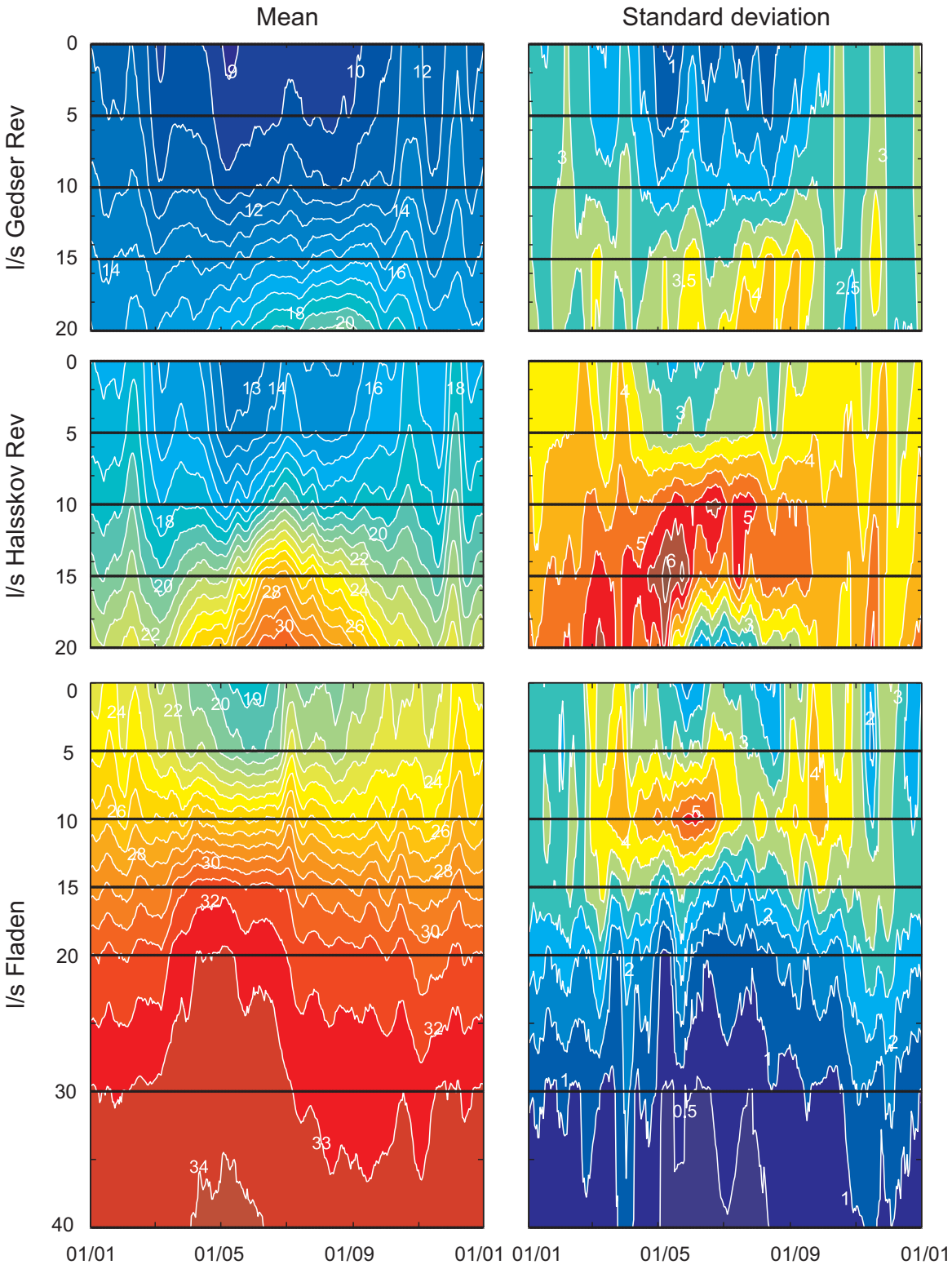

Figure 16: Isopleths of observed seasonal salinity variations (as a function of the time of year and depth [m], 10 day running mean) from l/s Gedser Rev (top), l/s Halsskov Rev (middle), and l/s Fladen (bottom). Mean values left and standard deviations right.

l/s Gedser Rev can be of high salinity, and thus it seems reasonable that even small changes towards more stable summer weather can trigger the inflows.

The density field (Fig. 17) is dominated by the salinity, so in the climatological average, the water column is stratified throughout the year at all transition zone stations with water depths of more than 10 m. Typical density differences between surface and bottom are 5–12 kg/m^3. However, the seasonal variations in both temperature and salinity affect the density field, so the lowest deep water density is seen at the same time as the temperature maximum (early fall), and the strongest stratification occur in early summer, when the surface salinity is low and the summer heating has not yet propagated to the deep water. The standard deviation of the density follows the standard deviation of the salinity very closely, that is, the largest variability in the stratification is linked to the variable halocline depth in early summer.

The density variations give rise to variability in the steric height, which can be calculated as

$$\begin{aligned} h_{steric} &\equiv \rho_0 \int \left(\frac{1}{\rho(T(z), S(z), P(z))} - \frac{1}{\rho_0} \right) dz \\ &= \int \frac{\rho_0 - \rho(T(z), S(z), P(z))}{\rho} dz \\ &\approx \int \frac{\rho_0 - \rho(T(z), S(z), P_0)}{\rho_0} dz \end{aligned}$$

where $\rho_0 = \rho(T = 0, S = 35, P_0)$ is the reference density and P_0 is the surface pressure. This formula gives the local steric effect. When an area with varying depth experiences a homogene change in density, this formula will show a large response in places with large water depths. However, a dynamic adjustment will take place, and on the small scales described here, the adjustment can be assumed instantaneous. If the water depth at the time of the measurements was known and taken into account, and the measurements were detailed enough vertically, the adjustment would thus be accounted for in the observations. However, this is not the case, and the following calculations should therefore only be seen as first order calculations.

If looking at the thermosteric effects only, that is, $h_{thermo} \approx \int \frac{\rho_0 - \rho(T(z), 35, P(z))}{\rho_0} dz$, the seasonal cycle is well defined, with an amplitude of 1–4 cm and a peak in late August at all stations. However, the halosteric effect, $h_{thermo} \approx \int \frac{\rho_0 - \rho(0, S(z), P(z))}{\rho_0} dz$, shows variability with an amplitude of 5–10 cm at the typical time scale of salinity variations (5–10 days), and if a harmonic fit is made, the amplitude is less than 2 cm. Thus steric effects are of some importance to the variability of the sea surface height in the transition zone, but the main variability occurs on the time scale of the salinity variations and not seasonal.

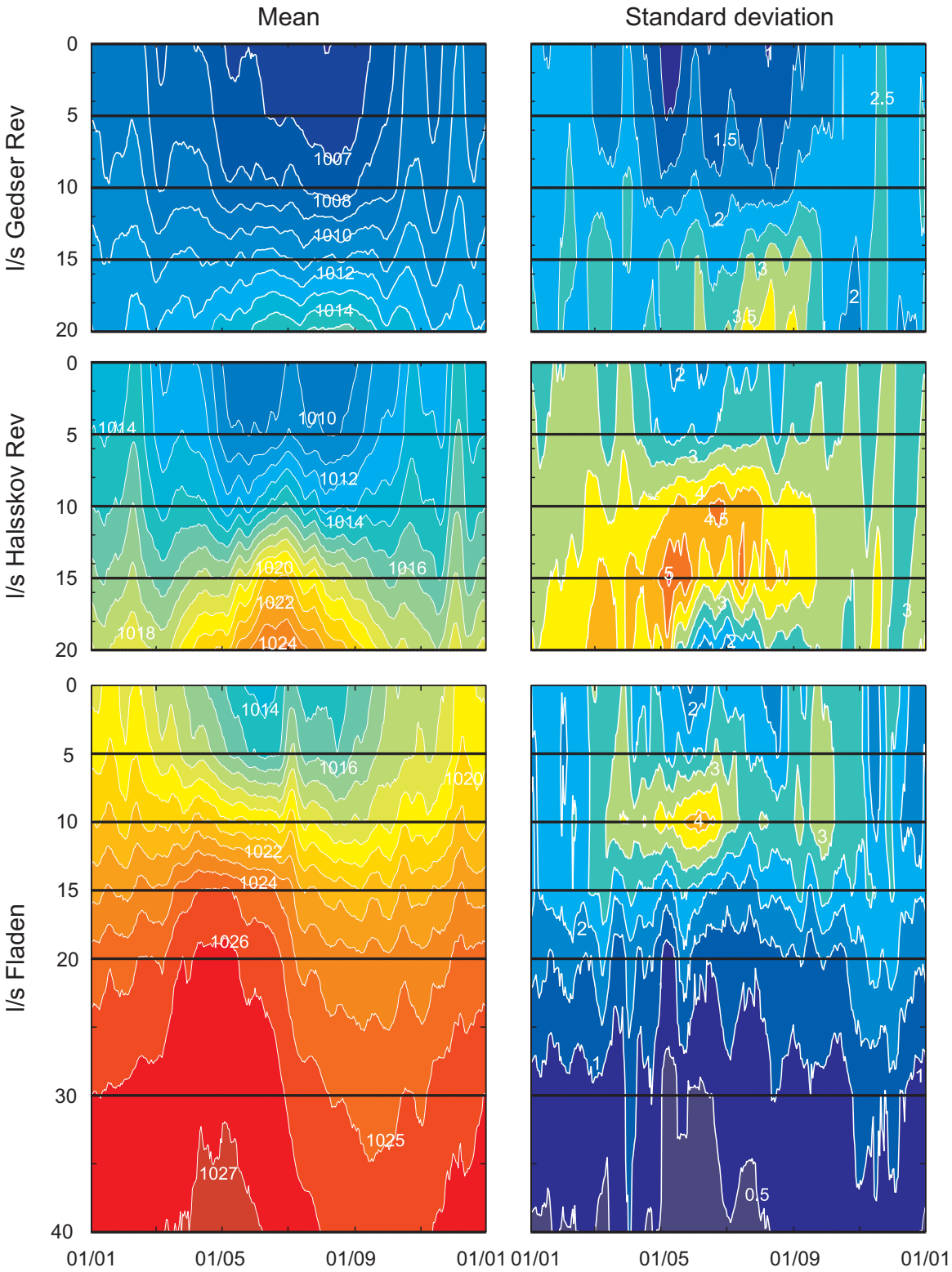

Figure 17: Isopleths of observed seasonal density variations (kg/m^3 as a function of the time of year and depth [m], 10 day running mean) from l/s Gedser Rev (top), l/s Halsskov Rev (middle), and l/s Fladen (bottom). Mean values left and standard deviations right.

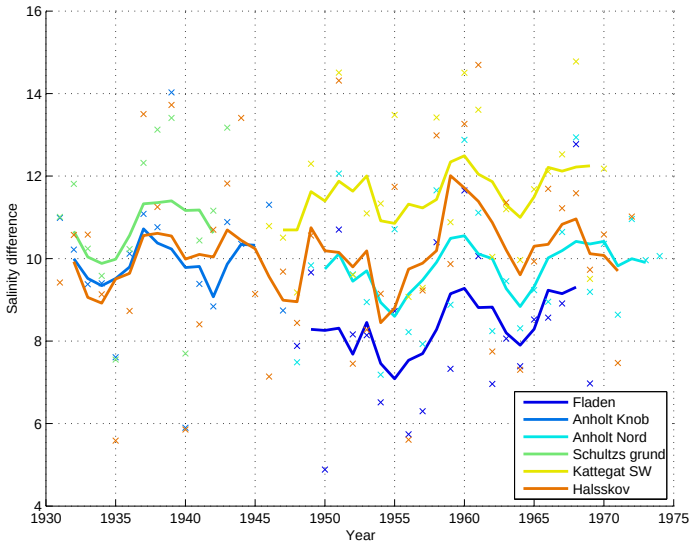

Figure 18: 5 year running mean August–October salinity difference between 5 and 20 m at selected lightships in the Kattegat and the Great Belt.

4.6 Late summer stratification

The late summer stratification in the transition zone, especially in the Great Belt, is important for the bottom oxygen conditions (Bendtsen et al., 2009). The strength of the stratification can be measured by the difference between surface and deep water density. Alternatively, since the vertical density structure in this area largely depends on salinity, the difference between surface and deep water salinity has been used as a simple measurement of the stratification by the Danish National Environmental Research Institute (NERI), and was used here to allow comparison.

For this study the salinity difference between 5 m and 20 m depth was used, since these depths are on opposite sides of the pycnocline when it is present (see Chapter 4.5), and there are measurements from most lightships at these depths. The four lightships l/s Halsskov Rev, l/s Schultz Grund/Kattegat SW, l/s Anholt Knob/Nord and l/s Fladen were used.

The single year mean and 5 year running mean salinity difference averaged over the months August–October is shown in Figure 18. It should be noted that within this 3 month period, large variations in the stratification can occur, and there is a tendency for stronger stratification in the beginning of the period (Fig. 16 (middle), page 41). An example of the variability is shown for year 1951 in Figure 19.

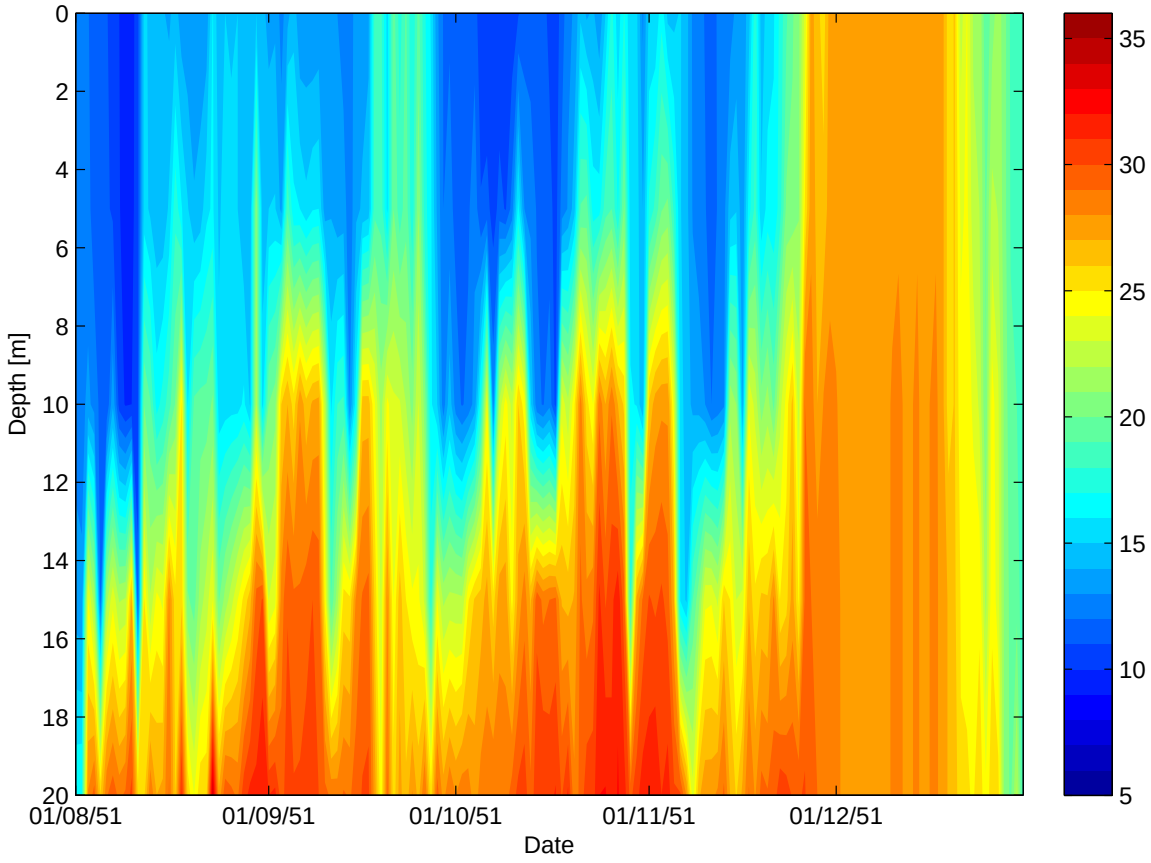

Figure 19: Isopleth of the daily salinity measurements from l/s Halsskov Rev August 1 to December 31, 1951.

The 5 year running mean salinity difference shows decadal variations, with the largest values at l/s Halsskov Rev around 1960, 2 units above the average. Any trend in the data is masked by the large interannual variations.

The 1931–1970s stratification investigated here shows smaller variations than results for recent years, where a 4 units peak has been shown around year 2000 in the northern Great Belt (Jørgen L.S. Hansen, pers. comm.). This indicates that the long period with increased late summer stratification around year 2000 in the Great Belt is unusual, and, together with changing nutrient loadings, is connected to the large oxygen depletion event in 2002 (Conley et al., 2007).

The daily lightship data also show how variable the Great Belt system is, and thus caution should be taken when working with less frequent, or irregularly timed data, to avoid sampling errors. One possible solution to this could be a data assimilation system (*e.g.* Wilkin et al., 2005).

4.7 The inflow event of 1951

The inflow event of 1951 was the largest observed in the 20th century. It lasted 25 days, from November 25 to December 19, 1951, with a precursory period of 12 days, and was caused by a combination of preceding low sea levels in the Baltic Sea and three weeks of strong westerly winds (Wyrtki, 1954; Matthäus & Franck, 1992; Schinke & Matthäus, 1998).

To illustrate the possibilities with the digital data set, focus was put on the daily salinity measurements at selected depths at 6 lightships for the time period 1 October, 1951 to 1 March, 1952 (Fig. 20), and on all available surface salinity measurements at three selected dates, chosen to show the buildup of the inflow (Fig. 21. An animation of the day-to-day development of the inflow can be found online at `www.gfy.ku.dk/~kristine/publications/ber08_ani.gif`). A two-dimensional linear interpolation between available data has been calculated and is shown with contour curves.

The inflow is also reflected in the water level difference between the two tide gauges in Hornbæk and Gedser (Fig. 22). The two stations are selected to give the best possible estimate of the water level gradient of the narrow parts of the transition zone. Starting from hourly observations (Hansen, 2007), tidal effects were removed by a 25 hour running mean, and the 1900–2000 mean was subtracted to remove differences in reference level.

The salinity data show that the water in the transition zone was stratified before the inflow event (Figs. 19 and 20), with bottom salinities of 33 in the Kattegat, falling to 23 at l/s Gedser Rev and surface salinities rising from 10 at l/s Gedser Rev to 22 at l/s Læsø N. The thickness of the surface layer is not constant, but is in most cases between 8 and 15 m. At l/s Skagens Rev, the water is less stratified, and has a higher salinity.

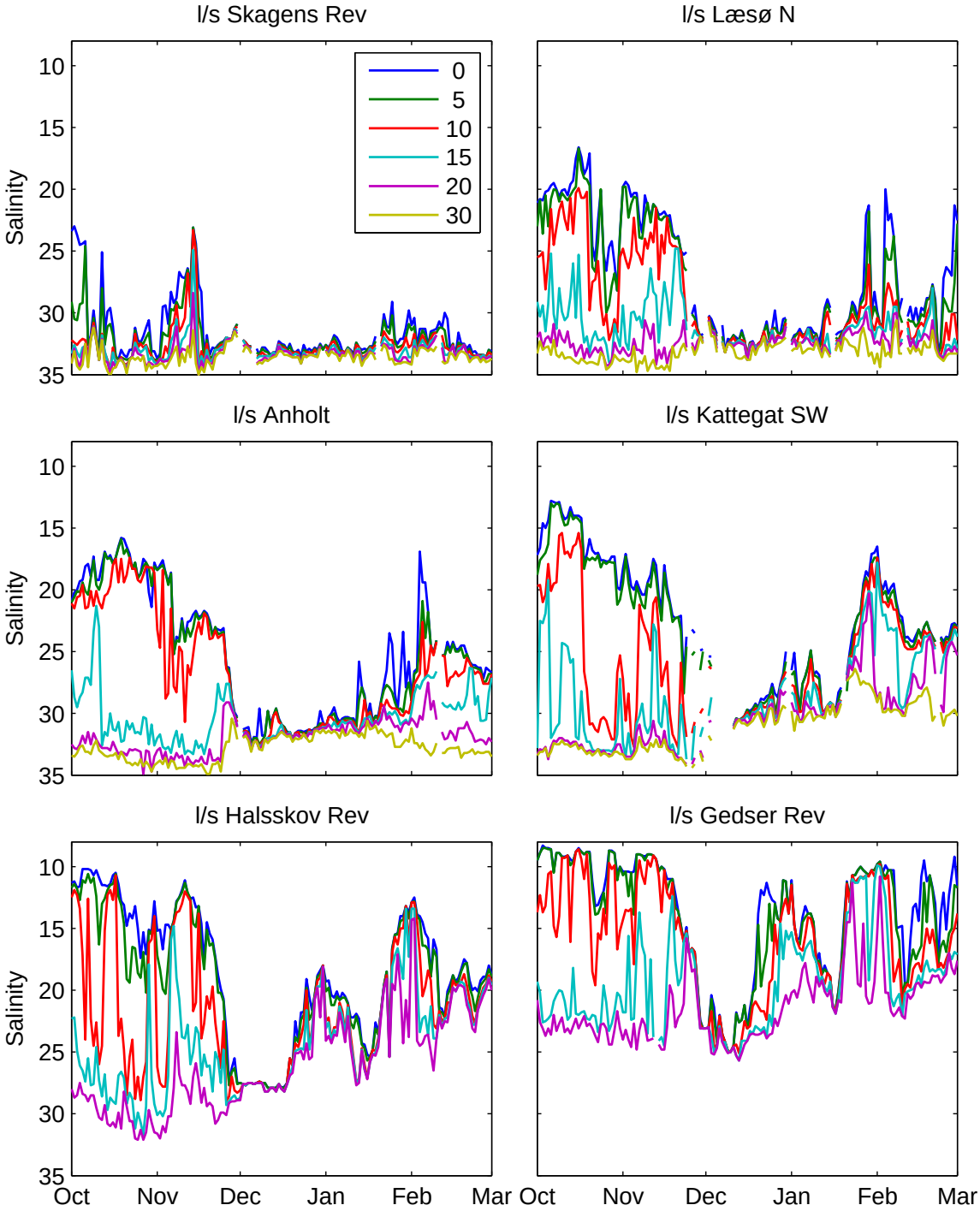

Figure 20: The salinity at six lightships throughout the transition zone at selected depths and for the time period 1 October, 1951 to 1 March, 1952. Note that the y-axis is reversed.

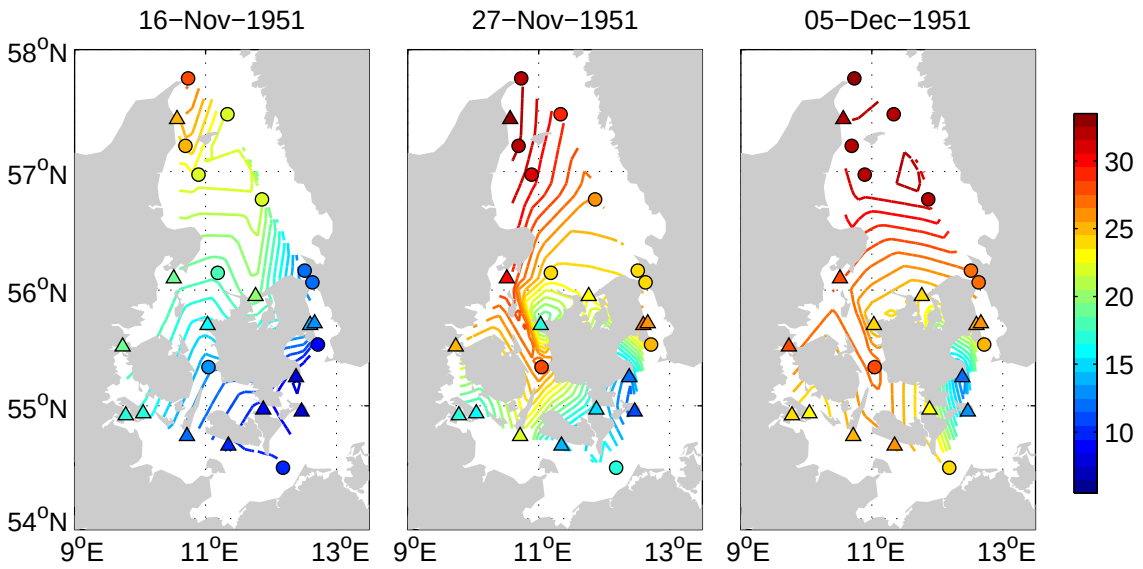

Figure 21: Surface maps of salinity at three selected dates during the precursory and inflow periods with contour curves of interpolated salinities (one salinity unit per curve).

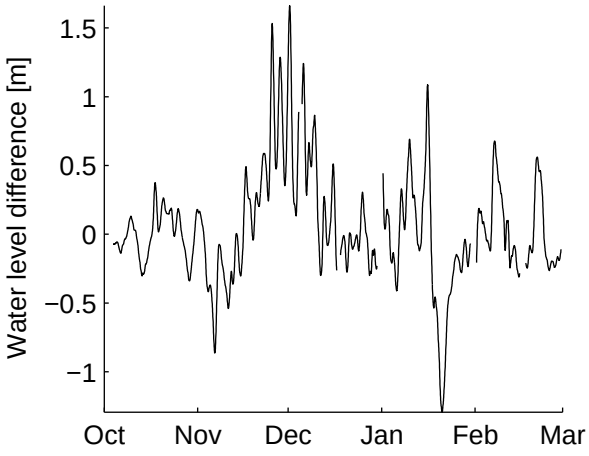

Figure 22: The 25 hour running mean water level difference between the Hornbæk and Gedser tide gauges for the time period 1 October, 1951 to 1 March, 1952. Positive values indicate higher water level at Hornbæk than at Gedser, and thus possibilities for inflow.

The inflow event is clearly seen as a collapse of the stratification, with salinities above 30 in the whole water column in the Kattegat, 27.5 at l/s Halsskov Rev and about 23 at l/s Gedser Rev. These numbers correspond well with the findings of Wyrtki (1954). The salinity at l/s Gedser Rev is approximately the same as that of the water that enters the Baltic Sea, as the station is close to the Darss Sill.

After the inflow, the water is again stratified at l/s Gedser Rev, while it remains mixed in the Kattegat for another month. This makes way for a smaller inflow in the middle of January 1952, and then the stratification is reestablished all the way to l/s Anholt.

This salinity pattern is supported by the surface maps (Fig. 21). On November 16, in the beginning of the precursory period, a normal situation with an increase in salinity from 10 at l/s Gedser Rev to 25 at l/s Skagens Rev is seen. On November 27, the inflow event is in its initial phase, and high salinity water is pressed through the Great Belt and the Sound. On December 5, the inflow is fully developed, with high salinity water all the way to l/s Gedser Rev.

The inflow signal is also clearly seen in the water level measurements, with a water level up to 1.66 m higher in Hornbæk than in Gedser and a mean water level difference of 0.50 m during the 25 day inflow period. This is a large deviation compared to the 30 cm mean sea surface topography difference between the central Baltic Sea and the Skagerrak (Ekman & Mäkinen, 1996) and to the standard deviation of the year 1900–2000 time series of 0.34 m. A simple estimate of the resulting current velocities can be made based on the assumption of a one layer channel flow with friction (Stigebrandt, 1980). According to this, the velocity is

$$u = \sqrt{\frac{2g}{1 + \frac{2kL}{H}} \Delta\eta} \tag{3}$$

where g is gravity acceleration, k is a drag coefficient, L and H are the channel length and depth, and $\Delta\eta$ is the water level difference between the ends of the channel. Stigebrandt uses $g = 9.8$ m/s^2, $k = 0.003$, $L = 40$ km, and $H = 20$ m, resembling the Great Belt system. With this, the mean and maximum inflow speeds in our case are estimated to 0.9 m/s and 1.6 m/s respectively.

5 Model description

The DMI-BSHcmod model is a 3D primitive equation ocean model developed for regional ocean modeling, especially of the North Sea–Baltic Sea area (Kleine, 1994; Dick et al., 2001). It was developed at Bundesamt für Seeschifffart und Hydrographie (BSH) in Hamburg, Germany, and further development and updating of the code has taken place at DMI. It is used operationally at both BSH and DMI for ocean forecasts, especially for storm surge warnings, and in various national and international research projects. In the following, DMI-BSHcmod will be denoted cmod for short.

5.1 Setup, physics, and numerics

The cmod model is characterized by its 2-way nesting system, which allows for higher resolution in the North Sea–Baltic Sea transition zone than in the rest of the model area. Therefore, it offers a much better description of the water exchange between the North Sea and the Baltic Sea than could be obtained with the same computational effort and no nesting, and model boundaries in the transition zone are avoided. This naturally gives a better description of the transition zone, but also of the Norwegian Coastal Current in the North Sea and of the water exchange to and from the Baltic Sea.

The model code is based on the shallow water equations set in horizontal spherical coordinates and a vertical z-coordinate system, assuming hydrostatic balance and the Boussinesque approximation (*e.g.* Cushman-Roisin, 1994). This implies volume conservation instead of mass conservation, which again means that steric effects will not be reflected in the sea surface height.

The current model setup is chosen to be as close as possible to current DMI standards, as used in the EU FP6 project Mersea project (`www.mersea.eu.org`). The model uses a k-omega turbulence scheme and includes a simplified thermodynamic sea ice module. The surface heat flux is parameterized using bulk quantities of both the atmosphere and the ocean (or sea ice) surface. In previous model versions, and for operational purposes, precipitation is not included, and the evaporation flux is only taken into account in the heat budget calculations. For the current simulations, a new module has been developed to include the evaporation-precipitation balance regarding water volume and salinity. The new scheme is based on the simple assumptions that evaporation and precipitation consist of fresh water, and that the precipitation has the same temperature as the surface water (Gosnell, Fairall, & Webster, 1995). A further simplification is that the module ignores any sea ice. This assumption is necessary with the current sea ice model, since the sea ice module does not communicate changes in water volume and salinity with the ocean model.

For use in climate change experiments, the model has been changed to expect a 360-day year, with 30-day months. This is common standard in climate modeling.

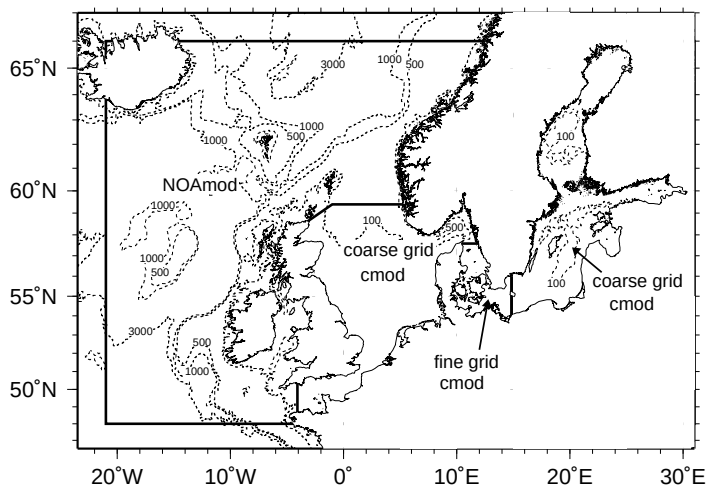

Figure 23: Map of the cmod and NOAmod model areas.

Table 7: Ocean model grids.

	Longitude	Latitude	Horiz. res.	No. of z-layers
Fine grid	9.35°E–14.85°E	53.59°N–57.59°N	1 nm	52
Coarse grid	4.08°W–30.25°E	48.45°N–65.85°N[a]	6 nm	50
NOAmod grid	21.08°W–13.25°E	48.2°N–66.3°N	6 nm	1

[a] 59.25°N in the North Sea

The changes are mainly a matter of bookkeeping in the date string routines. However, an adjustment of the calculation of tides and surface heat flux should have been implemented, and it is recommended for future experiments. Since this has been overlooked in the current simulations, an abrupt change in the tidal boundary conditions in the North Sea is seen on January 1 of every model year. The problem has been analyzed, and all effects decayed quickly, and disappeared within about 36 hours. All affected data were left out of the further analysis. The surface heat flux calculation skips 5–6 days in the end of December when calculating the solar height. This is not visible in the model results, but may cause a small warm bias.

The model is set up with a 1 nm horizontal model resolution in the transition zone (fine grid), see Figure 23 and Table 7. In this domain, the surface layer is 2 m thick; the following layers are 1 m thick down to 30 m, then 2 m thick to the deepest layer at 76 m. Figure 33 (page 70) shows an example of a small area of the grid. In the North Sea–Baltic Sea area (denoted the coarse grid), the horizontal resolution is 6 nm (about 11 km). The surface layer is 8 m thick to avoid complete drying, even in areas with large tides. The following layers are 2 m thick down to 80 m, then stepwise increasing to 50 m thick layers. To provide realistic sea level boundary conditions for the open boundary in the North Sea, a 2D barotropic version of the model, NOAmod,

Table 8: Overview of performed model simulations. In the v10 scenario run, both the precipitation and the other atmospheric forcing were taken from the S12 scenario, whereas the F12 control run precipitation was used for v12.

Name	Atm. forcing	Precip. forcing	Spin-up period	Simulation period
Control run	F12	F12	$1960 \times 2\frac{5}{12}$	1960–1990
Scenario run v10	S12	S12	$2070 \times 2\frac{5}{12}$	2070–2100
Scenario run v12	S12	F12	$2070 \times 2\frac{5}{12}$	2070–2100

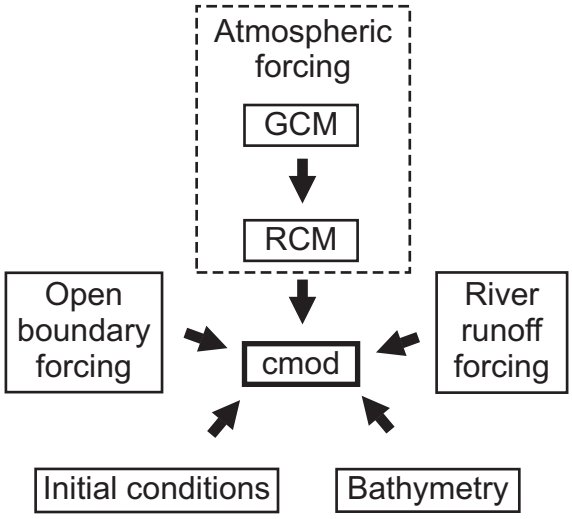

Figure 24: Overview of required input to cmod for climate simulations.

has been set up for the North East Atlantic. It has the same horizontal resolution as the coarse grid, but only one layer in the vertical.

The bathymetry of the Danish straits is very complex, with deep and narrow channels that are important for the inflow to the Baltic Sea, and these features cannot be fully resolved in the 1 nm model grid. Therefore, the grid has been optimized to contain the deep channels and still be volume-conserving (She, Berg, & Berg, 2007).

An overview of cmod model simulations used in this thesis is provided in Table 8.

5.2 Atmospheric forcing

The climate simulations described in this thesis can be seen as the third link in a chain of models. First, a global circulation model (GCM) is used to make simulations of past and future climate. Then a regional atmospheric climate model (RCM) is used to downscale the results dynamically, in the current example to the European area. Thirdly, the ocean model receives the atmospheric forcing from the RCM (Fig. 24).

The GCM used for this experiment is the Hadley Centre model HadAM3H (Jones, Murphy, Hassell, & Taylor, 2001). It is a 1.875°×1.25° global atmospheric model which has been run from 1960 to 1990 (control run) and from 2070 to 2100 (scenario run). For the scenario run, the IPCC SRES A2 emission scenario was used (Nakicenovic et al., 2000). The ocean sea surface temperature and sea ice extend were prescribed from observations in the control run, and for the scenario, the modeled changes from a coarser ocean-atmosphere GCM, HadCM3, were added to the observations.

The model has been validated for the European area and showed a reasonable location of the Icelandic storm track and seasonal mean land surface temperatures within 3°C of observations. As to changes in the scenario simulations, the GCM shows a deepening of the cyclonic anomaly centered over the northern North Sea during winter, an increase in temperature rising from 2°C over the North Atlantic towards east in the winter and south east during summer, with maximum changes of more than 7°C (Jones et al., 2001).

The HadAM3H simulations, as well as other GCM datasets, have been used extensively to force different RCMs for the European area within the EU project PRUDENCE (Christensen, Carter, Rummukainen, & Amanatidis, 2007, and other papers in this special issue). It has been found that HadAM3H gives a strong bias over the Baltic Sea when used as forcing for atmosphere-only RCMs, because the Baltic Sea is not properly resolved in the underlying HadCM3 model. This was solved by the Swedish Rossby Centre by using an RCM with a coupled model of the Baltic Sea, the RCAO model (Räisänen et al., 2004).

The RCM used for the current experiment is the atmospheric DMI HIRHAM RCM with extra high resolution (12 km), forced by the HadAM3H, but with sea surface temperatures over the Baltic Sea from RCAO (Ole B. Christensen, pers. comm.). The temporal resolution of the ocean model input is 3 hours (24 hours for specific humidity). These RCM simulations have been named F12 for the control run and S12 for the scenario run. The main characteristics of the RCM data are analyzed in the following chapters.

5.2.1 Sea level pressure and NAO index

The sea level pressure over the North Sea–Baltic Sea area is characterized by a south east going gradient in fall and winter. F12 shows the largest gradient in the January mean values, with 1007 hPa in the northern parts of the North Sea and the Baltic Sea, and 1015 hPa in the southern parts. During spring and summer, the sea level pressure is more uniform, with a maximum in May of 1014–1015 hPa over the whole sea area (Fig. 25).

When comparing with the ECMWF ERA40 reanalysis data for the same period (`data-portal.ecmwf.int/data/d/era40_mnth` , not shown), the average sea level pressure is very similar. The same gradient is seen in winter, but in ERA40, the

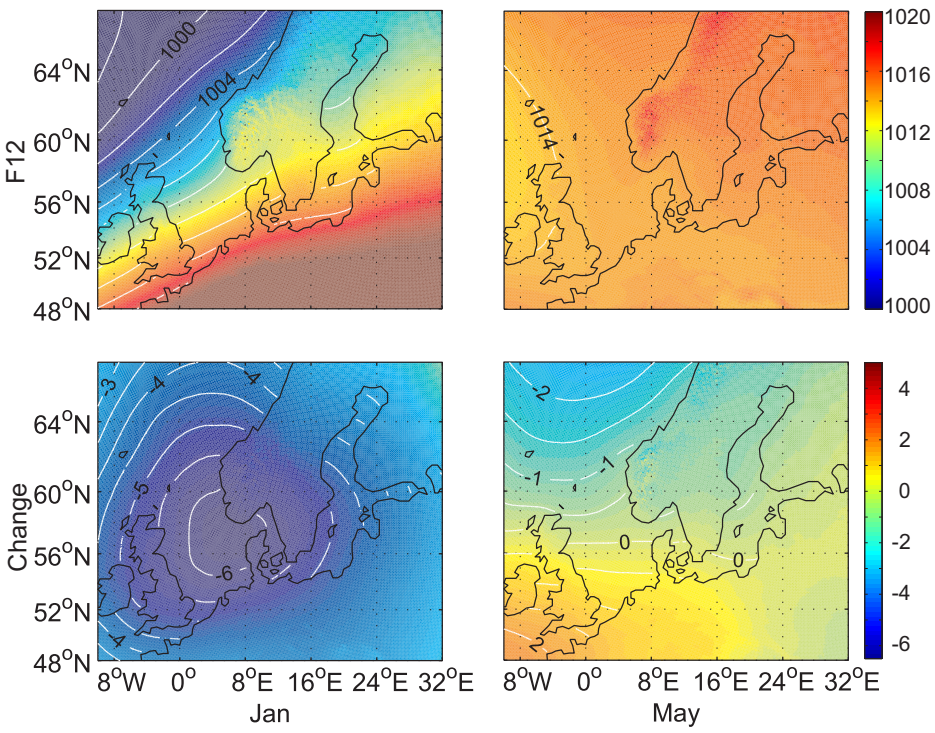

Figure 25: Monthly mean sea level pressure [hPa]. Top F12, bottom change from F12 to S12. Left January, right May.

Baltic Sea gradient is largest in December. A maximum in sea level pressure is also seen in May, of the same magnitude as in F12.

For S12, the total averaged sea level pressure over the area is almost unchanged, but the interannual variability is increased, with annual means varying from 1009 hPa to 1016 hPa. There is also an increased seasonality, with a mean decrease of 6 hPa over the central North Sea in January in agreement with HadAM3H, and a general increase in April, September and November. Other months have more patchy variations (Fig. 25).

The larger-scale state of the atmosphere over north-west Europe is often described by the NAO index. One way of calculating it is by the difference between normalized sea level pressure anomalies in Lisbon, Portugal and Stykkisholmur, Iceland, averaged over December–March (Hurrell et al., 2003, Fig. 26). This method was chosen over a pattern based method, since the HIRHAM model area does not include the whole North Atlantic Ocean.

The NAO index of F12 is lacking the general increase over the modeling period seen in the observational record, and there is no correlation between the two, but if the linear trend of the observational record is removed, the standard deviation of

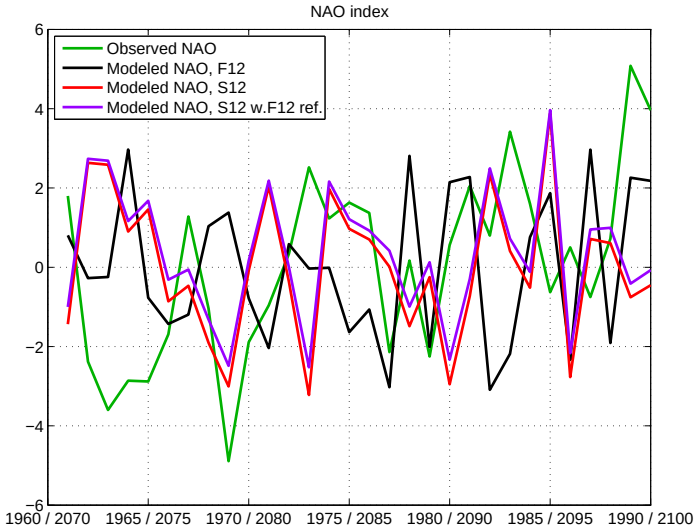

Figure 26: Observed and modeled NAO index, see text for details.

both records is 1.9 units. Thus, the F12 NAO does not resemble the observed interannual variability or the general trend over the modeling period, but the interannual variability has the same magnitude.

The S12 NAO can either be calculated based on pressure data normalized relative to the S12 values or to the F12 values. When the S12 values were used for normalization, the characteristics were almost identical with the F12 values (std. = 1.8), but with no correlation. When the F12 values were used for normalization, the index increased by 0.35 units on average, and the standard deviation was reduced by 0.2 units. This reflects a 1.2 hPa lowering of the Icelandic winter mean pressure and a small decrease in the interannual variability. Positive NAO anomalies lead to a more oceanic climate over southern Scandinavia, with relatively warm, wet, and windy winters.

5.2.2 Wind

Winds over water are generally stronger than over land. The following results are for the 10 m wind over ocean only.

The mean wind speed in F12 is 6–8 m/s over the whole area, and the average direction is from west and north west (Fig. 27). As for air pressure, there is a seasonal variation in the wind, with mean wind speeds of 10 m/s in the North Sea and 8 m/s in the Baltic Sea in December and January. In the summertime, the wind is more uniform over the area, with mean wind speeds of 5–6 m/s in June and July, on average coming from west. Another remarkable feature is a large variability in the mean wind

direction in April, with an average direction over the Baltic Sea and the transition zone from south east.

The monthly maximal wind speed in the control run shows the same seasonality as the mean wind speed, with highest values in December and January and lowest in June and July (Fig. 28). Averaged over the years, the northern North Sea has a January max of 21 m/s, decreasing to 19 m/s in the southeastern North Sea, and 16–18 m/s in the transition zone and the Baltic Sea.

The mean wind speed is within 10% of the climatological values based on observations in the Baltic Sea and the transition zone (Schmager, 2008), but for the maximum wind speeds, the model is missing a gust parameterization. This results in a much too low number of strong wind events, and the observed number of storm events (26 m/s) over the North Sea roughly corresponds to the modeled number of gale events (19 m/s) (Rockel & Woth, 2007). Over open areas in the Baltic Sea, the strongest winds in F12 are 2–6 m/s lower than the climatology of Schmager (2008).

The mean wind speed change between F12 and S12 is close to zero in the central North Sea, increasing to 0.3 m/s in coastal areas and the transition zone, and 0.4 m/s in the eastern part of the Baltic Sea (Fig. 27). However, there is a large difference from month to month. In the winter months, the largest increase is seen over the southern and eastern North Sea, the transition zone, Bothnian Bay, and Gulf of Finland, with average increases up to 1.2 m/s. These changes are very sensitive to the GCM and emission scenario, and the current atmospheric simulations shows relatively small changes (see *e.g.* Woth, 2005). During summer, there is a wind speed increase centered over the central Baltic Sea, with increases of up to 1.3 m/s in July. This is linked to the large temperature gradient between land and sea described below, and it is therefore considered spurious. There is a decrease in wind speed in spring and fall, most noticeable over the North Sea in September.

A general change in wind direction is seen, with winds that are more northerly in winter and more southerly in summer. Most noticeably, the tendency for southeasterly winds over the Baltic Sea in April is less uniform in S12.

The wintertime changes in extreme wind are largest over the North Sea, with a change of 1.5 to almost 2 m/s, or 7-10% (Fig. 28). The spurious summertime changes are also seen in the extreme wind, with an increase of 3 m/s over the Baltic Sea. However, the summer winds are still weaker than the wintertime winds.

5.2.3 Air temperature

The mean 2 m air temperature in F12 increases towards south and west, the modeled annual mean temperature in the Bothnian Bay is 2°C, while it is 12°C over the English Channel (Fig. 29). The seasonal cycle is much larger over the Baltic Sea than the North Sea, with a 24°C change from winter to summer over the Bothnian Bay and only

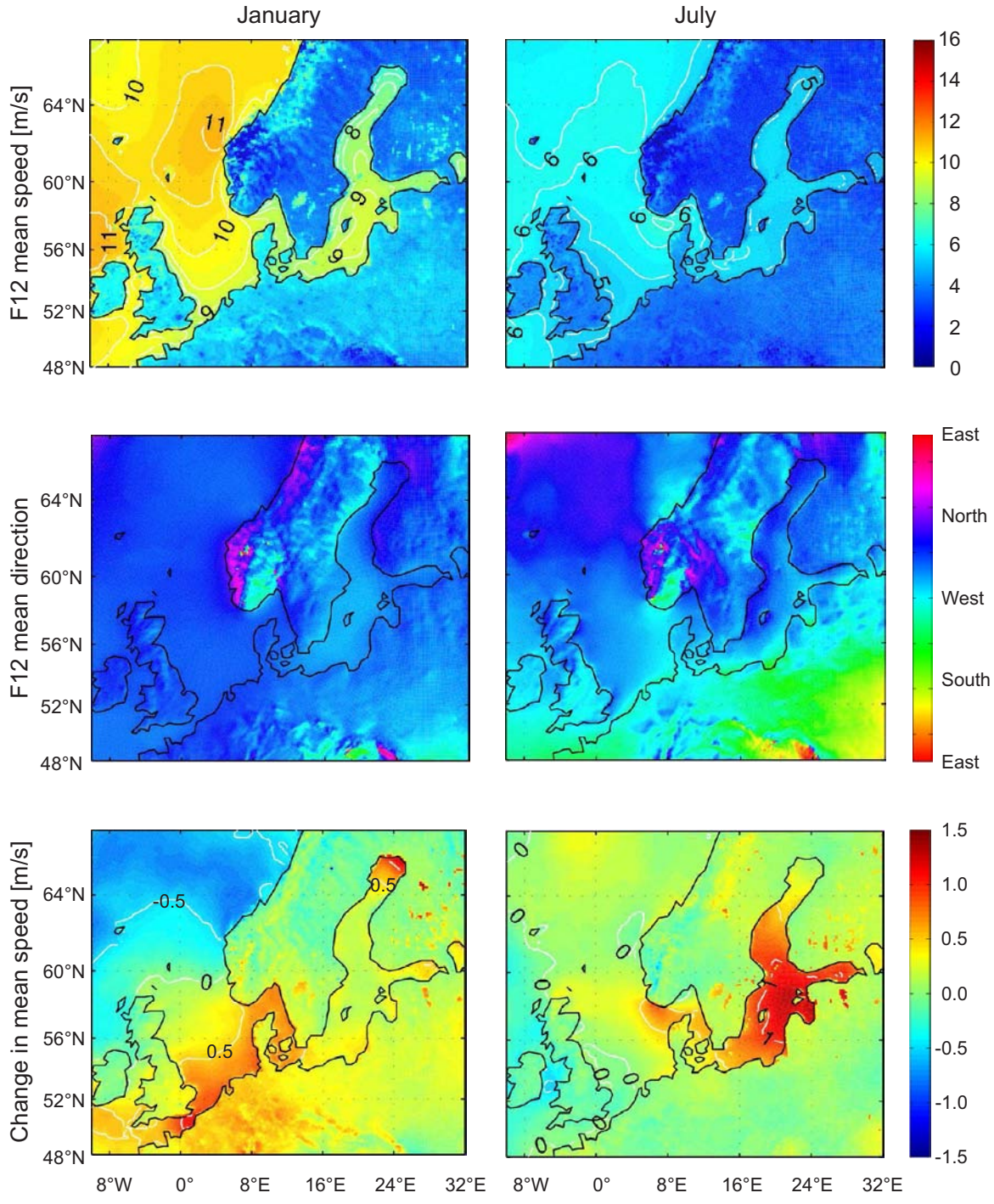

Figure 27: Monthly mean wind. Top: F12 wind speed [m/s], middle: F12 wind direction, bottom: change from F12 to S12. Left: January, right: July. Note that the changes in July are artificial (see text).

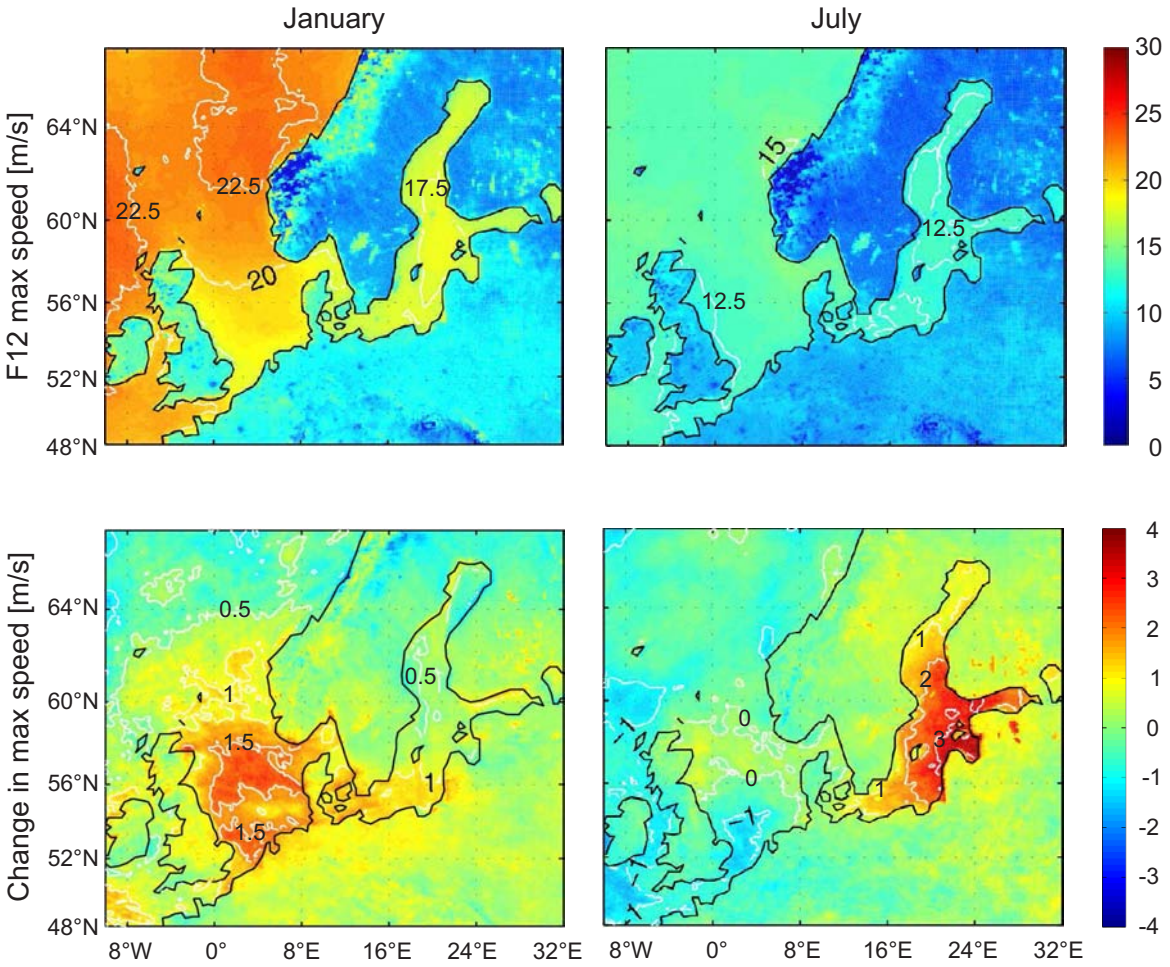

Figure 28: Monthly max wind. Top: F12 wind speed [m/s], bottom: change from F12 to S12. Left: January, right: July. Note that the changes in July are artificial (see text).

7°C in the northwestern North Sea. These results agree very closely with the ERA40 reanalysis results for the same time period, both in mean value and seasonality.

The changes in the air temperature between F12 and S12 are on average 3°C over the North Sea and 4–5°C over the Baltic Sea. There are seasonal variations, but the average change is positive in all months and all locations. The largest increases are seen in the deepest parts of the Bothnian Bay and Gulf of Finland in the wintertime and over the central Baltic Sea in the summer and early fall. The wintertime increase is linked to the reduction of sea ice. The summertime increase is an artifact of the combination of HadAM3H and RCAO forcing, and the larger changes over water than over land must be considered artificial. It creates unwanted effects in wind

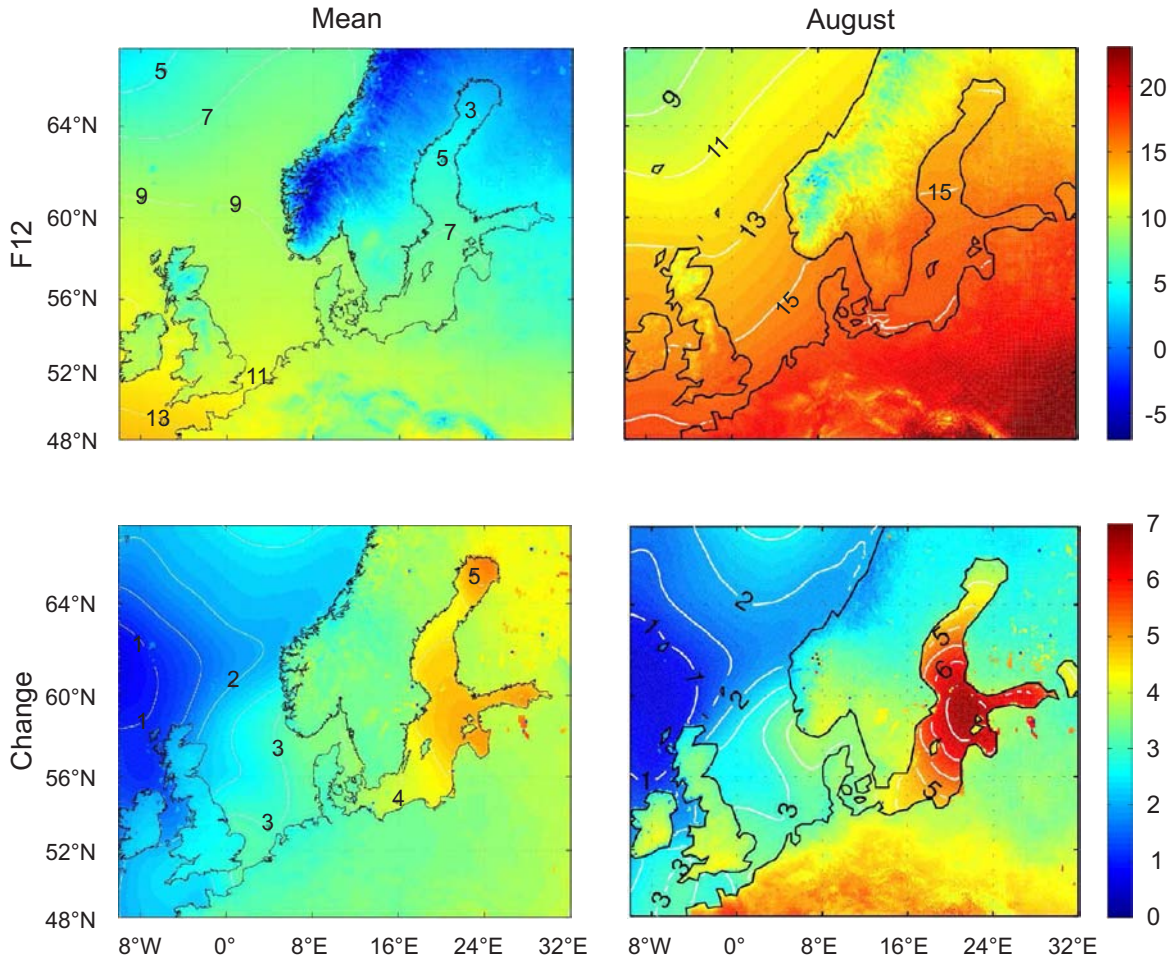

Figure 29: Mean temperature [°C]. Top: F12, bottom: change from F12 to S12. Left: annual mean, right: August. Note that the changes in August are artificial (see text).

and precipitation over the central and eastern Baltic Sea in the summertime. The precipitation increase is further discussed in Chapters 5.2.5 and 5.6.

5.2.4 Specific humidity and cloud cover

The specific humidity in F12 increases towards south and west, as for temperature. The overall mean range is from 4 g/kg over the Bothnian Bay to 7 g/kg over the English Channel. The seasonal variation also follows the temperature, with larger differences between the North Sea and the Baltic Sea during winter (1.5 g/kg difference) than during summer (close to zero difference). The data agree very well with ERA40.

The whole area has increased specific humidity in S12; this also follows the increase in temperature. The largest increase is over the eastern Baltic Sea in July, in connection with the large temperature increase described above.

The fraction covered by clouds in F12 has a mean value close to 0.6 in the whole model domain, which is 5–10% lower than ERA40. There is slightly larger seasonal variation over the Baltic Sea than over the North Sea, with most clouds in December and January, and the least in June and July. There is a small increase in cloud cover in S12, less than 10%.

5.2.5 Precipitation

The annual mean precipitation in F12 is 2.8 mm/day over the North Sea and 1.9 mm/day over the Baltic Sea (Fig. 30). Over the North Sea, there is a distinct annual cycle, with 3.7 mm/day in November and 1.7 mm/day in May. Over the Baltic Sea, the seasonal variation is smaller, and has a maximum in September of 2.5 mm/day. One very noticeable feature in the geographical distribution is the large amounts of precipitation on the west coasts of Norway, Scotland, and Ireland, and west of this, which is seen throughout the year and peaks in January. Most of this area is outside the model domain, but the north-eastern North Sea is affected by it.

These values are higher than the ERA40 results, but according to Omstedt, Chen, and Wesslander (2005), the ERA40 precipitation amount over the Baltic Sea is 18–38% lower than observed during 1997–2001, depending on location. The F12 results for the Baltic Sea are close to these observations.

In S12, the precipitation is increased over the entire area. The strong precipitation during winter close to the coast is enforced, especially southwest of Norway, leading to a precipitation increase of 2 mm/day over the northeastern North Sea. This is a natural consequence of the increased number of low pressure systems over the North Sea. A new area of heavy precipitation (up to 5 mm/day on average) is created during summer in the eastern Baltic Sea. This is a consequence of the large temperature increase in S12 and increased difference between land and ocean temperatures described above. These data should therefore be used with caution, see discussion in Chapter 5.6.

5.3 Open boundary forcing

Regional ocean models require that a closing boundary condition or some data input is provided at all open vertical model boundaries (Fig. 24). cmod needs information on the synoptic sea level, tides, temperature, and salinity on the northern North Sea boundary (59.25°N) and in the English Channel (4.08°W). The North Sea boundary points are numbered 1–50 from west to east, and the English Channel points are numbered 51–65 from north to south.

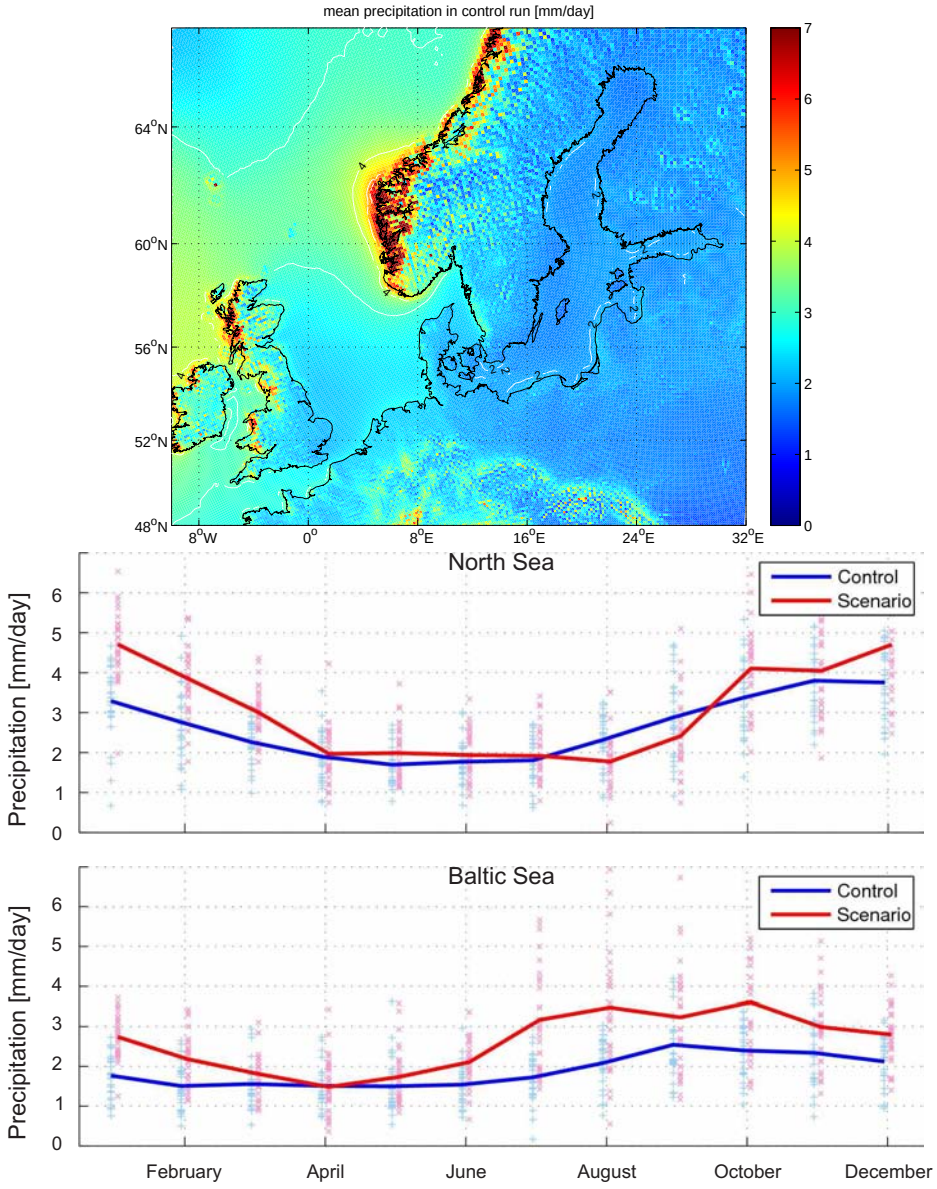

Figure 30: Top: mean precipitation in F12 [mm/day], below precipitation by month averaged over the North Sea and the Baltic Sea respectively. Blue is F12, red is S12, markers are single year values and curves are climatological means. Note that the S12 summer values over the Baltic Sea are considered artificial (see text).

The synoptic sea level information is provided by NOAmod, which has a radiation boundary condition (thus, no sea level information needs to be provided to NOAmod). Tides are prescribed in the form of period, amplitude, phase, and long-term variability of the 14 largest constituents. The description of long-term tidal variations has kindly been extended to cover the entire simulation period by Stephan Dick, BSH.

Temperature and salinity boundary conditions for the control run are derived from ICES data, using observations within 0.5° (56 km) of the boundary. Data have been grouped in boxes, with 4 horizontal × 3 vertical boxes in the western part of the northern boundary, 11 horizontal × 6 vertical boxes in the eastern part of the northern boundary, and one box covering the whole English Channel boundary (Fig. 31). In the English Channel, the observational data in the ICES database were so sparse that it was decided to keep the original cmod boundary, and only use the observations for comparison. The boxes have been defined based on the number of available data and the need for high resolution in the Norwegian Trench. For each box, the monthly 10-year running mean temperature and salinity have been calculated for the years 1960–1990 and any missing data has been interpolated from neighboring boxes, or if several boxes were missing, interpolated in time. The box values have been transferred to the cmod grid, smoothed spatially, and checked for stability. These observationally based boundary conditions clearly show the Norwegian Coastal Current with lower salinity than in the western and the deep parts of the northern North Sea border (on average 32 vs. 35, Fig. 31). Also, the English Channel border is warmer and saltier than the northern North Sea border.

For the future scenario run, the temperature has been perturbed according to the downscaling results obtained by Ådlandsvik (2008). The average temperature increase is 1.1°C, with large spatial and seasonal differences (Fig. 31 lower right). The inflowing water in the western side of the Norwegian Trench shows the largest increase, varying from 1.2°C in August to 2.5°C in April. On the opposite, the deep, western-most part of the northern boundary showed a decrease in temperature for large parts of the year, with −1.5°C in early summer. No change in salinity has been made for the scenario run, because no results have been found with sufficient details of the Norwegian Coastal Current.

5.4 River runoff

For the freshwater input from rivers to the model, a monthly climatology has been compiled from available data, with the great help of Corinna Schrum, University of Bergen, Ralf Weisse and Katja Woth, GKSS, and Phil Graham, SMHI, see Table 9.

The river runoff to the Baltic Sea is on average 13500 m^3/s, 1200 m^3/s to the transition zone, and to the North Sea including the Skagerrak, it is 9000 m^3/s (Fig. 32). 42% of the runoff to the Baltic Sea comes from the Bothnian Bay and Sea, and the runoff from this area shows a strong seasonality, with a peak in May connected to the

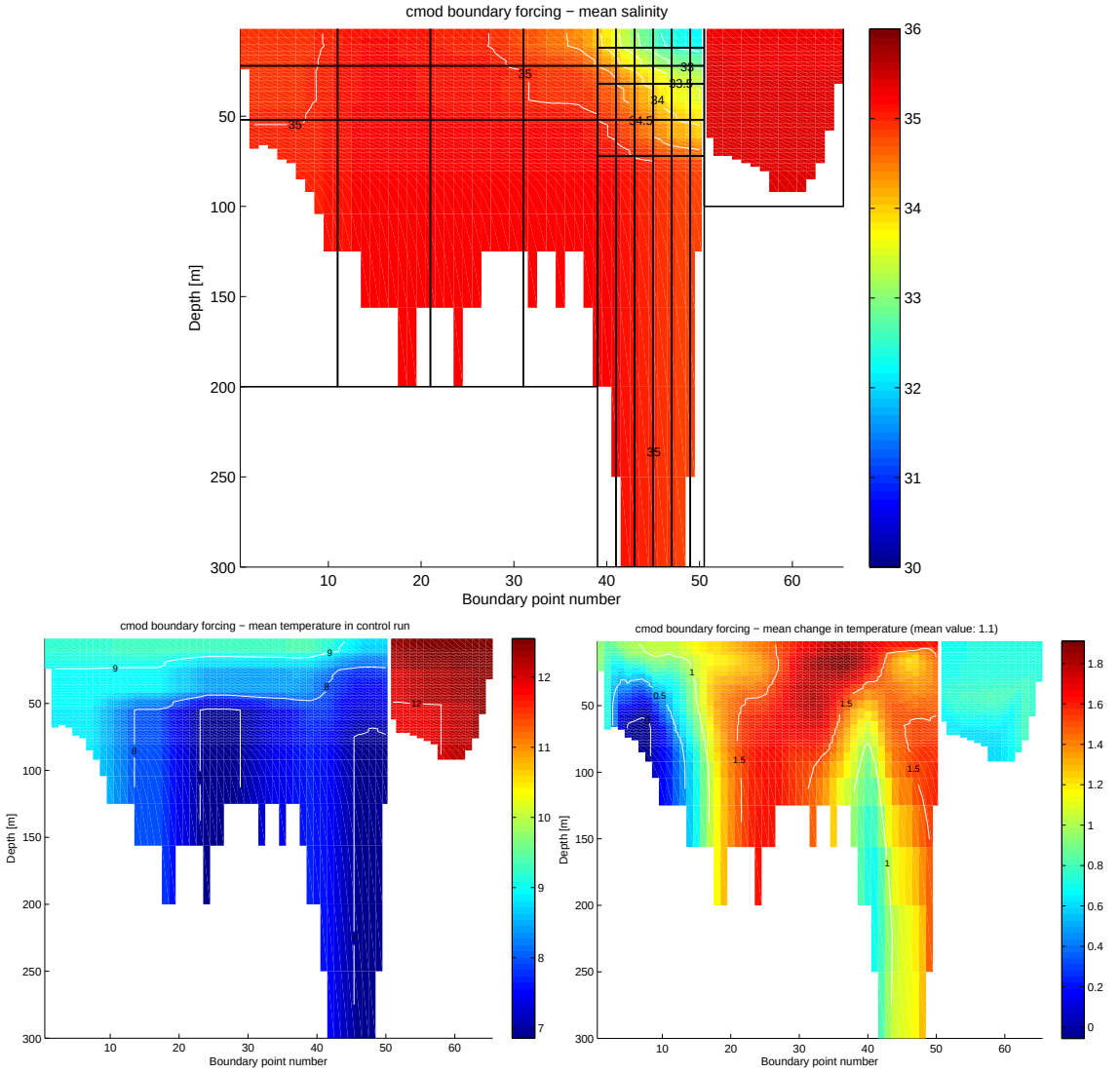

Figure 31: Vertical boundary conditions for the coarse grid model. Top is mean salinity, bottom left is mean temperature, and bottom right is mean change in temperature. Boundary point no. 1–50 are on the northern North Sea boundary, no. 51–65 are in the English Channel. The black lines in the salinity figure shows the boxes used for grouping observations.

Table 9: Data sources for river runoff climatology

Area	Data type	Period	Reference
Baltic Sea and transition zone	monthly observations	1921–2005	Bergström and Carlsson (1994, extended by Phil Graham, pers. comm.)
Norwegian coast	grouped monthly mean observations	1945–1979	Damm (1997)
Continental North Sea coast *Alternative source for German and Dutch rivers (not used)*	monthly mean observations *Daily observations*	start 1975–1977, end 1992–1994 *1977–2002*	Damm (1997) *Pätsch and Lenhart (2004)*
British coast	Monthly climatology	-	Corinna Schrum, pers. comm.

spring melt. Here the runoff is more than doubled compared to the annual average. The runoff to the North Sea shows less seasonality, but a summer minimum is seen.

No changes have been made for the scenario simulations, since the uncertainties in the size of change of future runoff in the Baltic are large (The BACC Author Team, 2008), and to this authors knowledge, no detailed studies of changes in future runoff which covers the whole model area have been made to date. Some increase in the mean Baltic Sea runoff, as well as changes in the seasonality are likely, when more precipitation falls as rain instead of snow. Manmade effects from damming in connection with hydropower plants are also significant for the seasonality in the northern Baltic Sea (*e.g.* Graham, 2004; Jacob & Omstedt, 2005; Thodsen, 2007; Kjellström & Lind, 2009).

5.5 Initial conditions

For the control simulation, the model was started on August 1, 1960, with temperature and salinity fields taken from the Mersea version of cmod from the same time of year and adjusted to match ICES observations. August 1 was chosen to benefit from the many observations around this time of year, and to avoid sea ice in the initial field. All velocities and the sea surface height were set to zero when starting the model.

To let the model adjust any errors in these starting fields, a 2 year, 5 month spin-up period was used before starting the actual model run. This spin-up length was chosen so that the model would start on January 1 after spin-up, and to match the characteristic time scales of the system. The only parameter that has a much longer characteristic time scale is the Baltic Sea salinity. It has a characteristic time scale of 30–40 years (Stigebrandt & Gustafsson, 2003; Omstedt & Hansson, 2006), thus it is not possible to do a proper spin-up with the current model and computer

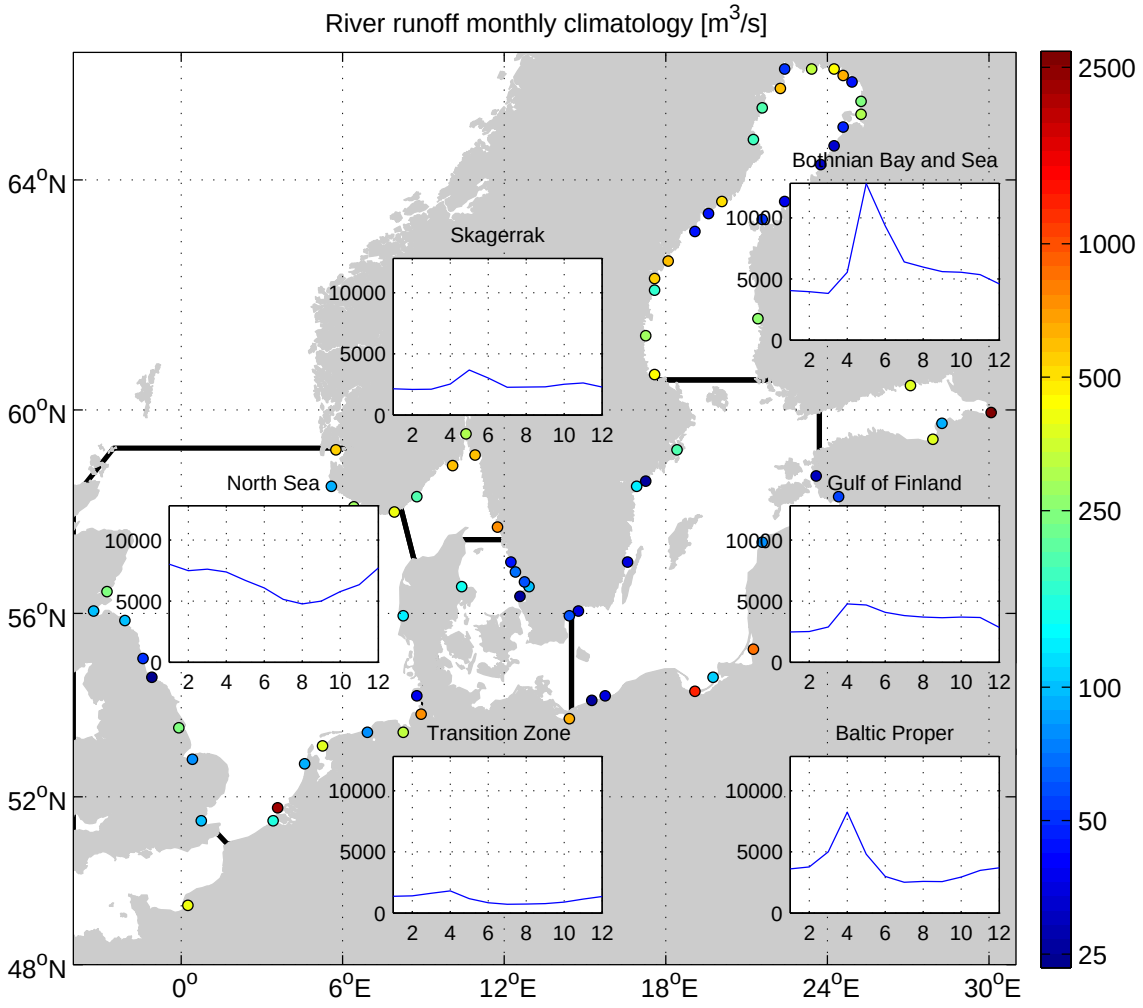

Figure 32: Map of rivers included in the model. The dots indicate the mean runoff [m^3/s, logarithmic scale] of each river. The inserted diagrams show the seasonality for each of the areas limited by black lines.

resources. Instead, care was put in making the initial salinity field as realistic as possible, minimizing the need for spin-up.

For the future simulations, the only change in initial conditions was a temperature increase of 1.3°C in the entire model area, corresponding to the changes modeled by Ådlandsvik (2008). Again a 2 year, 5 month spin-up was made, this time with atmospheric forcing for year 2070. The initial temperature increase in the Baltic Sea was too low, but the model adjusted this during the spin-up period.

5.6 Discussion

Atmospheric forcing

The ocean simulations never become more accurate than the provided forcing, and there is room for further studies and improvements. The simulations presented in this thesis are based on one atmospheric forcing scenario, with one emission scenario, one GCM, and one RCM. The atmospheric forcing has been compared with other forcing scenarios as described above, but making more simulations with alternative atmospheric models and emission scenarios would allow for assessment of the uncertainty range in the state of the ocean induced by the atmospheric forcing. This has been done by Woth (2005) for storm surges in the North Sea and by Meier (2006) focusing on salinity and stratification in the Baltic Sea. For the current work, a first step is taken in this direction, as the results presented here are included in the climate simulation comparison work package of the ongoing EU project ECOOP (European coastal–shelf sea operational monitoring and forecasting system, `www.ecoop.eu`). The project will not provide a full ensemble of regional ocean climate simulations, but different realizations of climate change in the North Sea and the Baltic Sea, including the effects of using different ocean models, are investigated. Detailed ensembles investigations of changes in the transition zone are left for future studies.

Also, as described in Chapter 5.2.3 and shown by Kjellström, Döscher, and Meier (2005) for the Baltic Sea, the modeling system would be greatly improved if the atmospheric RCM and the ocean model were coupled, since the ocean surface input to the RCM when provided by the current GCM is not realistic in these coastal areas. In addition, especially the storm surge modeling would benefit from the high temporal resolution of the wind forcing in a coupled system. Here it should be noted that the atmospheric forcing used for the current studies has high spatial resolution compared to most RCMs, and this is equally important for the storm surge modeling. Alternative to using a coupled system, a newer GCM with a more realistic description of the Baltic Sea could be used for boundary forcing of the RCM. This approach is used for the DMI simulations in the ongoing EU project ENSEMBLES (`ensembles-eu.metoffice.com`).

Scenario freshwater forcing

As noted in Chapter 5.2.5, the modeled change in precipitation in the eastern Baltic Sea was unrealistically large. When looking at the S12 precipitation increase over the Baltic Sea as a whole, it was on average 2500 m^3/s, or 38%. Other studies of the Baltic Sea indicate a general increase in wintertime precipitation and a decrease in summertime precipitation in the southern parts, resulting in a likely annual mean increase in precipitation (The BACC Author Team, 2008), but the S12 results must be considered in the high end. However, changed precipitation will naturally lead to changed river runoff, and this effect was not included in the current simulations. The modeled average river runoff to the Baltic Sea was 13500 m^3/s and the precipitation in F12 was 6400 m^3/s. Thus, if looking at the total freshwater forcing increase, it was $\frac{2500\ m^3/s}{13500\ m^3/s+6400\ m^3/s} \cdot 100\% = 12.6\%$, which is within the range of earlier studies (Graham, Hagemann, Jaun, & Beniston, 2007; The BACC Author Team, 2008). Thus, when considering the Baltic Sea as a whole, and the annual averaged data, the increased freshwater forcing in the S12 simulation is not unrealistic. Still, the scenario freshwater forcing is a major uncertainty factor in the atmospheric forcing. The two different ocean model scenario simulations with and without changed precipitation were made to assess the importance of the freshwater forcing, but further studies are needed to identify a proper level of scenario precipitation increase.

6 Modeled sea level

6.1 Introduction

Coastal areas of Denmark are storm surge risk areas and coastal protection is needed to mitigate the storm surge effects of rising mean sea level and changes in wind patterns (Hallegatte et al., 2008, Chapter 3). This requires good estimates of the expected ranges of future mean sea level and storm surges.

DMI has the national responsibility for storm surge forecasts in Denmark, and a 60 hour forecast is made 4 times a day. The forecast is made by using the operational version of cmod, which is forced by the in-house atmospheric model HIRLAM. No data assimilation of sea level information is performed, but the model results are adjusted to fit real-time sea level measurements from tide gauges before forecasts are sent out. The non-adjusted forecasts are validated on an annual basis, and the 12 hour forecast of storm surges has peak error levels of 0–20 cm, depending on location (ocean.dmi.dk/validations/surges/index.uk.php and J. W. Nielsen, 2001). Similar forecast systems exist in most countries around the North Sea and the Baltic Sea and cooperation takes place in the NOOS and BOOS communities under EuroGOOS, as well as in numerous research and development projects. From this, cmod is well tested and known to be comparable to other storm surge models in the area (Gästgifvars, Müller-Navarra, Funkquist, & Huess, 2008).

The overall geographical pattern of mean sea level of a regional model arises in a complex interplay of the model zero level value and the physical processes included in the model, and the cmod mean sea level has not previously been investigated. Variations in the operational model sea level in non-surge situations are currently being validated in the transition zone (Vibeke Huess, pers. comm.), and have been validated in the Gulf of Finland (both DMI and BSH setup) and the German North Sea coast (BSH setup only) (Dick et al., 2001; Gästgifvars et al., 2008).

Storm surges in tidally dominated areas are always a sum of the weather-generated surge and the tides. Thus a large weather-generated surge hitting at low tide may cause much less damage than a smaller surge hitting at high tide. The Danish tradition is to analyze storm surges with tides included, but in a climate change perspective it can be useful to remember that the tidal cycle is unchanged by changes in the extreme wind climate.

At DMI, one other storm surge climate simulation which covered the North Sea – Baltic Sea area has been performed (Nicolai Kliem, pers. comm. and unpublished data). The atmospheric forcing was similar to the one used in the present study,[9] but the MOG2D ocean model developed by LEGOS, France, was used. MOG2D is a finite element model, and thus has the ability to run with very high resolution in coastal

[9] Nicolai Kliem used the CONWOY data set (Søndergaard, Kronvang, Pejrup, & Sand-Nielsen, 2006) with 25 km resolution

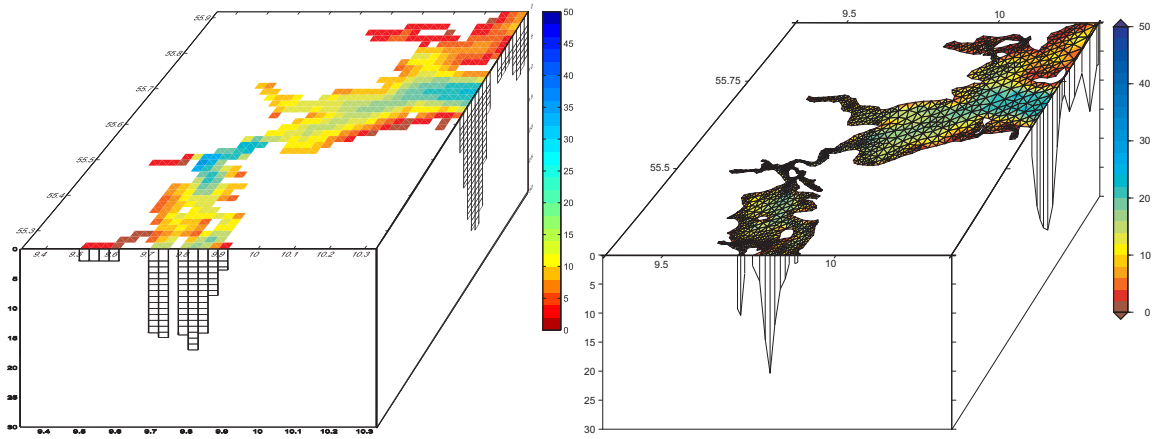

Figure 33: Visualizations of the 3D finite difference grid of cmod (left) and the 2D finite element grid of MOG2D (right) for the Little Belt area (55°15'–55°55'N, 9°20'–10°20'E). The colors show the depth in meters.

areas (Fig. 33), but works only on the vertically integrated water column (Lynch & Gray, 1979). MOG2D has been shown to work approximately as well as cmod on the Danish North Sea coast and for the Bornholm area, but less good in the transition zone (`ocean.dmi.dk/validations/surges/2008/compare.php`).

The short term sea level variability in the model relies heavily on the atmospheric forcing, especially the wind. As discussed in Chapter 5.2.2, the mean wind speed field used for the control run is of reasonable quality, whereas the strong winds are systematically underestimated. The model wind stress on the water is given by

$$\tau_{surf} = \rho_{air} C_D W^2,\ C_D = 6.3 \cdot 10^{-4} + 6.6 \cdot 10^{-5} W$$

where ρ_{air} is the air density and W is the wind speed (Dick et al., 2001). Thus, the wind stress scales with the cube of the wind speed for large wind speeds, and an underestimation of strong winds will lead to a large underestimation of storm surge heights. For this thesis, the delta change approach is taken, where it is assumed that any model errors will be similar in the control and scenario runs, and thus cancel out when looking at the change in the signal. However, even if this approach is valid for the strong wind speeds, the storm surge height changes will be systematically underestimated because of the non-linearity of the problem, and thus this method provides a lower estimate of the actual changes.

In the following, I will first give a brief review of existing sea level modeling relating to climate change from the study area (see Chapter 2.2 for a broader review), and then analyze the modeled changes in mean sea surface height, seasonal variations, and storm surge heights. For each of these subjects, the control simulation will first be validated against observations. The validation has been made bearing in mind that

the model is already well tested for operational purposes, but the forcing used here is of a different nature, and the simulation period is much longer. The model results presented here do not include all effects that are important for sea level changes. As described in Chapter 5, two scenario runs have been made, with and without changed precipitation (v10 and v12 respectively). In v12, the only sources of changed sea level are changes in the atmospheric forcing (wind, air pressure, and air density) and in the dynamics. In v10, additionally, the added freshwater forcing both has a direct effect on the sea level and an indirect effect through the alteration of model dynamics. In the analysis of the mean sea level and seasonal variations, both were included. For the storm surge analysis, only v10 was used. Common for both scenarios is that sea level rise originating outside the model area, as well as steric effects and land uplift effects are not included. These additional effects will be discussed in Chapter 8.

6.2 Review

Future sea level changes in the North Sea, and especially changes in storm surge statistics, have been modeled by several authors in recent years, including ensemble studies (Debernard & Røed, 2008; Woth, 2005; Woth et al., 2006). These studies give a best estimate of the 99th percentile, where the scenarios show an increase along the German, Danish, and Norwegian coasts of 8–20% by the end of this century, with the largest changes in the German Bight[10]. With the general mean sea level rise (Chapter 2.2), the tides will also be affected. Flather and Williams (2000) estimated an increase of the high tides along the eastern North Sea coast and in the Kattegat of 2–4 cm for a 50 cm mean sea level rise (that is, 4–8%). However, close to the coast, local conditions have large influence on tidal variations so detailed studies are needed (Huess, 2001).

Fewer studies have focused on the Baltic Sea extreme sea level change, most likely because the global sea level rise will partly be compensated by isostatic land rise, especially in the northern parts of the Baltic Sea. Meier (2006) found that the magnitude of changes depend on the underlying GCM and forcing scenario, with results based on the Hadley Centre GCM showing a smaller wind increase than for the ECHAM/OPYC model. Changes were largest in the eastern part of Gulf of Finland and Gulf of Riga, while sea level rise in the northern Bothnian Bay was compensated by land rise for small and midrange climate change scenarios. The rate of land rise at Kemi in the northern Bothnian Bay is 7.20±0.27 mm/year, at Hamnia in the eastern Gulf of Finland it is 1.62±0.26 mm/year (www.fimr.fi , Leppäranta & Myrberg, 2009). According to Suursaar, Jaagus, and Kullas (2006) the winter mean sea level in the Gulf of Riga may rise up to 10 cm and the variability may increase.

[10] These studies use the threshold approach, see Chapter 3.1.

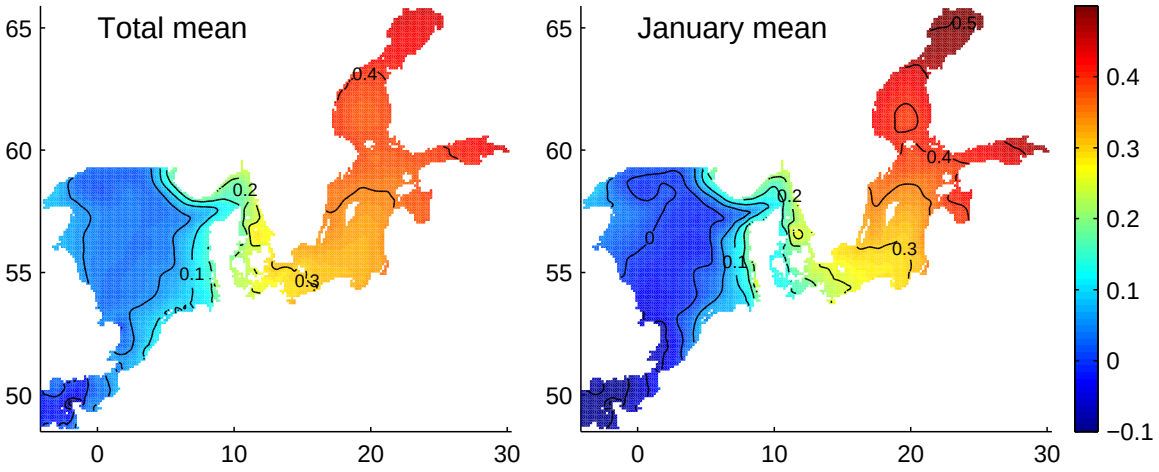

Figure 34: Model mean sea level in control run [m]. Left: total mean; right: January mean.

To my knowledge, the studies presented in this thesis are the first long-term model studies that include both the North Sea and the Baltic Sea, where the model grid resolution is sufficient to simulate storm surge situations in the transition zone.

6.3 Variations in the mean sea surface height

The model mean sea surface height (Fig. 34) was shaped by wind setup, river runoff, and net precipitation surplus in the Baltic Sea, in combination with the restricted water exchange through the transition zone and the model dynamics. Since the model is volume conserving, steric height signals were not included.

The wind and freshwater surplus created a mean sea level gradient from the North Sea to the northern and eastern Baltic Sea of 40–45 cm, with about 15 cm change through the transition zone. The currents had large influence on the detailed sea surface topography. In Skagerrak, the combined effects of wind setup and counter-clockwise circulation created a trough, and the model showed a large bulb in Kattegat, corresponding to a clockwise circulating eddy. This baroclinic circulation and its connection with the Kattegat–Skagerrak front has been investigated by the use of lightship surface velocity measurements, dedicated cruises, and models (Jakobsen, 1997; M. H. Nielsen, 2005; Pedersen, 1993).

During winter, the modeled wind generated sea level gradient in the North Sea and from the North Sea to the northern and eastern Baltic Sea was increased, so the mean January sea level difference between the English Channel and the Bothnian Bay was 60 cm (Fig. 34).

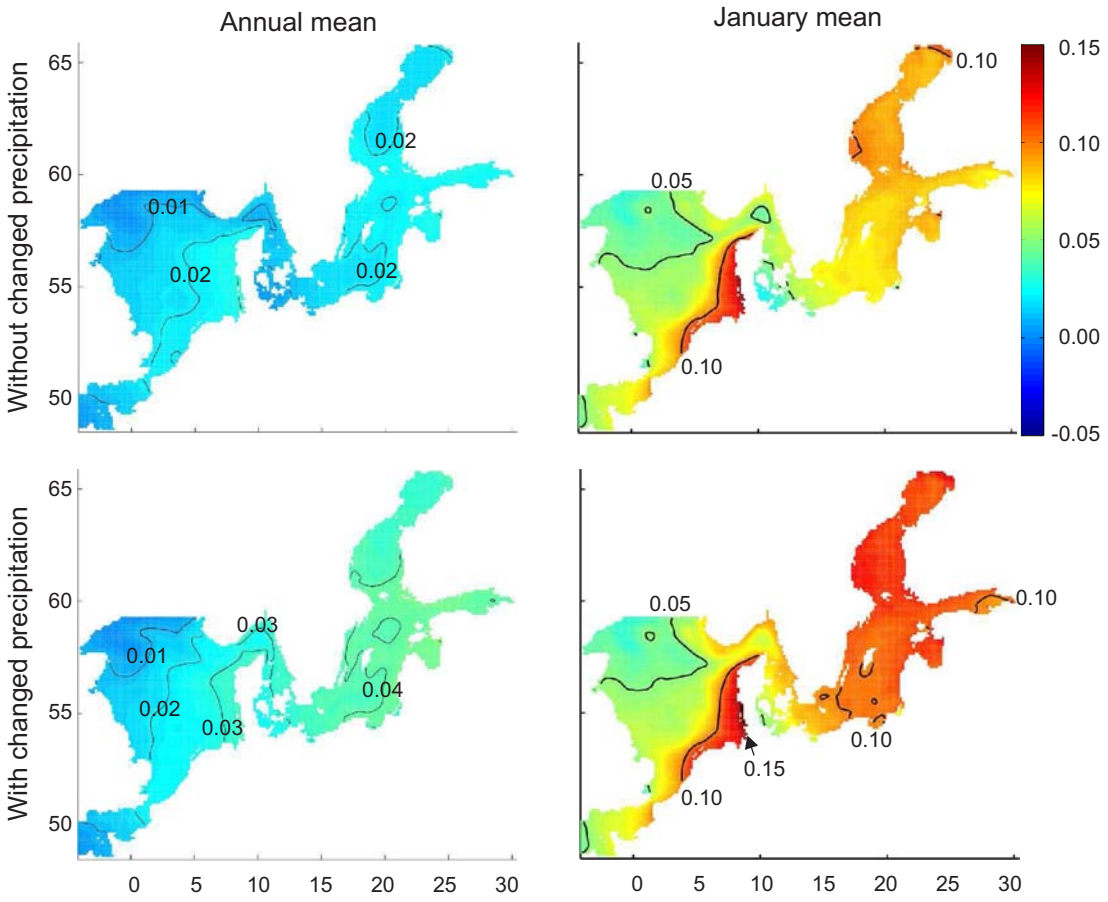

Figure 35: Changes in model mean sea level [m]. Left: total mean changes; right: January mean changes. Top: scenario without changed precipitation (v12); bottom: with changed precipitation (v10).

The changes in mean sea level between the control simulation and each of the two scenario simulations were small (Fig. 35). In the v12 run, an increase of 2 cm was seen in the Baltic Sea, in v10 this was 4 cm. Thus, the increased freshwater forcing and the changed wind/air pressure setup each contributed with about 2 cm (excluding steric effects). The differences between v10 and v12 was smaller in the North Sea, both simulations show a small increase in the north east–south west gradient.

If looking at the January mean changes, the simulations showed an increased sea level in the whole domain, with 4–5 cm at the open boundary. On top of this, the North Sea gradient increased by about 10 cm, much more than in the annual mean, and the Baltic Sea increased by 3–6 cm from the wind/air pressure setup and about 3 cm from the increased freshwater forcing. It is also noticeable that the Skagerrak

eddy area stands out as an area with less increase in sea level than the surroundings, indicating increased circulation.

6.4 Seasonal variations

The seasonal variations in sea level were compared to detrended monthly mean GLOSS data (see Chapter 2.3), see Figure 36 and the electronic supplement. In general, the amplitude of the seasonal cycle is comparable, and the standard deviations show the same size and seasonality. However, the model tends to show a phase shift towards an earlier peak in sea level, with relatively higher sea levels than observed in June–August and relative lower than observed in November–January. The differences are up to 8–10 cm. Similar differences have been observed in a 2005–2008 validation study of the operational (ECOOP) setup of cmod, but there, the relative higher-than-observed sea levels peaked in April and May (Vibeke Huess and Peter Nørtoft Nielsen, unpublished data). The differences between model and observations can partly be explained by the lack of steric effect in the model, but also, Ekman (1999) has reported a change in the Stockholm sea level seasonality with a shift from late summer maximum to early winter maximum, linked to wind pattern changes and NAO. Thus uncertainties in the wind pattern are also a possible explanation.

The modeled changes in sea level are largest in winter with a peak in January, especially at coastlines exposed to westerly winds (14 cm increase in January at Esbjerg). In the Baltic Sea, relatively large changes are also seen in the summertime (6–7 cm at Stockholm in July), which must be seen as a result of the spurious summertime changes in wind (Chapter 5.2.2). The increased precipitation in the v10 simulations are seen as a small extra general increase in sea level at Stockholm and the transition zone stations; the effect is 1–3 cm and almost constant over the year.

6.5 Extreme sea level

The model storm surge statistics have been calculated at all tide gauges marked in Fig. 40, which are selected from the NOOS and BOOS networks of stations (`www.noos.cc` and `www.boos.org`).

A comparison between modeled and observed top hundred independent storm surge events offers a simple measurement of the model's ability to simulate storm surges. Here, the comparison is made for selected Danish stations, with two datasets, DMI's records and KDI's records, of the highest sea levels at individual stations (Chapter 2, Sørensen et al., 2007). The KDI dataset is used here to supplement the DMI records, because these are lacking data from a few events, and at Hirtshals the DMI record only goes back to November 1971. In the observational record and

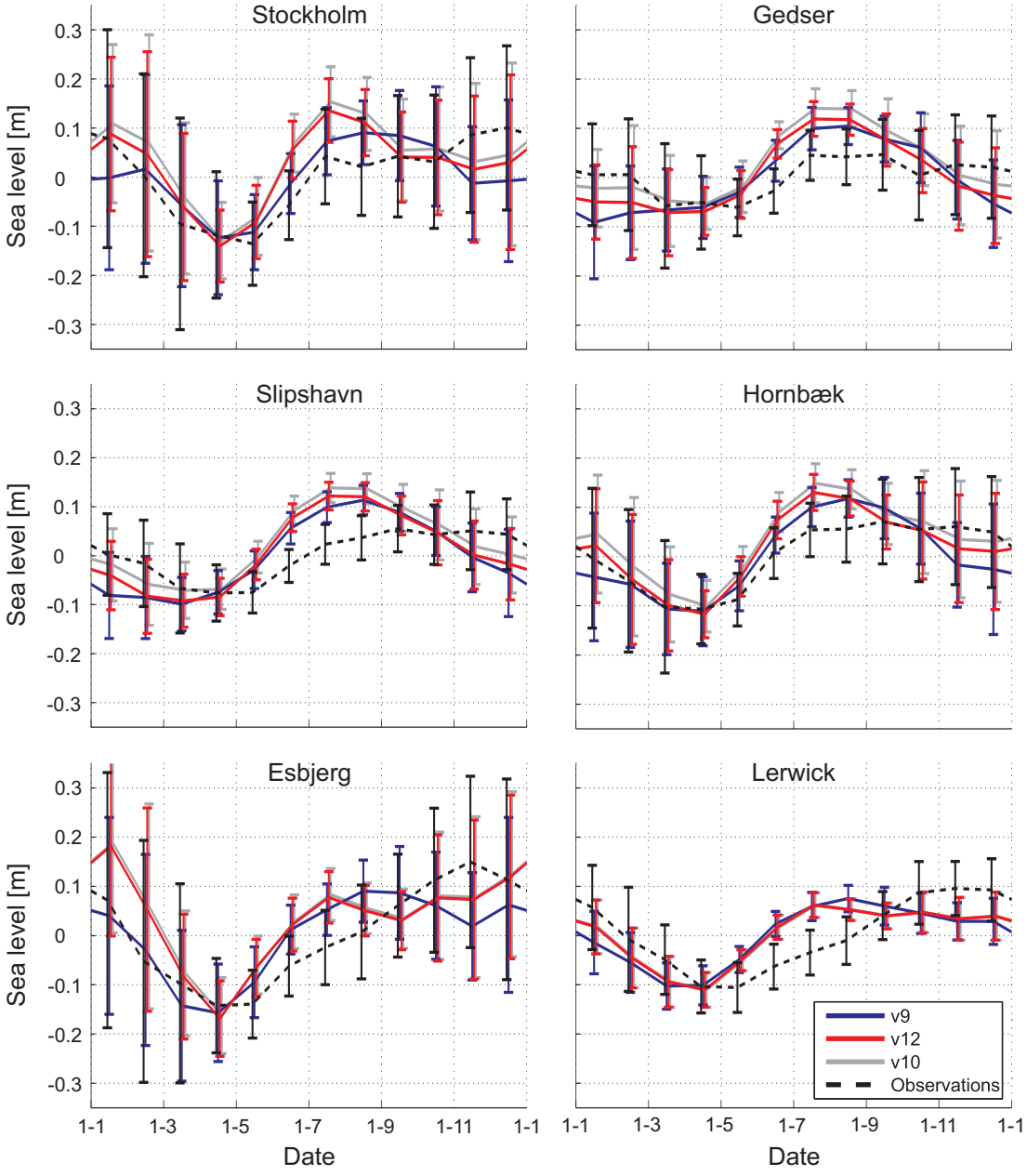

Figure 36: Seasonal sea level variations at selected tide gauges (error bars indicate one standard deviation). Black dashed: observed, blue: control run, red: scenario run without changed precipitation, gray: scenario run with changed precipitation. The observed mean value has been subtracted from observations; the control run mean value has been subtracted from all model data. Note that the v10 and v12 simulations are nearly identical at Lerwick.

the cmod results, tides are included. MOG2D was run without tides, so to allow comparison, the cmod results are analyzed with and without tides included.[11]

As expected, the model surge heights are smaller than observed at most stations (Fig. 37). The difference in the transition zone is about 10–20 cm depending on the station, and at Esbjerg the top 100 average is 52 cm lower than the similar DMI observations, while the top 10 records are 1.05 m lower than the KDI top 10 for the same period. At Hirtshals, cmod has a few higher events than observed, but this may be due to the limited observational record. The detided top 100 storm surges modeled by cmod and MOG2D largely agree on the distribution of storm surges (the way the curves fall off in Figure 38 are similar), but the MOG2D results are generally 20–30 cm lower than the cmod results. For the top 5 storms, the differences between the two models, and between control- and scenario runs, is more variable. An offset between MOG2D and cmod is also seen in the southern and central Baltic Sea and in the southern North Sea (not shown).

The scenario run shows higher maximum values than the control run at most stations. At Esbjerg the top 100 mean increase is 14–18 cm, depending on model and whether the data are detided. At Hirtshals, the change is down to 6–9 cm, and in the transition zone, the changes are even smaller, in the southern parts sometimes negative. The changes are thus close to the modeled rise in winter mean sea level. The cmod and MOG2D changes are very similar, so the changes can be considered characteristic for the atmospheric forcing, more than for the ocean models.

As for the observational records, a truncated Weibull distribution has been fitted to the highest model sea levels, to estimate the return heights (see also Chapter 3). For the model results, it was chosen to truncate at the 31st highest event, corresponding to one event per model year on average, to use a consistent method for all stations and simulations. As long as the estimates are used well within the data range, the results are not very sensitive to the truncation level, but for return periods longer than about 10 years, the truncation dependency goes up, as does the uncertainty in the estimate. Note also that the fit to a Weibull distribution was chosen to follow the KDI standards. A log-normal distribution (straight line in Figure 39) could fit the data equally well, with almost the same results for a 10-year event.

The change in the 10-year event was 15–31 cm at Esbjerg (largest with tides included), 1–5 cm at Copenhagen and 8–13 cm at Helsinki (Fig. 39, other stations in electronic supplement). Most changes in the 10-year events are statistically insignificant (changes are within the bounds of the confidence intervals), but for the south western North Sea coast, the Norwegian coast, and the far ends of the Baltic Sea, statistically significant increases are seen (Fig. 40).

[11] Detiding has been performed using the Matlab utility t_tide (Pawlowicz, Beardsley, & Lentz, 2002).

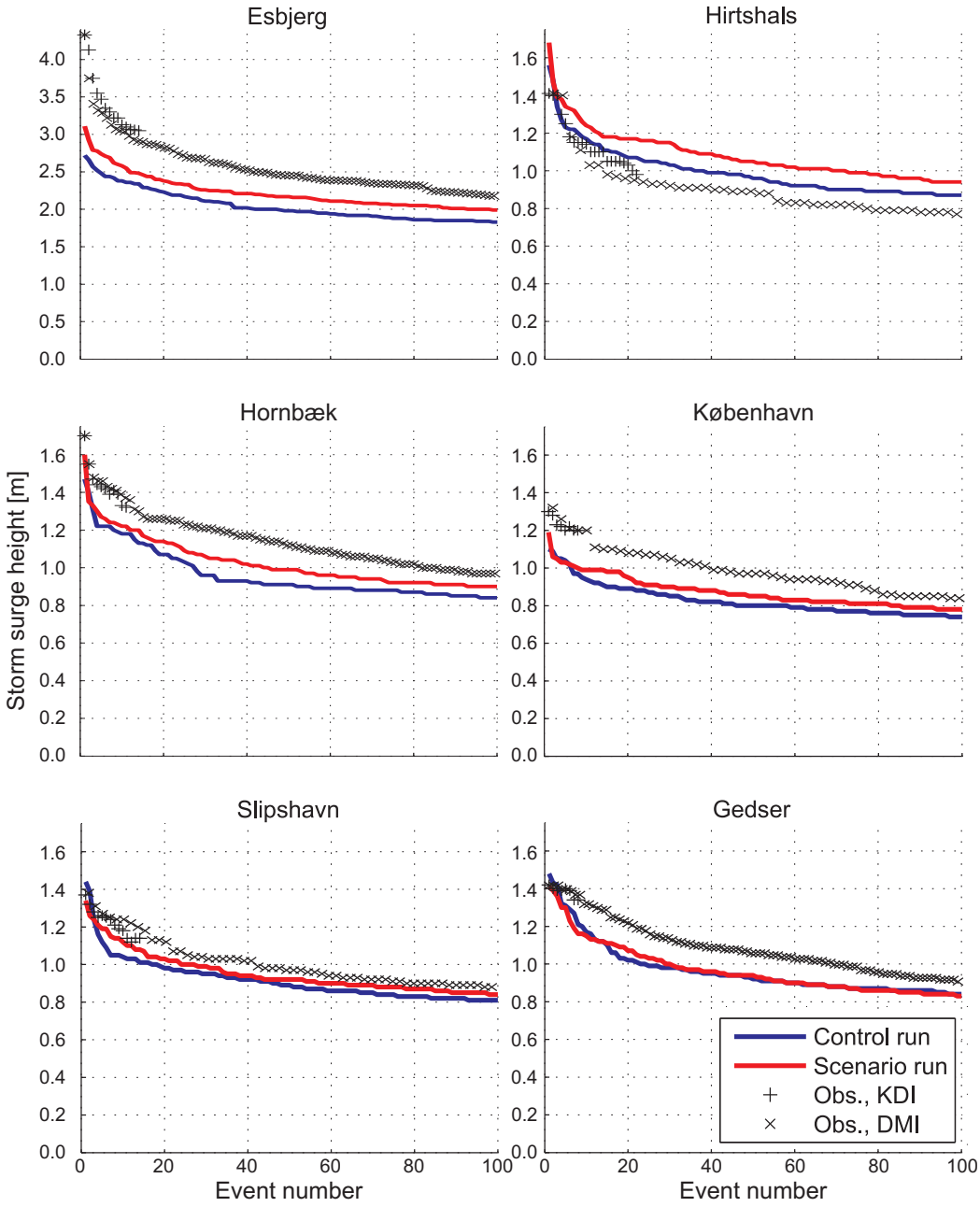

Figure 37: The modeled 100 largest independent sea level events and corresponding observations at 6 selected stations, tides included. Note that the y-axis scale is different at Esbjerg than at the other stations, and that the difference between the model and observations is larger at Esbjerg than at the other stations, especially for large events (see text for details).

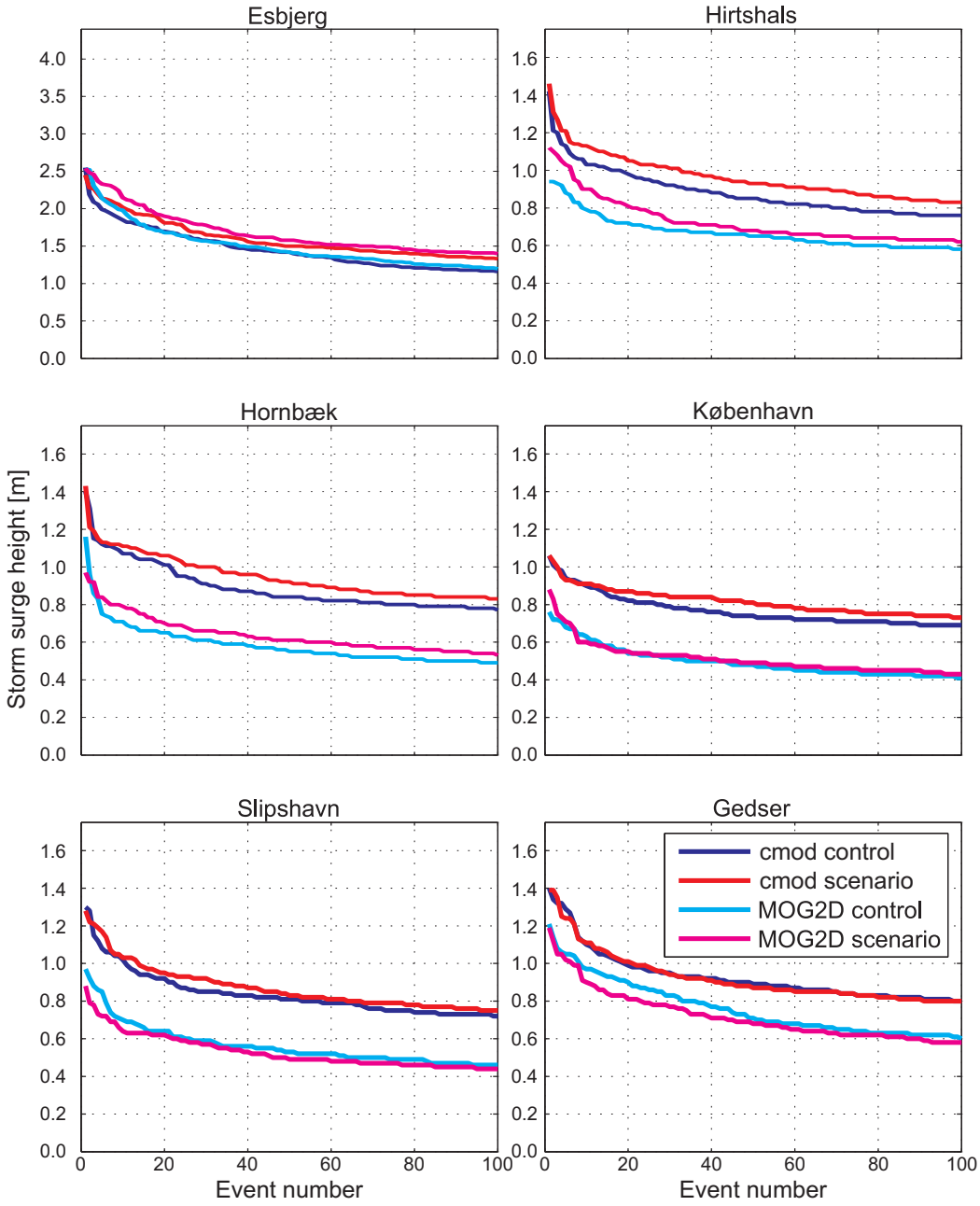

Figure 38: The modeled 100 largest independent sea level events by cmod and MOG2D at 6 selected stations, tides not included. The scales are the same as in Figure 37.

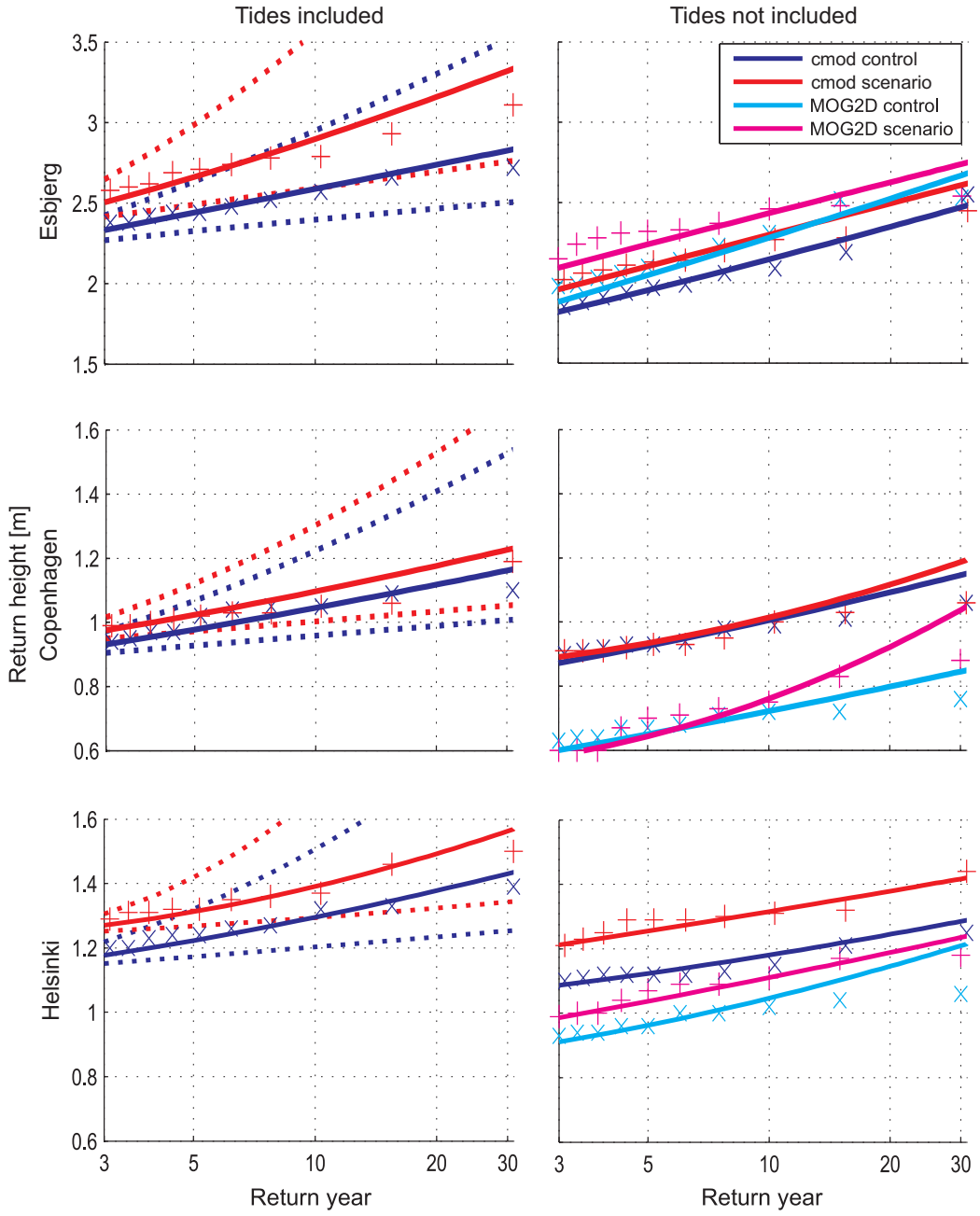

Figure 39: Return heights calculated from the cmod and MOG2D control and scenario runs at the Esbjerg, Copenhagen, and Helsinki stations. Left: tides included, dashed line shows 90% confidence levels. Right: tides not included. Note the logarithmic x-axis and that the y-axis scale is different at Esbjerg than at Copenhagen and Helsinki, and does not go to zero.

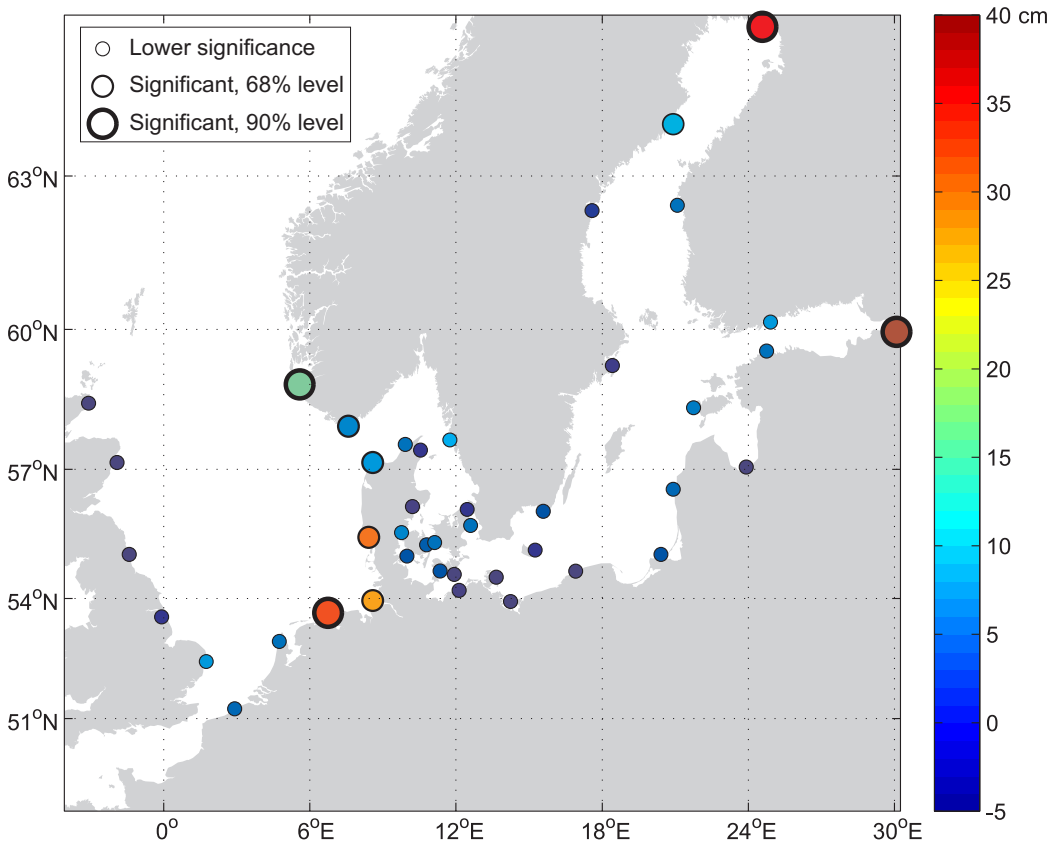

Figure 40: 10 year return height changes calculated from the cmod model with tides included. The size of the markers shows how significant the changes are.

For the transition zone, the southern and central Baltic Sea, and the British North Sea coast, the best estimates of the model scenario changes are generally below 5 cm. Thus, according to this scenario, the wind generated effects will cause little change in the storm surge statistics in these areas. In this connection, it is worth to note that the model setup allows for external surges generated over the North Atlantic to build up in the NOAmod model and propagate into the cmod area. It is likely that some of the storm surges hitting the Norwegian and Danish coasts build up over the North East Atlantic, but the simulations did not show a significant increase of externally generated surges that traveled around the North Sea as Kelvin waves.

7 Modeled temperature and salinity

7.1 Introduction

The temperature, salinity, and stratification of the North Sea and the Baltic Sea are important for the ecosystem, and several model studies have looked at the climatic changes in these parameters. For the Baltic Sea, the main concern is a possible decrease in salinity because of increased freshwater input, which is likely not to be fully compensated by inflows through the transition zone (Stigebrandt & Gustafsson, 2003; Meier, Kjellstrom, & Graham, 2006; The BACC Author Team, 2008). Major inflows may be increased by increased wind, and observations show that inflows are decreased in periods with increased freshwater forcing to the Baltic Sea (The BACC Author Team, 2008, and references therein). Decreasing salinity may have a negative effect on the fish population of the Baltic Sea (MacKenzie, Gislason, Möllmann, & Köster, 2007), whereas E. O. Gustafsson and Omstedt (2009) argue that increased freshwater forcing may improve the oxygen conditions at intermediate depths due to weaker stratification.

The temperature is projected to increase in both the North Sea and the Baltic Sea. The Baltic Sea volume mean temperature has been projected to increase 2–4°C from the 1961–1990 period to the 2071–2100 period, depending on the emission scenario and underlying GCM (Doscher & Meier, 2004; Meier, 2006). The North Sea temperature increase is likely to be smaller, with a volume mean warming of 1.4° C and SST warming of 1.7°C over 100 years, according to Ådlandsvik (2008), but no ensemble studies have been made.

Temperature and salinity changes in the transition zone were studied as a part of the CONWOY project (Søndergaard et al., 2006), using the DHI model Mike 3 and focusing on the transition zone and eastern Skagerrak (9.3E–13.5E). The atmospheric forcing was similar to the forcing used here. They found an average transition zone SST increase that varied with season between 2–2.5°C in spring and more than 3.2°C in winter. They also found changes in the difference between surface and bottom salinity. These were area dependent, but in general they showed increased stratification in spring because of increased outflow of low salinity water from the Baltic Sea, and decreased stratification in winter because of increased wind mixing.

The HAMSOM and ECOSMO[12] models have been used for long hindcast simulations with a model setup similar to the cmod coarse grid used here, but with no nesting to a finer grid in the transition zone (Janssen, Schrum, Hübner, & Backhaus, 2001; Schrum, Alekseeva, & John, 2006). No detailed studies of the transition zone have been made with HAMSOM or ECOSMO.

[12] ECOSMO is based on the physical ocean model HAMSOM and an ecosystem model.

The operational version of cmod is used routinely for temperature and salinity forecasting (see `ocean.dmi.dk`) and has been compared to observational data in the transition zone, showing that the temperature was a bit too warm, especially in summertime (bias up to 0.8°C, standard deviation 0.7–0.8°C) and that the stratification in the Great Belt has been improved with the introduction of the k-ω turbulence scheme (Per Berg and Vibeke Huess, pers. comm.).

In the following, the modeled changes in integrated and surface temperature and salinity will be analyzed, as well as the implications for the steric effect and stratification. Also, the model data will be compared to the observations presented in Chapter 4.

7.2 Volume integrated heat and mean salinity

The volume integrated heat was calculated as

$$Q = \int\int\int (T(x,y,z) - T_0)\rho\, c_P \, dx\, dy\, dz \tag{4}$$

where $T_0 = 0$°C and $\rho = 1026\text{kg/m}^3$ and $c_P = 3970$ J/(kg K) were kept constant to comply with the standards in the ECOOP project.[13] c_P is also kept constant in cmod, while the fixed value for ρ results in an overestimation of less than 2%, especially in the Baltic Sea.

Similarly, the mean salinity was calculated as

$$S = \frac{1}{V}\int\int\int S\, dx\, dy\, dz \tag{5}$$

where V is the total volume.

The North Sea integrated heat content in the cmod control run had a mean value of $11 \cdot 10^{20}$ J, corresponding to 8.7°C and a seasonal variability with an amplitude of $2.5 \cdot 10^{20}$ J. The mean value is in agreement with the heat content calculated from the climatology of Janssen et al. (1999, hereafter referred to as the Janssen climatology); the seasonal cycle is about 30% smaller but has the same phase (Fig. 41). The top 10 m values agree well with the Janssen climatology, in both mean value and seasonal variations. The interannual variations are smaller than modeled by a hindcast study with the ECOSMO model (The BACC Author Team, 2008, and Corinna Schrum, pers. comm.), but the decadal variability of the two simulations have common features, with cool periods in the late 1960s and in the 1980s, and warming towards the end of the simulation (Fig. 42).

[13] 3970 J/(kg K) is a low value for c_P and corresponds to a salinity of 38 and a temperature of 10°C.

Correspondingly, the Baltic Sea volume integrated heat content in the cmod control run had a mean value of $5 \cdot 10^{20}$ J, corresponding to 5.8°C. Here, both the model mean value and size and phase of the seasonal cycle were very close to those calculated from the Janssen climatology, and the same is true for the top 10 m values (Fig. 41). The interannual variations were of comparable magnitude as modeled by the ECOSMO model, but the long-term variability had a higher correlation with the North Sea variability than what the ECOSMO model showed (Fig. 43).

The spin-up phase is marked with green in Figure 41. As the forcing for the spin-up phase and the first year of simulations is the same, these can be directly compared to investigate the development during the model spin-up. The initial field was slightly too cool to balance the atmospheric forcing and open boundary conditions, but the model adjusted this within the first year of spin-up. The later part of the spin-up and the first year of simulations are almost identical.

In the future scenario, the volume integrated heat content in the Baltic Sea increased from around $7 \cdot 10^{20}$ J in the beginning of the simulation to around $8 \cdot 10^{20}$ J towards the end, corresponding to a mean warming of 2.7°C (Fig. 43). The warming is larger in the summertime (2.9°C in September) than in the winter (2.5°C in March, Fig. 44), which, according to Kjellström et al. (2005), is a feature of the spurious changes in the atmospheric forcing. The increasing heat content in the scenario simulation originated from the atmospheric forcing, where the annual mean 2 m temperature over the Baltic Sea increased from 10°C to 13°C during the scenario run. The North Sea volume mean warming was 1.5°C, with no large changes in the features of the interannual variations (Fig. 42) or the seasonal cycle (Fig. 44) and the transition zone volume mean warming was 2.7°C. The difference in the heat content between the scenarios with and without changed precipitation is insignificant.

The monthly mean volume averaged salinity of the North Sea in the cmod control run varied between 34.6 and 34.8. The seasonal cycle had an amplitude of 0.05 with the lowest values in early summer and the highest in late fall (Fig. 45). The top 10 m averaged salinity had a larger seasonal cycle, with amplitude of 0.1–0.2. The seasonal variations agree well with the Janssen climatology, though the surface amplitude was smaller in some years. The volume integrated mean values are almost identical, whereas the model top 10 m salinity was 0.2–0.3 too high most years.

The Baltic Sea volume averaged salinity for the control run varied between 6.9 and 7.3. The Janssen climatology average value for the same area is 7.3 (Fig. 45). Observations from Gotland Deep show a general decrease in salinity from 1980 to 1990 of 0.8–2 depending on depth (Feistel et al., 2008). This decrease is not seen in the cmod control run. Thus, the model is able to run stably for long simulations, but the current simulation did not catch the historic long term salinity variability. There is no significant seasonal cycle in the volume averaged salinity. For the top 10 m, the amplitude is smaller than in the Janssen climatology, but the phase is the same, with the lowest salinity in early summer.

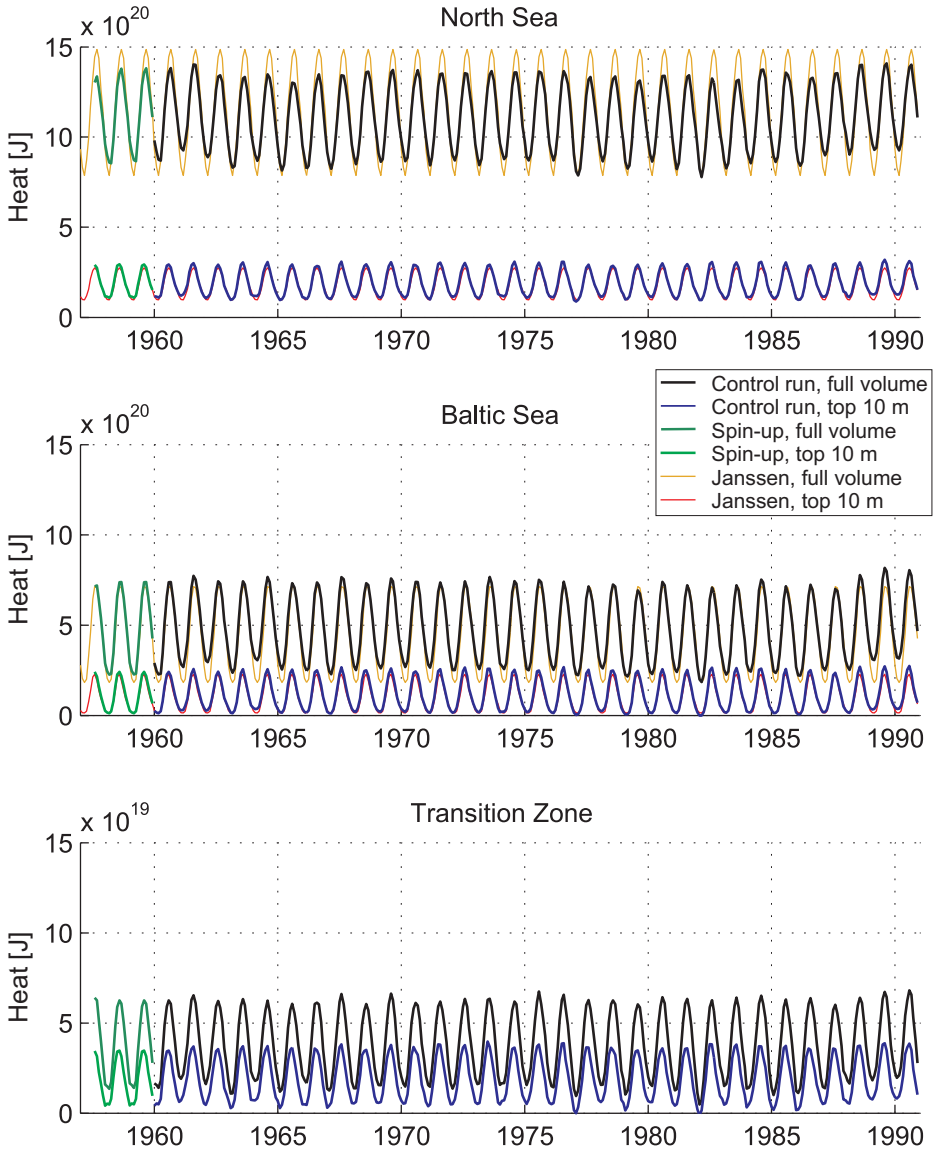

Figure 41: Top 10 m and volume integrated monthly mean heat content in control simulation, including spin-up phase, and from the Janssen climatology, for the North Sea, the Baltic Sea, and the transition zone. Note that the y-axis scale for the transition zone is a factor 10 smaller than for the North Sea and the Baltic Sea.

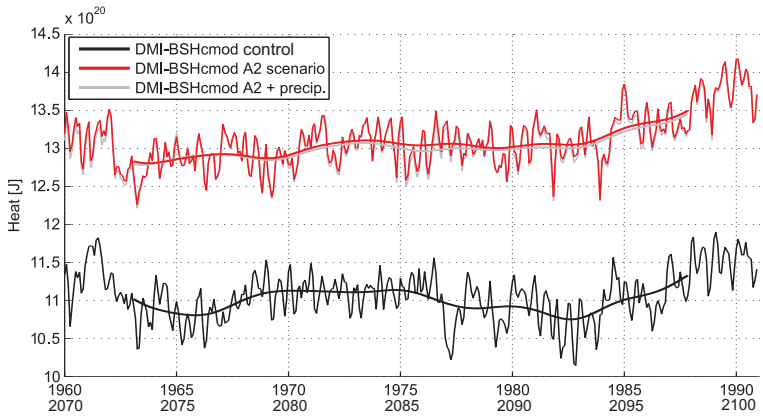

Figure 42: Monthly mean volume integrated North Sea heat content. Thin line: harmonic fit of seasonal cycle subtracted. Thick line: 3 years lowpass filtered (Lanczos filter).

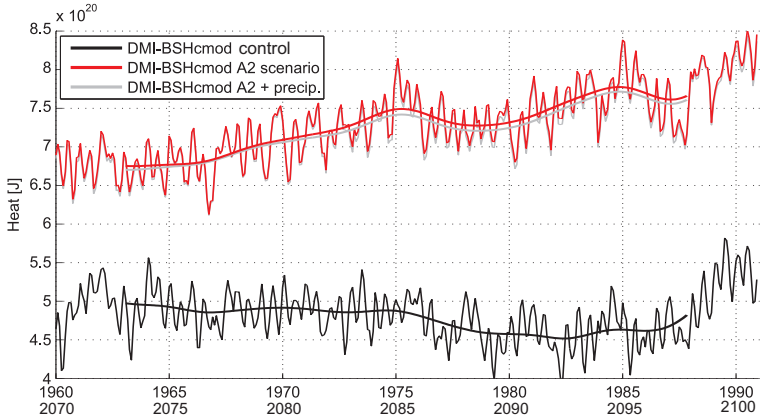

Figure 43: Monthly mean volume integrated Baltic Sea heat content. Thin line: harmonic fit of seasonal cycle subtracted. Thick line: 3 years lowpass filtered (Lanczos filter).

The transition zone volume averaged salinity shows a much larger variability than the North Sea or the Baltic Sea (note the different scale in Figure 45), but the interannual variability has many features in common with that of the Baltic Sea. Some seasonality is seen, especially in the top 10 m, where the wintertime salinity in some years is up to 4 units higher than the mean value for the rest of the year. In other years, no wintertime peak is seen.

From the green spin-up phase curves in Figure 45, it is seen that the initial salinity has been about 0.1 too salt for the model in the North Sea, so the salinity decreased in the spin-up phase, but appears stable in the first years of the model simulations. The Baltic Sea salinity seems more stable in the spin-up phase, but since the time scale for salinity changes in the Baltic Sea is long, it cannot be ruled out that the interannual variability in the Baltic Sea is affected by the initial conditions. The transition zone

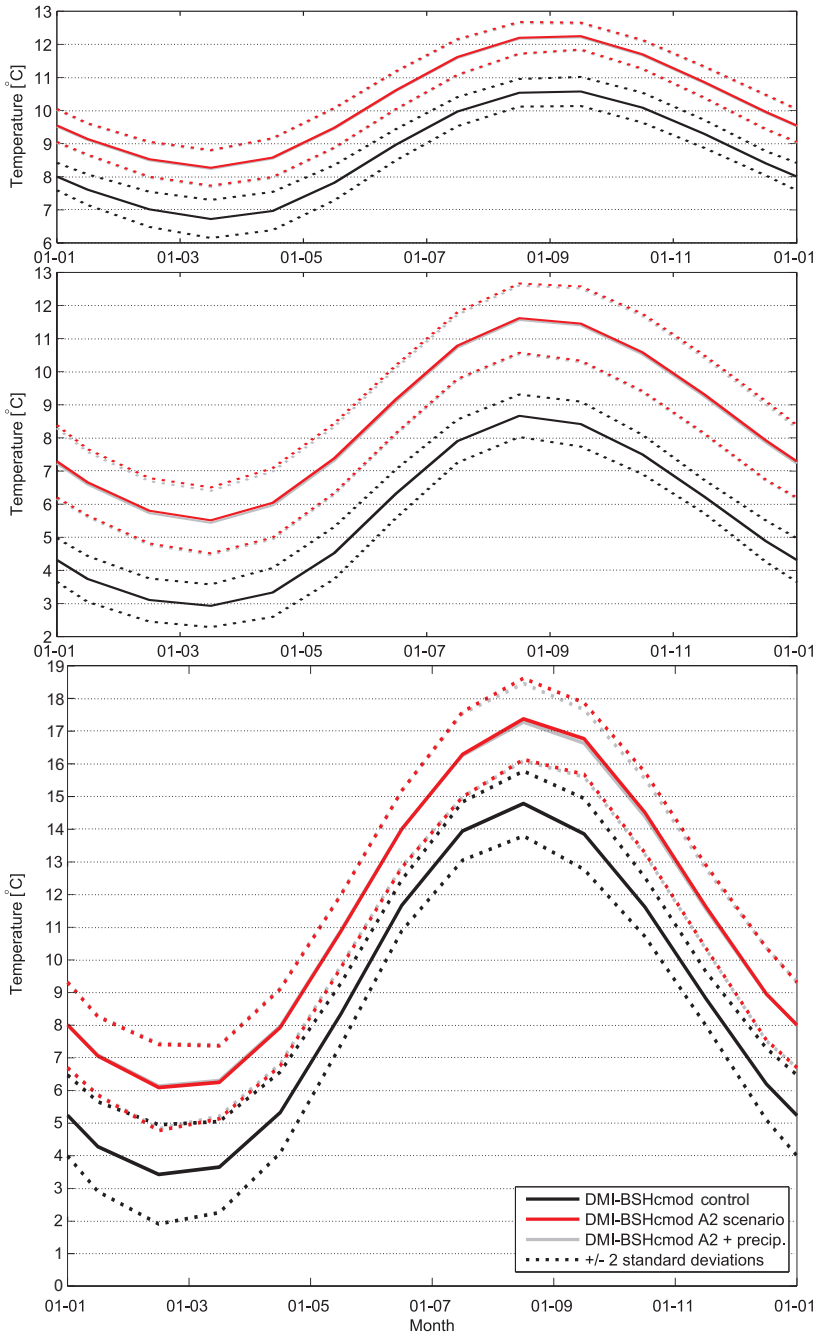

Figure 44: Mean seasonal variations in volume mean temperature. Top: North Sea, middle: Baltic Sea, bottom: transition zone. Note that the scale is the same for the three areas, but that the y-axis does not go to zero in the top two.

lowpass filtered salinity decreased in the first half of the spin-up phase, and again in the first years of the model simulations, especially in the surface.

The future scenario salinity of the Baltic Sea is highly dependent on whether the change in precipitation is included in the simulation. In the simulation where changes in precipitation were ignored (red curve in Fig. 46), salinity remained much like in the control run, with an increase towards the end of the simulation of 0.3. The increase may be due to increased salt water inflow (Chapter 7.7) or evaporation. When changes in precipitation were included, the salinity fell with a rate comparable to that observed in stagnation periods (*e.g.* Feistel et al., 2008). However, since the characteristic time scale of the Baltic Sea salinity is comparable to the length of the model simulations, and the scenario initial conditions are by nature unknown, the time slice simulations cannot be used to put an absolute value on the Baltic Sea salinity, only to indicate that the cmod model supports a stabile or decreasing future Baltic Sea salinity, in agreement with The BACC Author Team (2008) and references therein.[14]

The transition zone salinity changed both because of wind pattern changes and because of the increased freshwater forcing. In the scenario without changed precipitation, the volume averaged salinity was on average 0.3 higher than in the control run, while it was on average 0.4 lower than the control run in the scenario with changed precipitation. Most of the mean value difference between the two scenarios is explained by the difference in the Baltic Sea salinity, but the difference in interannual variability was not explained this way.

The North Sea salinity results depend on the scenario, too. If the changes in precipitation were ignored (red line in Fig. 46), a small increase in volume averaged salinity was seen, whereas the scenario including precipitation changes (gray line) showed a small decrease in salinity. In both cases, the magnitude of the changes was comparable to the interannual variability.

7.3 Spatial patterns and seasonal variations

To compare the spatial patterns of the model temperature and salinity with the Janssen climatology (Figs. 11 and 12, page 33 and 34), the monthly mean cmod control run fields averaged over all model years were calculated at 5 m and 25 m, and from these, the mean, minimum, and maximum values were found (Figs. 47 and 48). Also, the lightship values were duplicated for easy comparison.

To allow detailed comparison with the vertical structure of the seasonal variability observed at the lightships, the 10 day running climatological mean of temperature, salinity, and density and the corresponding standard deviation were also calculated from the model data at the closest grid point of each lightship. The control run

[14] This could be tested by running the model scenario with an ensemble of initial conditions, but time has not allowed this.

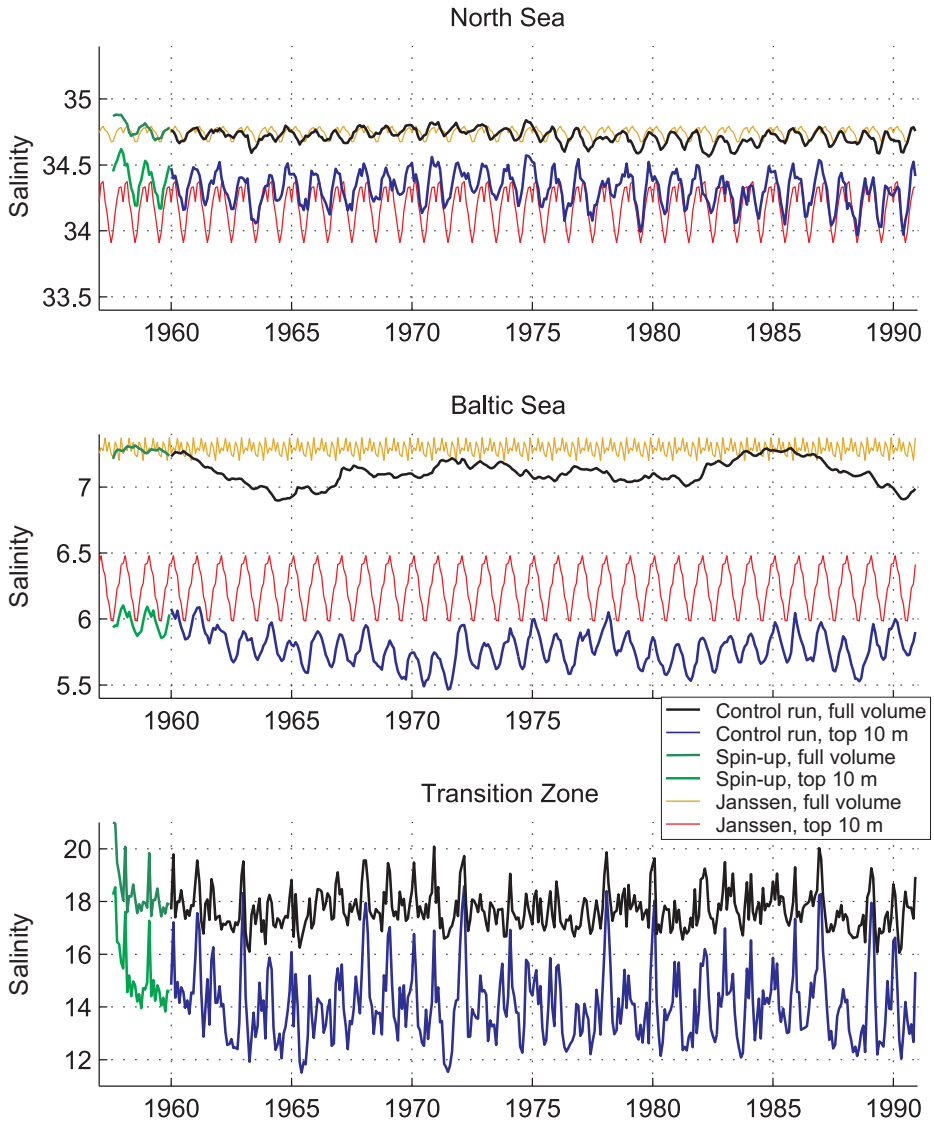

Figure 45: Top 10 m and full volume monthly mean salinity in control simulation, including spin-up phase, and from the Janssen climatology, for the North Sea, the Baltic Sea, and the transition zone. Note the different y-axis scaling in the transition zone.

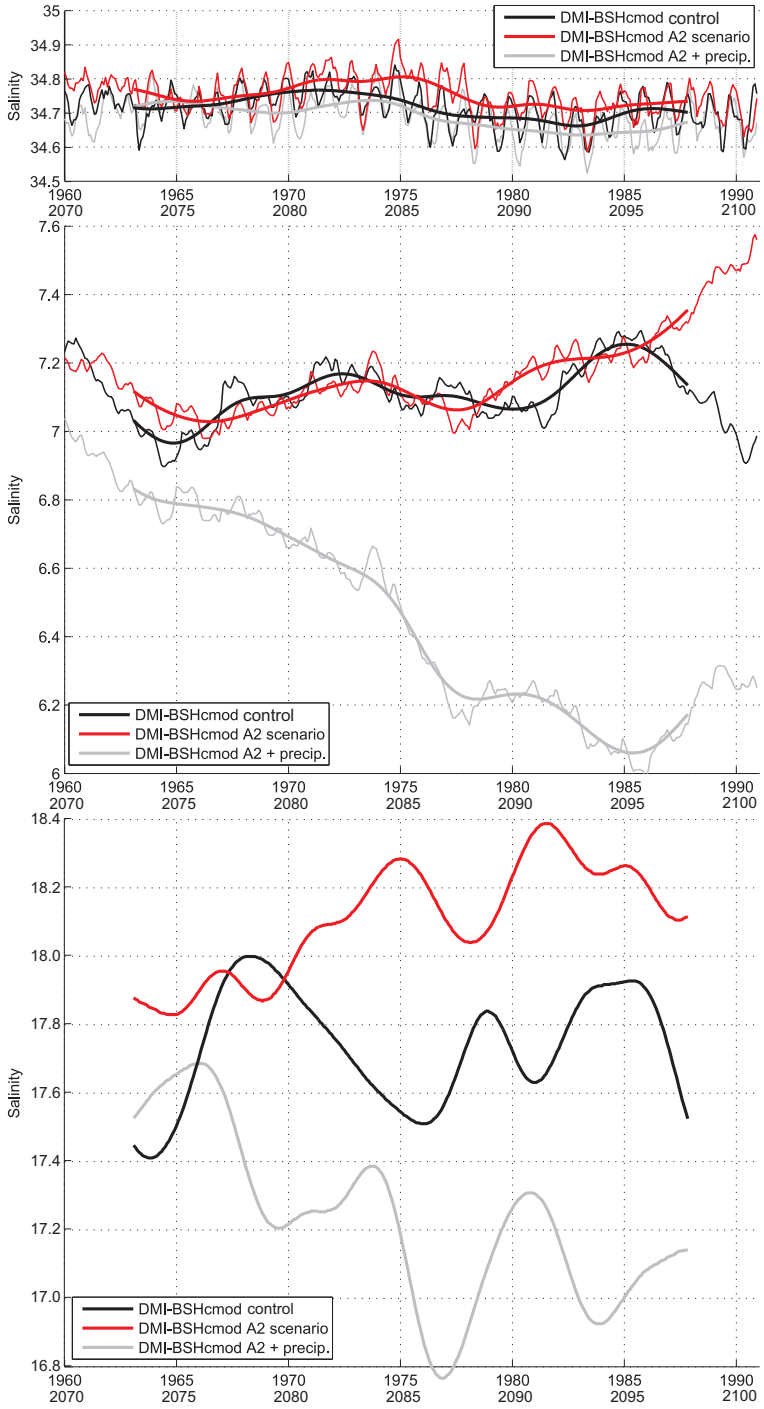

Figure 46: Monthly mean volume averaged salinity. Top: North Sea, middle: Baltic Sea, bottom: transition zone. Thin line: Monthly value. Thick line: 3 years lowpass filtered (Lanczos filter). The monthly values for the transition zone show large variability and have been left out (see Fig. 45).

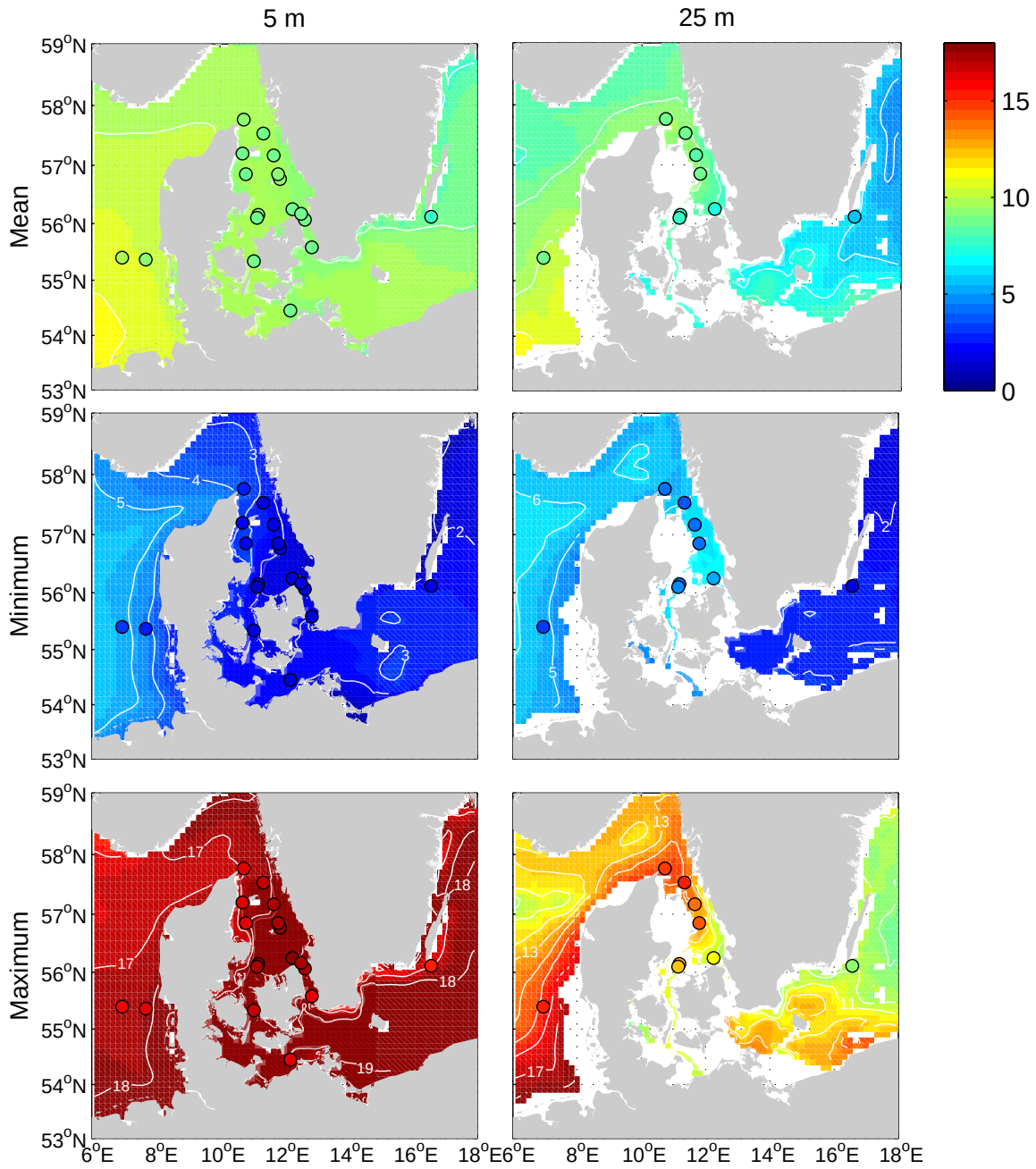

Figure 47: 5 m (left) and 25 m (right) temperature in the model control run and at the lightships (colored dots). Top: mean value, middle: minimum value from monthly means, bottom: maximum value from monthly means. Compare with climatology in Figure 11, page 33.

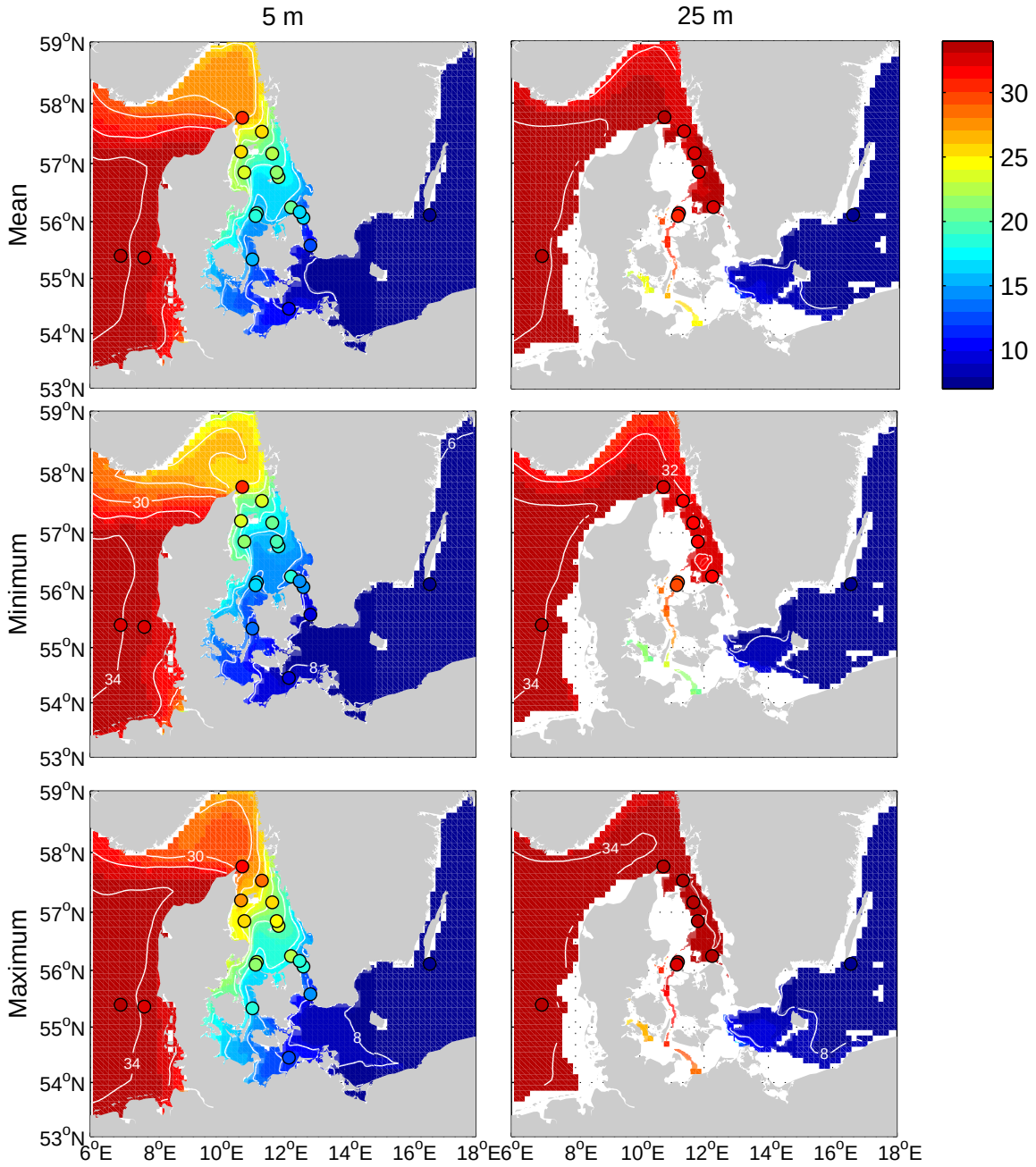

Figure 48: Spatial pattern of the 5 m (left) and 25 m (right) salinity in the model control run and at the lightships (colored dots). Top: mean value, middle: minimum value from monthly means, bottom: maximum value from monthly means. Compare with climatology in Figure 12, page 34.

temperature and salinity isopleths for l/s Gedser Rev, l/s Halsskov Rev, and l/s Fladen are shown in Figures 49 and 50 and the scenario salinity at Halsskov Rev is shown in Figure 51. Figures from other stations are available in the electronic supplement.

The model is in general 0.5–2°C warmer than the climatology and the lightship data. The main exception is the subsurface summer temperatures where the model showed cooler temperatures than the climatology at 25 m in the North Sea and the Baltic Sea as well as below the pycnocline in the transition zone. The geographical pattern of the control run model salinity in the open water of the North Sea and the Baltic Sea were close to the Janssen climatology. Below the pycnocline, the model control run and lightship data in Kattegat were also very similar, but the salinity above the pycnocline in the transition zone and in Skagerrak was generally too low. The difference can be described as a north-westward shift of the salinity gradient and means that the model monthly mean maximum has closer resemblance to the climatological mean than to the climatological maximum. Also, the transition zone halocline had a sharper vertical salinity gradient in the model than observed. The summertime peak in bottom salinity seen in the lightship observations (Chapter 4.5) is also seen in the model and it is stronger at l/s Gedser Rev, where the 20 m August mean salinity in the model control run was 26, 6 units higher than observed.

Since the modeled surface salinity was lower than observed and the salinity below the pycnocline was close to or higher than the observed, the model stratification was stronger than observed. This is further investigated in Chapter 7.6.

In this analysis the model control run representing year 1960–1990 was compared with lightship data mainly from the 1930s, 1950s, and 1960s, and to the Janssen climatology, which were based on data from 1900–1996, but with most data in the last part of the 20th century. Thus, stationarity of the temperature and salinity statistics were implicitly assumed. If considering the observed long-term variability (*e.g.* Fig. 14 page 37) this could introduce an error of up to 0.9°C and 0.9 in temperature and salinity, respectively, not taking the warming towards the end of the 20th century into account.

This possible sampling error covers the difference between modeled and observed temperature, but as shown in Chapter 7.5, it is not the case at the Drogden Station. The differences in transition zone surface salinity are larger than this possible sampling error.

The changes in surface salinity depend on the scenario, as also described for the volume averaged salinity (Chapter 7.2). In the scenario where the precipitation was not changed, the largest mean changes were seen in the northern Kattegat, with and increase of more than 1 (Fig. 53). The changes were largest in November–February and June–August (see electronic supplement). In the scenario with changed precipitation, the surface salinity was on average lower in almost the whole model domain, with the largest mean value changes in the southern Baltic Sea and in wind protected parts of

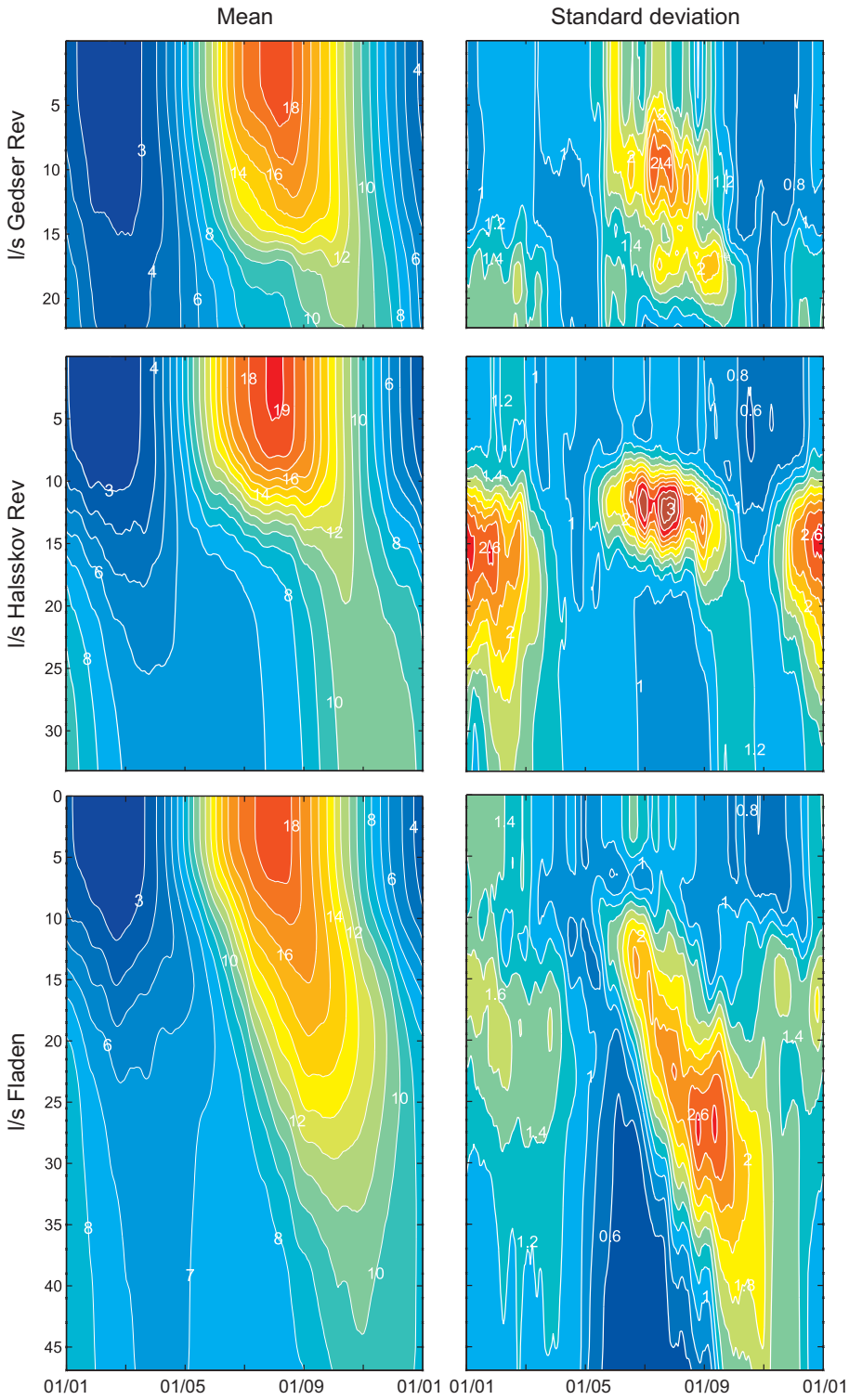

Figure 49: Isopleths of control run seasonal temperature variations (°C as a function of the time of year and depth [m], 10 day running mean) from l/s Gedser Rev (top), l/s Halsskov Rev (middle), and l/s Fladen (bottom). Mean values left and standard deviations right. See also similar plot for observations in Figure 15, page 40.

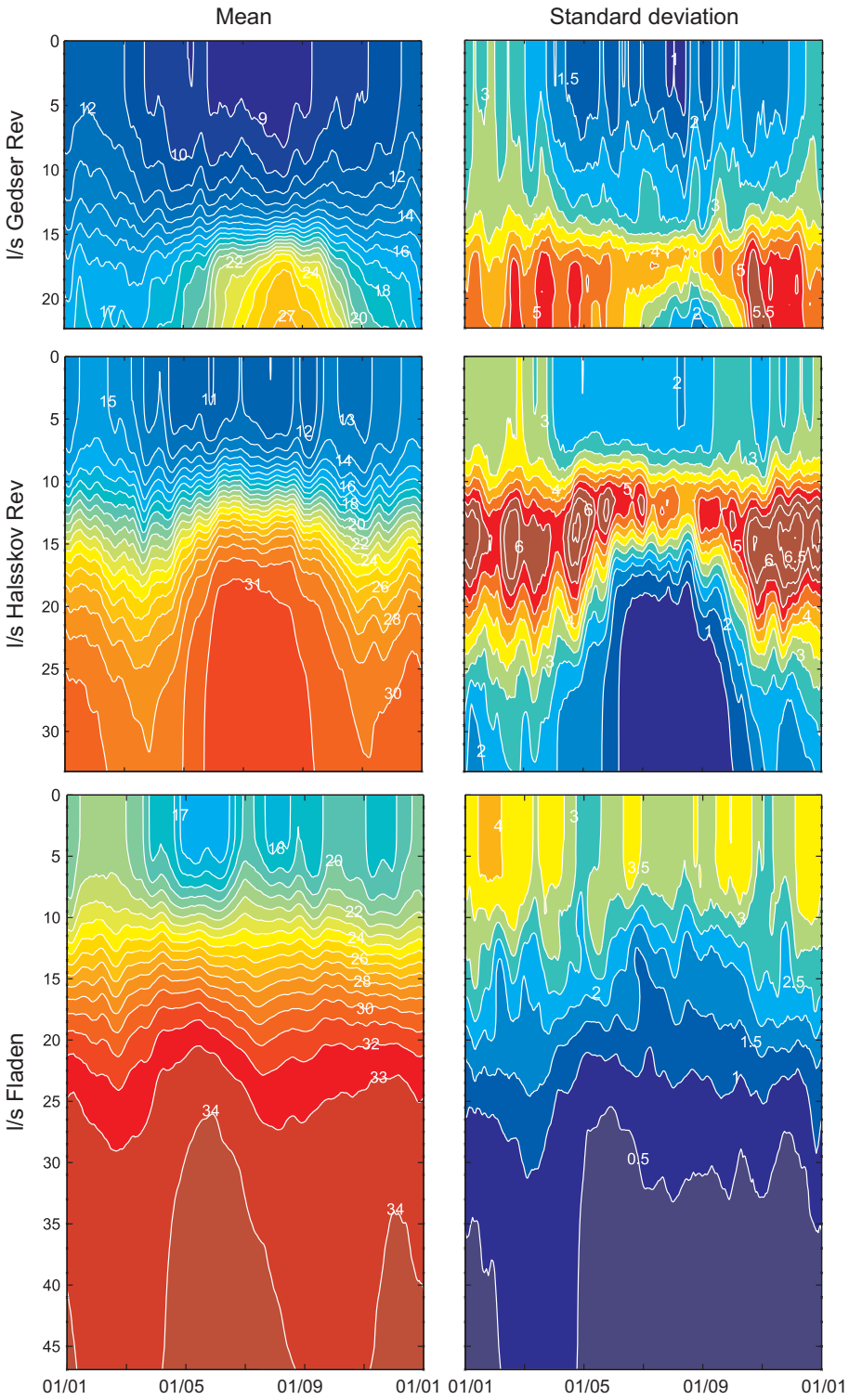

Figure 50: Isopleths of control run seasonal salinity variations (as a function of the time of year and depth [m], 10 day running mean) from l/s Gedser Rev (top), l/s Halsskov Rev (middle), and l/s Fladen (bottom). Mean values left and standard deviations right. See also similar plot for observations in Figure 16, page 41.

the transition zone. The salinity decrease was up to 0.7. However, the changes in the transition zone, the Skagerrak, and the Norwegian Coastal Current were very dynamic and in some months the transition zone salinity increased (see electronic supplement).

The salinity changes in the deeper parts of the transition zone were smaller than those at the surface, and similar in the two simulations (Fig. 51 and electronic supplement). Most of the year, a small decrease (less than 0.5) was seen below 20 m at l/s Fladen, but in September and October and in the spring a small increase was seen in both scenarios. The spring increase lasted longer in the simulation without changed precipitation. At l/s Halsskov Rev, the seasonal variation of the halocline depth was decreased in both scenario runs, and again the salinity below the halocline was slightly decreased in summer and winter but increased in late October and November and in March, April, and May. The spring increase and summertime decrease was reflected at l/s Gedser Rev as a broadening of the summertime deep water peak and a decrease of the maximum value. The decrease was largest in the scenario with changed precipitation.

The sea surface temperature in the model control run and the change in the scenario are seen in Figure 53 (note the different color scales if comparing with the air temperatures in Figure 29, page 60). The difference in warming between the North Sea and the Baltic Sea is clear and can be explained by the gradient in the air temperature change in combination with the relatively small temperature increase in the open boundary conditions. Even with these differences, the Baltic Sea surface temperature increase was smaller than the air temperature increase, especially in summer. The area mean sea surface temperature increase was 2.2°C in the North Sea, 2.9°C in the transition zone and 3.4°C in the Baltic Sea.

The temperature changes in the deep parts of the transition zone follow some of the same patterns as the salinity. In general, a warming is seen, but it is smaller than above the pycnocline. The dominant features at l/s Fladen are a relatively large increase in July and August, where it seems that much of the surface warming was transported downwards, and a relatively small increase (in the simulation with changed precipitation even a decrease) in September and October centered at 30 m (see figures in the electronic supplement). This could be linked to the increased water inflow from the North Sea to the Kattegat. The temperature increase is more uniform over the year at l/s Halsskov Rev and l/s Gedser Rev.

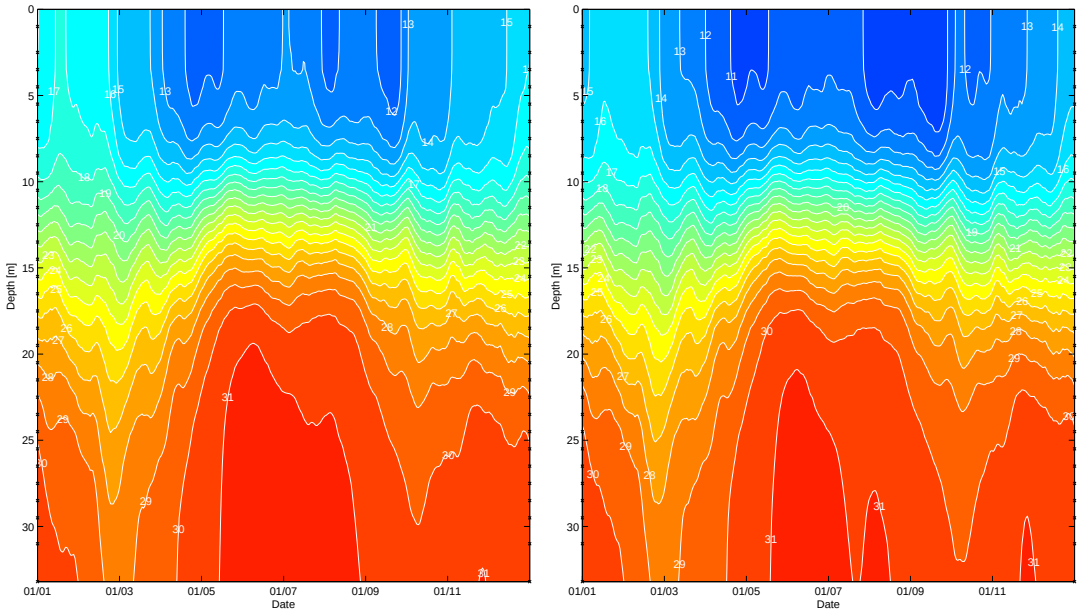

Figure 51: Isopleths of scenario run seasonal salinity variations (10 day running mean) from l/s Halsskov Rev. Left: scenario run without changed precipitation (v12), Right: scenario run with changed precipitation (v10). Compare with the control run isopleth in Figure 50.

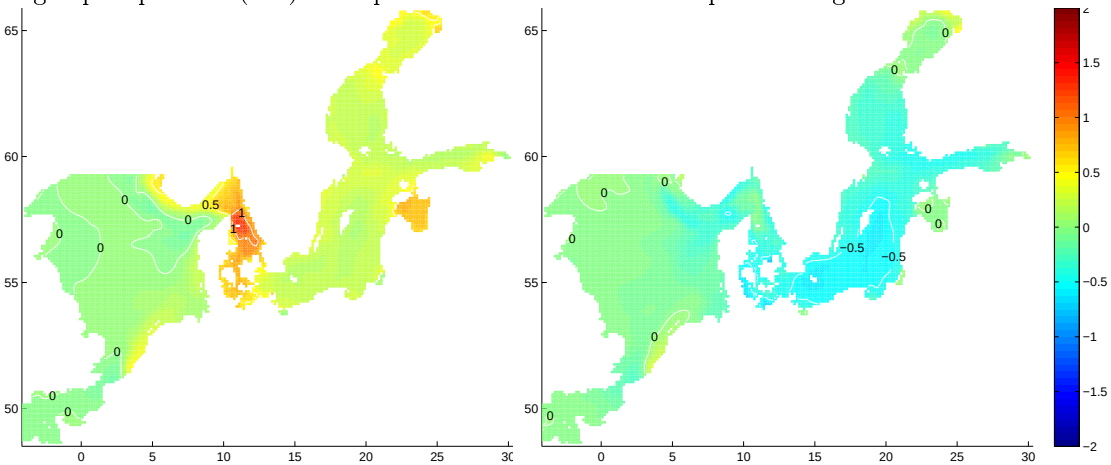

Figure 52: Mean change in surface salinity. Left: no change in precipitation (v12). Right: precipitation changed (v10).

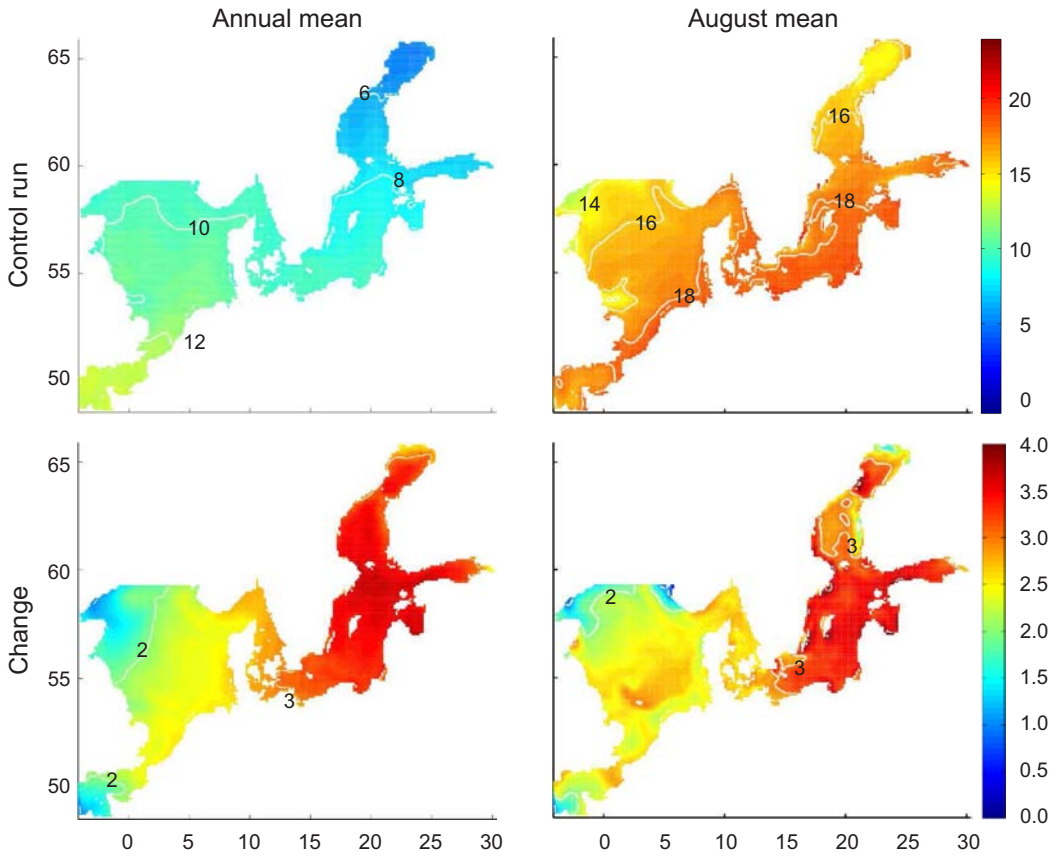

Figure 53: Surface temperature in model control run (top) and change between control run and scenario (below). Left is annual mean, right is August mean.

7.4 Steric effects

As described in Chapter 5.1, the steric sea level is not included in cmod, and since steric effects will be dynamically adjusted (Chapter 4.5). A dedicated study is needed to give a precise estimate of the local and regional effects in coastal regions. However, to provide a rough estimate of the order of magnitude of the locally generated effects and assess whether the local steric effects are important for the sea level rise budget, the basin mean steric effect changes were calculated for the North Sea, the Baltic Sea, and the transition zone. All height signals were calculated relative to the control run mean steric height of each basin. For computational reasons, the basin monthly mean temperature and salinity were used, neglecting the effects of the non-linearity of the equation of state. This is a rough assumption, especially for the Baltic Sea in the wintertime, where the northern and eastern parts with low salinity and temperature close to the freezing point may show contraction when heated.

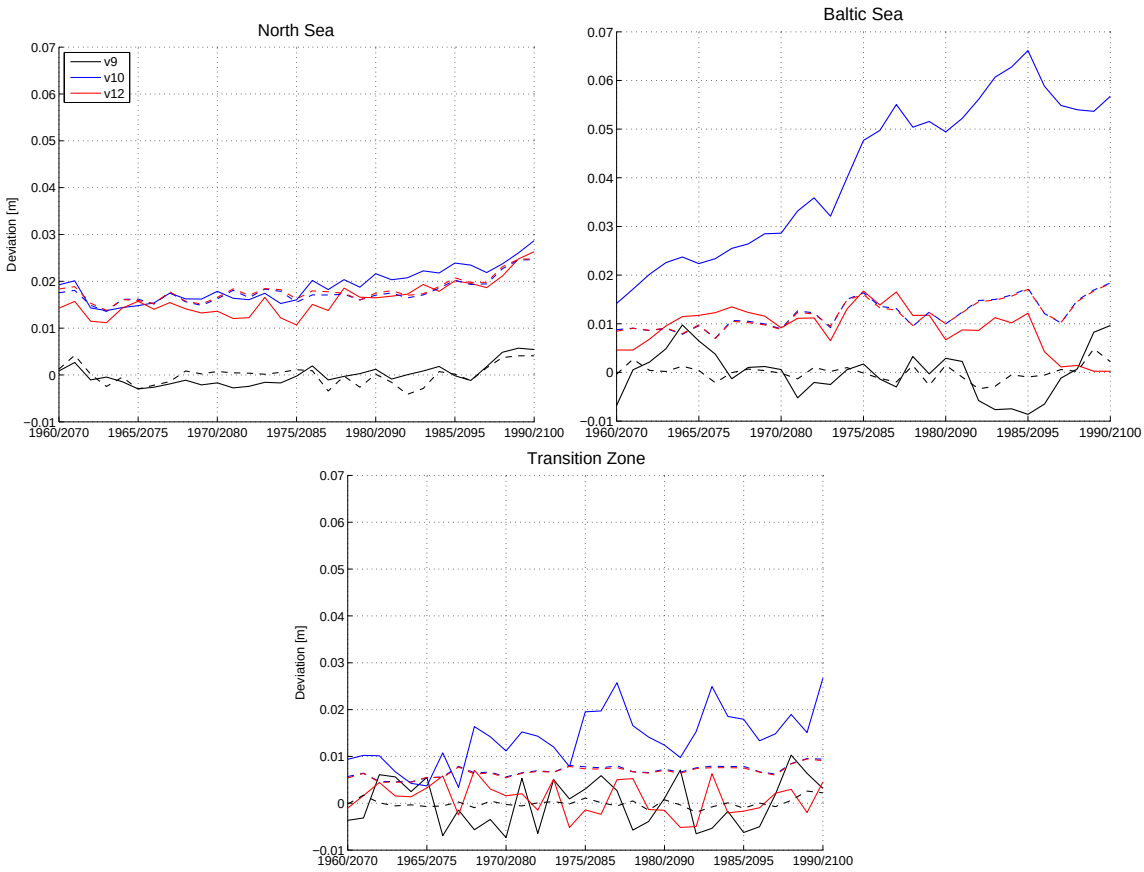

Figure 54: Rough estimate of the area averaged, annual mean static steric height for the North Sea (top, left), Baltic Sea (top, right), and transition zone (below), for the control run and two scenarios. Solid lines indicate the steric height taking both temperature and salinity into account, for the dashed lines only temperature is taken into account (salinity is kept at control run average).

Table 10: Estimated mean change in area averaged static steric height.

	North Sea	Baltic Sea	Transition zone
Scenario without changed precipitation	0.016 m	0.009 m	0.001 m
Scenario with changed precipitation	0.019 m	0.04 m*	0.024 m
Temperature change alone	0.018 m	0.012 m	0.008 m

* Increasing from 0.02 m to 0.06 m.

With these precautions, the interannual variability in the control run was small, below 1 cm (Fig. 54). The temperature generated increase in steric height was estimated to be 1–2 cm for both scenarios. The total steric effect change in the North Sea was largely independent of salinity. In the transition zone, the increased salinity in the scenario without changed precipitation (v12) compensated for the heat expansion, while the decreased salinity in the scenario with changed precipitation (v10) roughly doubled the signal. For the Baltic Sea, the v10 scenario stands out, with increasing steric effect corresponding to the decreasing salinity and a maximum annual mean of 6.5 cm.

Thus, even with the coarse assumptions made for these calculations, it is clear that the locally generated changes in steric effect will be small compared to those of the North East Atlantic Ocean, basically because of the relatively shallow water depths. The main steric contribution to the sea level rise budget will thus be that of dynamical adjustment of the global and regional changes.

7.5 Salinity and temperature at the Drogden Station

The Drogden Station is located in the southern end of the Drogden Sill, and in this shallow area the water column is mixed at most times. At the Drogden Station, daily surface temperature and salinity measurements have been made during the entire modeling period. As shown in Figure 55B, the daily salinity measurements show a base level of 8–10 (lowest in summer), corresponding to outflowing Baltic Sea water, and a number of spikes of varying magnitude of up to 25 in this 3 year window, corresponding to Kattegat water. The model control run showed the same type of dynamics, but the salinity rarely exceeded 20, and the base level also often had slightly lower salinity than observed. The annual mean salinity in the control simulation was generally about 1 unit lower than the observed, and the interannual variability is not like the observed, but of similar magnitude (Fig. 55A).

The future scenario salinity at Drogden showed the same general features as the transition zone integrated salinity (Figs. 46 and 55A), with a small increase in salinity in the scenario without changed precipitation and decreasing salinity in the scenario with changed precipitation. However, as seen in Figure 55B, the climate change signal was much smaller than the short term variability, and the dynamical features had the same characteristics in the control and scenario runs. Also, since the forcing in the two future scenarios was the same except for precipitation, the daily variability was almost the same, and the difference is only seen as a small offset (in Figure 55B, the gray curve is almost hidden by the red curve).

Figure 56 is an extension of Figure 13, page 36, where the annual mean and 10-year running mean temperature observations from the Copenhagen area are overlaid with the mean modeled results from the location of the Drogden Station. Here, the cmod control run (v9) mean temperature is 0.6°C warmer than observed. Also, the

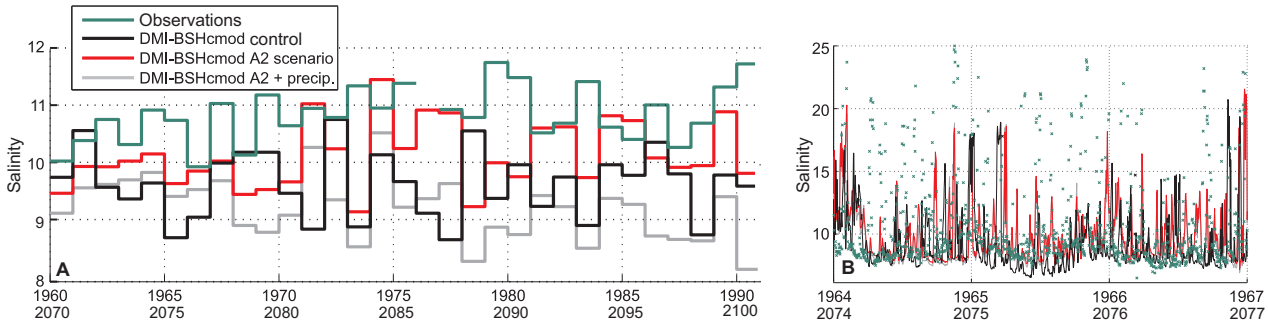

Figure 55: Salinity at the Drogden Station in the Sound (55.53N, 12.72E). A) Annual mean values. B) Daily observations (green marks) and model daily mean values for year 1964–1966 (arbitrarily selected).

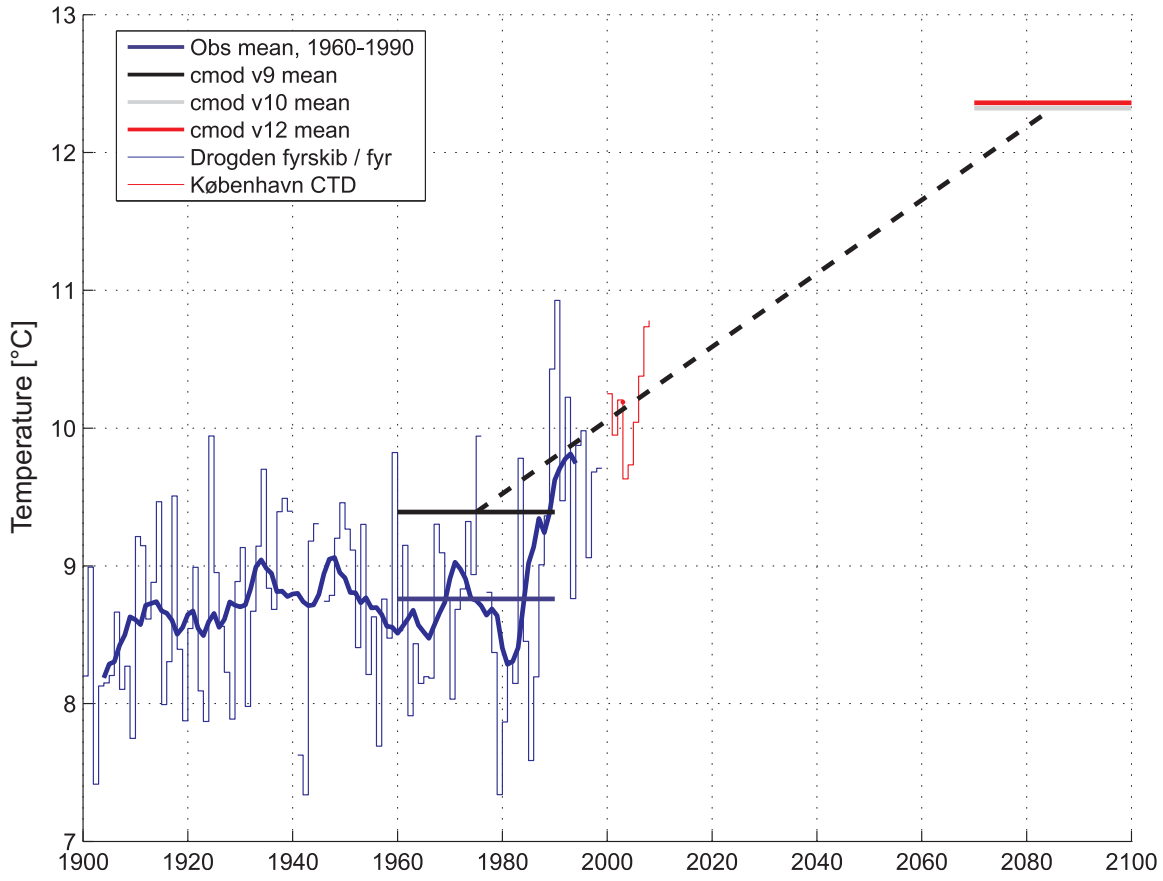

Figure 56: Observed and modeled sea surface temperature in the Copenhagen area. The observational data are copied from Figure 13 page 36 and the blue horizontal line show the observed 1960–1990 mean value. The other horizontal lines represent the model mean values for the grid point closest to the Drogden station. The two scenario results (gray and red lines) lay close together. The dashed line represent the average rate of temperature increase needed to obtain the projected changes.

projected 21st century warming of 2.9°C is large compared to the changes of the 20th century, but the rate of change is not unrealistic when comparing to the changes seen in recent years. Finally, the mean changes for the two future scenarios are almost identical, so the surface temperature change projections are not affected by the large diversity of the salinity projections.

7.6 Stratification

As for the observational data (Chapter 4.6), the model stratification is analyzed based on the difference between the 20 m and 5 m salinity, and the model coverage allows a mapping of the difference (Fig. 57 and electronic supplement). In Kattegat, the maximum control run stratification was seen in May, while the south-eastern transition zone showed a maximum in July and August. The main pycnocline in the Arkona Basin is below 20 m, and thus the 20 m−5 m salinity difference is not a good indicator of the stratification in that area. As noted above, the model surface salinity is lower than observed, and the stratification is stronger than observed. However, the geographical distribution with relatively low stratification at l/s Fladen and high stratification at l/s Kattegat SW is resembled in the model. The relatively high values in southern Kattegat were due to a relatively high average stratification lasting throughout the fall and winter seasons.

The projected future changes are scenario dependent. In the scenario without changed precipitation, the surface salinity increased in the transition zone, and thus the stratification was weakened, especially in the Kattegat (Fig. 57C). In the scenario with changed precipitation, the surface salinity on average decreased, and the stratification increased. There, the largest changes in the late summer and fall were seen in the Great Belt and the southwestern and northern Kattegat (Fig. 57D). In both scenarios the changes were less than 10%.

If the cmod simulations are compared to those of the CONWOY project (Søndergaard et al., 2006, Figure 7.1, note the reversed color scale), it is obvious that the results are sensitive to the forcing and model setup. However, in both of the present cmod simulations and in the CONWOY simulations, the winter stratification is in general decreased, and the spring stratification in the southern part of the transition zone is increased. For the late summer and fall, where oxygen depletion is most likely, the results are model dependent, and should thus be used with care.

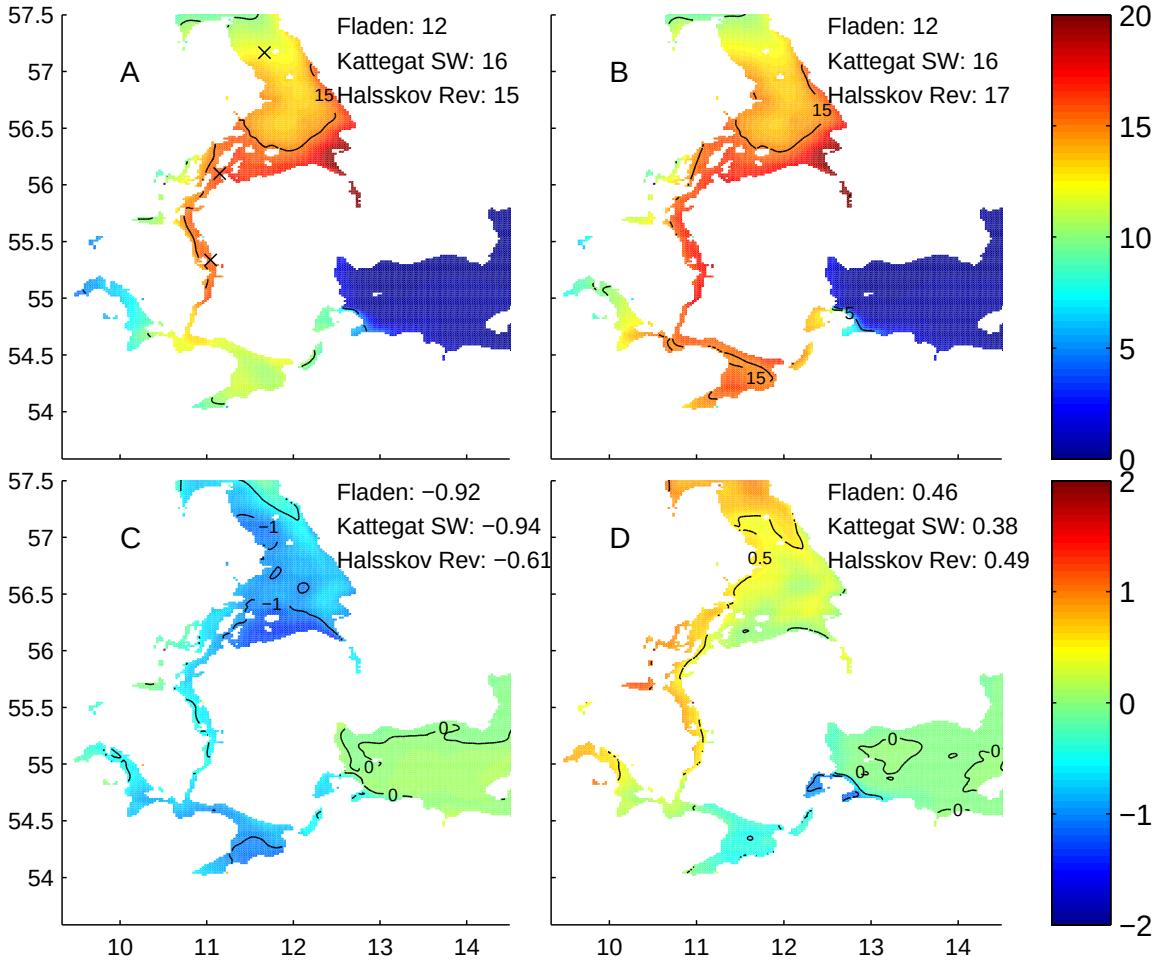

Figure 57: Model stratification calculated as the difference between the 20 m and 5 m salinity. The white areas represent land areas and areas where the water depth is less than 20 m. A: mean value for control run. B: same for August, September and October (ASO). C: ASO mean increase in scenario without changed precipitation. D: ASO mean increase in scenario with changed precipitation. In panels A and B, high values indicate high stratification. In panels C and D, positive values indicate increased stratification. The overlain text displays the model results at three selected lightships, l/s Fladen, l/s Kattegat SW, and l/s Halsskov Rev. The ship locations are marked with 'x' in panel A.

7.7 Inflows to the Baltic Sea

The observed and modeled major inflows to the Baltic Sea were quantified using the inflow index of Franck, Matthäus, and Sammler (1987) (here following Matthäus and Franck (1992)):

$$Q = 50\left(\frac{k-5}{25} + \frac{S-17}{7}\right)$$

where k is the number of consecutive days where the salinity at l/s Gedser Rev fulfills the criteria

$$1 - \frac{S_{0\text{ m}}}{S_{20\text{ m}}} \leq 0.2 \text{ and } S_{20\text{ m}} \geq 17$$

and $S_{0\text{ m}}$, $S_{20\text{ m}}$, and S are the surface, 20 m (bottom), and mean salinity at l/s Gedser Rev, respectively. This index was chosen to allow comparison between model and observations. The index was designed to measure winter inflows with high salinity in the whole water column. Franck et al. (1987) set up several criteria to determine the exact duration of each inflow. I have simplified this, and allowed interpolation across single days of missing observations and merged inflows which were up to two days apart. l/s Gedser Rev was moved on March 31, 1976, so for the observational record, data were only used between January 1, 1960 and March 31, 1976 (52% of the modeling period of 1960–1990). The observational index was based on daily observations (made in the morning), while the model based index was based on daily mean values.

Figure 58 shows the detected inflows as a function of time and the distribution of inflows when categorized by intensity ($Q \leq 15$: weak, $15 < Q \leq 30$: moderate, $30 < Q \leq 45$: strong, and $Q > 45$: very strong). When considering that the observational period was only approximately half as long as the modeling period, it is clear that the model control run has too few weak inflows, and possible also too few strong and very strong inflows, though the modeling period is too short to confidently determine that. The number of moderate inflows was approximately as observed.

When looking at the differences between the control and scenario runs, the number of detected weak and moderate inflows has gone up by 63% and 50%, respectively, in the simulation without changed precipitation. In the simulation with changed precipitation, the number of moderate inflows is diminished. From the time series plot, it is seen that the timing of inflows is often the same in the two scenarios, which is a natural consequence of the identical wind- and pressure forcing. However, the inflows in the scenario with changed precipitation are generally weaker. Thus, the simulation without changed precipitation indicates that increased wind forcing may increase the number of detected inflows. The effect on the Baltic Sea salinity was limited, but many of the inflows occurred in the last 10 years of the simulations, where the Baltic Sea salinity also increased. The results indicate that decreased mean salinity in the transition zone may limit inflows to the Baltic Sea, even though the

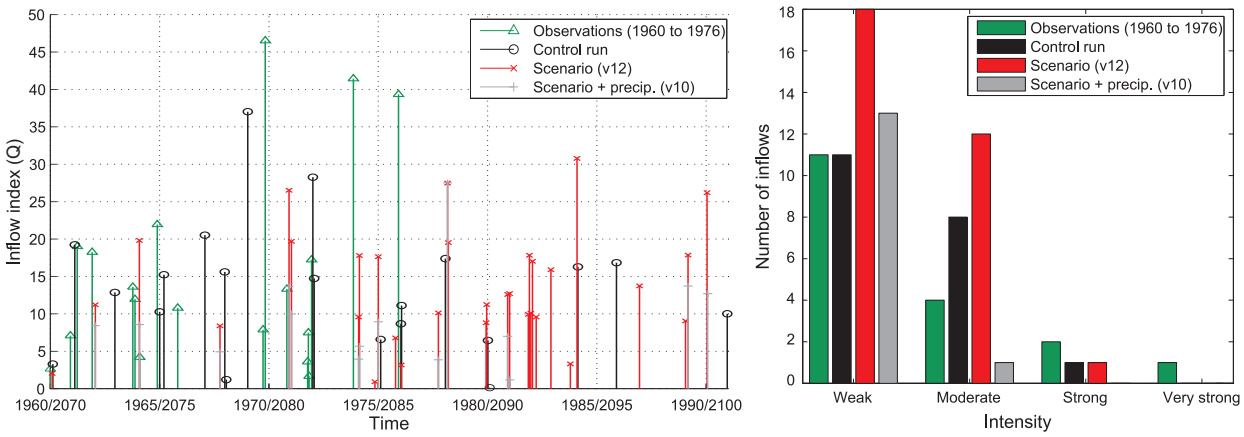

Figure 58: Observed and modeled inflow indices for inflows to the Baltic Sea. Left: ordered by date, right: sorted by magnitude ($Q \leq 15$: weak, $15 < Q \leq 30$: moderate, $30 < Q \leq 45$: strong, and $Q > 45$: very strong). Note that the observations only cover 52% of the model period, and the model results could be expected to have an accordingly larger number of inflows.

changes in the transition zone bottom salinity were smaller than the surface changes. The simulations do not include variations in the river runoff, which have been shown to be important for the decadal variability (Matthäus, 2006), nor the effects of externally forced increased mean sea level, which may raise the bottom salinity (see Chapter 8).

8 Overall discussion

Methods and materials

The observational records in the transition zone have proven to be a valuable source of climate change information for the 20th century. The accuracy of the lightship temperature and salinity measurements does not live up to the international standards (UNESCO, 1988), but the spatial coverage and temporal resolution, as well as the large signals compensates for this. The tide gauge records live up to the standards for the GLOSS database (see Chapter 2.3) and also give detailed information on past storm surges.

The modeling part of this study can be seen as a proof of concept that cmod is suitable for long-term climate simulations. Throughout both test runs and the final simulations presented in this thesis, it has proven to be stable for multi-year simulations, also regarding sensible parameters such as the Baltic Sea salinity. No re-initialization or nudging towards climatology has been performed during the simulations. The nested system has allowed simulations without model boundaries in the transition zone. This has enabled a detailed analysis of the transition zone itself, but also opens up for future studies of the interaction between the North Sea and the Baltic Sea on climatic time scales. Regarding future modeling approach, Kjellström et al. (2005) have shown the value of a coupled ocean–atmosphere model, especially for the Baltic Sea region. Several other simulations with the current setup would also be valuable, and has become more feasible, since cmod has been ported to DMI's new supercomputer after the completion of the simulations presented here. At the time of the submission of this thesis, a simulation based on downscaled ERA40 reanalysis data is on the way. It could be interesting to assimilate the historic ocean observations in this type of simulations, and the simulation makes way for sensitivity experiments and detailed process-oriented studies. If focusing on the Baltic Sea salinity and inflows to the Baltic Sea, transient simulations would also be of value.

Other ocean models have been used for climate simulations in the North Sea and the Baltic Sea, each with their advantage, such as coupling with an atmospheric model or an ecological model, or a model domain covering the North East Atlantic shelf sea (*e.g.* Meier, 2006; Schrum et al., 2006; Hjøllo, Skogen, & Svendsen, 2009; Ådlandsvik, 2008). The major advantages of using cmod have been the two-way nesting in the transition zone and the fact that the model is well-tested for operational use, giving confidence in the model, especially regarding storm surges.

The atmospheric forcing has allowed detailed simulations of a future climate change scenario. The forcing has uncertainties common for most RCM simulations. As the scenario forcing is one member of an ensemble of atmospheric simulations within the PRUDENCE project, the uncertainty could be addressed by running the model with other members of the ensemble. However, computer resources have been lim-

ited, and the present forcing was chosen for its high temporal and spatial resolution, which is not generally available. Two factors stand out as extra challenging for ocean simulations. The missing gust parameterization cause systematic underestimation of extreme winds. This is especially important for storm surge simulations, and means that this thesis can only provide a lower estimate of the changes associated to the selected scenario. The other item is the unrealistic summertime changes over the central and eastern Baltic Sea, which could be avoided with a coupled model. The atmospheric forcing has proven to be a stable basis for the ocean simulations, but is probably the main source of uncertainty.

Sea level

Table 11 shows a budget of the most important terms regarding sea level rise at Danish coasts, based on the literature review and results of this thesis. The individual terms are discussed below.

The sea level trends observed by satellite altimetry show the collected global and regional changes for recent years. For the North Sea, the trend is likely to be lower than the global mean (Chapter 2.4.1). This agrees well with the findings of the Deltacommissie (Veerman, 2008), who did not find an increased sea level trend at the Dutch coast. The rise seen in recent years at the Danish North Sea coast is larger, possibly due to wind setup (Chapter 2.4.2). Interestingly, an initial study of the satellite data indicates that the Baltic Sea sea level trend may be higher than the global mean for the measuring period of the satellites. The interannual variability in the Baltic Sea sea surface height is large, but a best estimated rise 3 times larger than for the North Sea raises the need for future investigations.

The future regional changes induced by changes in the wind and air pressure, as well as additional freshwater input, are projected to be small in the annual mean (Chapter 6.3). Steric effect changes generated in the North Sea and the Baltic Sea will also be small (Chapter 7.4). Thus the annual mean regional signal is likely to be dominated by gravitational effects, which depend on the amount of ice melting, especially from Greenland, and possibly dynamic and steric changes in the North-East Atlantic Ocean which are projected to be on the order of 0.1 m (Mitrovica et al., 2001; Bindoff et al., 2007).

The most important local factor in Denmark is the isostatic land rise, which has canceled out previous sea level rise in northern Denmark, and will continue to ease the effects of sea level rise. The 19 year running mean in-situ observations also show decadal variability on the order of a few centimeters and especially the exposed stations at Hirtshals and Hornbæk show high correlation with NAO, in agreement with earlier studies (Andersson, 2002; Wakelin et al., 2003; Tsimplis et al., 2006), while the stations further inside the transition zone show little correlation with the NAO index (Chapter 2.4.1).

Table 11: Budget of observed and future mean sea level change components and additional change in high water situations.

	Observed change	Scenario increase by year 2100
Global mean	20th century: 1.7 ± 0.3 mm/yr.[1] 1993–2008: 3.1 ± 0.1 mm/yr.[2]	IPCC: 0.18–0.59 m plus up to 0.17 m from linear increased ice melt rates.[3] Others: 0.55–1.2 m is possible.[4,5]
Regional mean		
Steric	North-East Atlantic ∼0 mm/yr.[6] North Sea ≤ 0 mm/yr.[A] Baltic Sea > 0 mm/yr.[A]	+0.1 m in the North East Atlantic.[8], *B*
Dynamic		< 0.1 m.[C,5]
Gravitational		−80% to +10% of ice melt, depending on source.[8]
Local mean		
Isostatic	−1.5 to −0.3 mm/yr sea level rise equivalents at tide gauges in Denmark, largest decrease towards north.[9]	Unchanged.
Wind generated	> 0 mm/yr on the Danish North Sea coast in recent years.[A,10]	Additional 0.10–0.15 m on the Danish North Sea coast.[C]
High waters		
Tides		High tide increased on the order of 4–8% of mean sea level rise.[11]
Storm surge	Tendency for increase at western Danish stations.[D]	Danish North Sea coast: 0.15–0.2 m for 10 year event at Esbjerg. Transition zone ∼ 0.[E]

[1] Church and White (2006)
[2] Cazenave et al. (2008)
[3] Meehl et al. (2007)
[4] Rahmstorf (2007b); Grinsted et al. (2009); Pfeffer et al. (2008)
[5] Veerman (2008)
[6] Church et al. (2004); Levitus et al. (2005); Ivchenko et al. (2007); Cazenave et al. (2008)
[7] Landerer et al. (2007)
[8] Mitrovica et al. (2001)
[9] Per Knudsen, pers. comm.
[10] Knudsen et al. (2008)
[11] Flather and Williams (2000)

[A] Chapter 2.4.1
[B] Chapter 7.4
[C] Chapter 6.3
[D] Chapter 3.3
[E] Chapter 6.5 and this chapter

Whereas the modeled annual mean scenario changes are small over the whole model domain, a spatially varying winter time sea level increase was seen, with a January increase on the order of 0.07–0.15 m on wind-exposed coasts in the North Sea and in the Baltic Sea (Chapter 6.3). The increase is similar to the results of Suursaar et al. (2006), though their results show a more local increase on the Estonian coast.

Overall, the budget of past changes is balanced on the global scale, but has some open ends in the regional and local scale. For the future changes, uncertainty still remains for most items. On the global scale, the largest uncertainty is the climate change response of the large ice sheets. On regional scales, the gravimetric response is a major uncertainty, both since the ice sheet melting is uncertain, and because the "gravimetric fingerprints" identified by Mitrovica et al. (2001) have yet to be observed in nature. Hopefully, this will be resolved in the near future by a combination of gravimetric and altimetric measurements by satellites. Other regional and local phenomena also add to the uncertainty, but less than the above.

Despite the uncertainty, it is clear that the sea level around Denmark will continue to rise in the future, and it is very likely that the rate will increase over the 21st century. As it can be assumed that the isostatic land adjustment will continue at the same rates as today, in this scenario, the southern parts of Denmark will experience almost the full rate of global and regional change, while the northern parts will start to experience permanently increasing sea levels as well.

Storm surges on the Danish North Sea coast are likely to increase more than the annual mean, for three reasons. The model scenario shows larger monthly mean sea level changes in the winter than the rest of the year, extreme wind speed increase can cause a change in the statistics, and the tides may increase if the mean sea level goes up (see Chapter 6.2). For the model scenario for the station in Esbjerg, this adds together to an increase in the 10-year return height of 19–37 cm, additional to changes in the annual mean sea level, depending on whether the tides are included in the storm surge calculations and assuming an increase in the maximum tides of 4–8 cm (Chapter 6.5, Flather & Williams, 2000). The 1961–1990 10-year storm surge height calculated from observations was 3.52 m (Chapter 3.3), so this corresponds to an increase of up to 11% on top of the mean sea level changes. This is in the lower end of previous estimates, which seems reasonable in the light of the lacking gust parameterization and non-linearity of the problem (Debernard & Røed, 2008; Woth, 2005; Woth et al., 2006). In the transition zone and on the Danish Baltic Sea coast, storm surges are not projected to increase more than the mean sea level. Still, the storm surge return periods, also in these areas, will change significantly with the projected mean sea level changes.

Temperature and salinity

In the discussion of current and future global climate change, the temperature rise is perhaps the best understood indicator. In this light, the long observational records especially from the Drogden Station, but also from other locations in the transition zone are of high value.

The 10 year running mean surface temperature at Drogden Station show no significant trend from 1904 to 1985, with running mean values ranging between 8.2 and 9.1°C, but then a noticeable strong climatic signal in the end of the time series is seen, with a 10 year mean value centered in 1992 of 9.8°C, 0.7°C higher than earlier running mean values. The high temperatures are persistent till today. Available data from the other stations support the observations from Drogden Station. The size of the detected warming is in line with results from the Baltic Sea and the North Sea (Feistel et al., 2008; Belkin, 2009; MacKenzie & Schiedek, 2007b), and the long record of direct measurements provide a high degree of reliability. The difference between the temperature increase at the Drogden Station and in the records from Rødby and the Great Belt may partly be due to the location of the stations. The Drogden Station measured the open water temperature, while the Rødby and Great Belt records are both measured from the coast. According to Ærtebjerg (2007), the cooling in the beginning of the 1980s was more marked in the open water transition zone surface temperatures than in fjords and coastal seas.

The model results indicate that the observed warming will continue, and that it will be larger in the Baltic Sea than in the North Sea and larger in the surface than volume averaged. The rise in ocean temperature is lower than the rise in air temperature. These results are the consequence of the east–west gradient in atmospheric heating over the model area and the relatively small warming at the vertical boundary with the north east Atlantic Ocean (Chapters 5.2.3 and 5.3). For the scenario used in this thesis, the mean temperature increase ranges from a North Sea volume mean of 1.5°C to a Baltic Sea surface mean of 3.4°C. The results are within the range of other model results from the area (The BACC Author Team, 2008; Ådlandsvik, 2008), and show that the mean transition zone warming lay in between the surface warming of the North Sea and the Baltic Sea.

Observations and model results from the Drogden Station were used to compare the past and projected warming in the transition zone (Fig. 56) and this indicated that the 21st century scenario warming will be large compared to the 20th century data record, but that the average rate of change needed to obtain this warming was comparable to the observed rate of change in recent years.

The model showed a warm bias in the transition zone when validating against lightship data, except for the summer temperatures below the pycnocline. A similar bias was seen in the validation of the operational version of cmod (Chapter 7.1). However, the modeled changes are larger than the bias (4.6 times for the mean value

at the Drogden Station), so I expect the major uncertainty for the future temperature development to come from the forcing, and not from the model.

The salinity in the transition zone shows large variability, dominated by synoptic time scales. No long-term trends have been observed, but the observational data allow detailed studies of past events, here exemplified by the Baltic Sea inflow event of 1951 (Wyrtki, 1954; Matthäus, 2006). The horizontal and vertical details of the digitized daily salinity observations allowed a detailed analysis of the event during precursory, inflow, and recovery periods for the transition zone. The breakdown of the stratification and salinities of up to 23 at the entrance to the Baltic Sea was seen in the observations, and the sea level gradient in the transition zone was up to 1.66 m.

The large spatial and temporal variability of the transition zone salinity makes it challenging to model. In the presented simulations, the mean salinity above the pycnocline was too low in the transition zone and Skagerrak, as if the salinity gradient had been shifted northwards and westwards. The salinity below the pycnocline, as well as in the North Sea and the Baltic Sea was closer to both observations and climatology in the model control run. The reason for the low salinity has not been found, but it is not seen in the operational model. The ongoing reanalysis simulations will help to investigate the causes.

In the model scenarios, the transition zone salinity was affected both by wind changes, which worked towards increased mixing and surface salinity, and by the possible decrease in the Baltic Sea mean salinity, which was reflected almost one to one in the transition zone salinity. The projected changes in the transition zone are smaller than the large natural variability, and the changes in wind and freshwater forcing may have opposite effects (but not the same seasonality), so in the presented scenarios, the direct impact of the salinity on the ecosystem will most likely be small.

One factor which is not taken into account in the model scenarios is the increased sea level imposed from outside the model domain. A sea level rise in the range proposed in this thesis will have little direct effect on the open water salinity of the North Sea, but it could be important for the propagation of bottom water in the transition zone, possible compensating or reversing the small decrease in bottom salinity seen in the model simulations.

The Great Belt and southern Kattegat stratification in late summer and early fall is important for the bottom water oxygen conditions. The observed stratification was tightly linked to the salinity difference over the pycnocline, and thus showed large variability, both on synoptic time scales and interannually. The seasonal mean bottom to top salinity difference, and thus stratification, had high values around 1960, but no overall trend was detected for the measuring period (1930s to 1970s).

The model stratification was generally too strong because of the low surface salinity discussed above. This also makes the detection of changes in stratification uncertain. However, the wintertime stratification was decreased in the whole transition

zone and the springtime stratification was increased in the south-western part of the transition zone in both model scenarios presented here and in the CONWOY projection (Søndergaard et al., 2006). For August–October, which is the most important period for oxygen depletion, the salinity determined stratification changes were scenario dependent and showed large geographical variations. However, the magnitude of the changes was less than 10% in the cmod simulations. The larger temperature increase in the surface than in the deep water may provide a small contribution towards increased stratification. The density difference increase can be derived from the equation of state and is on the order of 2% per degree increase in the difference between surface and bottom temperature. The oxygen conditions will also be affected by the temperature increase, through biological effects and the water's ability to dissolve oxygen. A discussion of the biological aspects is outside the scope of this thesis, but the maximum amount of dissolved oxygen will decrease approximately 2% per degree of warming.[15] Thus, the climate change may affect the oxygen conditions in the transition zone. However, the nutrient content is also important for the oxygen conditions, and the role of climatic changes in the ocean relative to the effects of changed nutrient input needs further investigation.

The modeled number of major inflows to the Baltic Sea in the control simulation was lower than observed, most likely due to the low transition zone salinity and weak extreme winds discussed above. The modeled changes in inflow events agree well with earlier studies; the increased wind in the scenario without changed precipitation enhanced inflows, but the decrease in salinity in the simulation with increased freshwater forcing resulted in a reduction of the number of inflows. The freshwater effect was larger for moderate inflows than for weak inflows.

[15] The maximum amount of dissolved oxygen in surface sea water in mg/l is given by

$$L = \frac{1}{0.7}\exp\left(-173.4292 + 249.6339\frac{100}{T} + 143.3483\ln\left(\frac{T}{100}\right) - 21.8492\frac{T}{100} + S\left(-0.033096 + 0.014259\frac{T}{100} - 0.0017\left(\frac{T}{100}\right)^2\right)\right)$$

where S is the salinity and T is the temperature in Kelvin (Gierloff-Emden et al., 1986, Chapter 3.4.5).

9 Conclusions

The North Sea and the Baltic Sea are undergoing climatic changes. In this thesis, I have presented new detailed knowledge on the observed climatic variability of the 20th century and presented a downscaling scenario of the changes in the 21st century, focusing on the sea level, temperature, and salinity of the North Sea – Baltic Sea transition zone.

Sea level has been measured at 10 Danish tide gauges throughout the 20th century, and 8 of these stations are considered to provide high quality data covering the whole century. The observed sea level rise for the period 1901–2000 varied between −0.23 and +1.15 mm/year with a 90% confidence interval of 0.08–0.26 mm/year. Most of this difference is due to isostatic land adjustments, and preliminary results of the land uplift show that the mean sea level trend after land uplift correction is 1.5 ± 0.5 mm/year.[16] The long records of tide gauge measurements also show natural variability of 2–3 cm with a time scale of several decades, showing how important long data records are for the assessment of long-term trends. Since 1993, the global sea surface height has been measured by satellite altimetry. A first investigation of these data indicated that the open water trend of the Baltic Sea during 1993–2008 may have been higher than that of both the North Sea and the global mean. This needs further investigation.

The sea level rise can be seen as the sum of global, regional, and local contributions. The main contributions to future sea level rise in the North Sea – Baltic Sea area are projected to originate outside the area. The rate of the 21st century global sea level rise is not well determined. The latest IPCC report indicate a change of 18–59 cm by the end of the century, but newer studies open up for the possibility of a larger rise, and a recent assessment gives an upper estimate of 0.55–1.2 m based on present knowledge. Regional steric and dynamic changes in the North East Atlantic Ocean are likely to be on the order of 10 cm, while gravimetric effects may partly counteract the global sea level rise due to melting in Greenland (Chapter 2.2). The main local contribution is the land uplift, which will continue with approximately the same rates as today, and thus work to compensate the sea level rise. However, with the current projections, all of Denmark will experience a mean relative sea level rise in the 21st century, and for long-term planning purposes the risk of a rise on the order of 1 m or more must be taken into account.

On top of the changes in mean sea level, increased extreme winds may increase storm surge heights. In the presented scenario, the changes are most significant at the eastern coastlines of the North Sea, including the Wadden Sea and the Danish and Norwegian North Sea coasts, and in the northernmost Bothnian Bay and easternmost

[16] An additional bias due to the reference frame realization of up to 0.5 mm/year cannot be ruled out at present (Per Knudsen, pers. comm.).

Gulf of Finland. The projected 10 year storm surge height increase in Esbjerg was 19–37 cm depending on analysis method. The results have large uncertainties, because the changes in wind are uncertain and because the extreme wind forcing is too weak. For the stations in the transition zone, the modeled changes were in general small, and thus the changes in storm surge statistics will be dominated by the relative mean sea level increase.

The sea temperature at the Drogden Station close to Copenhagen has been stable during the period 1900–1985, with 10 year running mean temperatures varying between 8.2 and 9.1°C. Then the mean temperature rose to 9.8°C, and it has stayed at that level since. The temperature increase is supported by data from coastal stations and monitoring cruises in the transition zone and from observations in the North Sea and the Baltic Sea, though natural variability cause the timing to vary.

The model scenario showed a mean warming ranging from 1.6°C for the volume averaged North Sea temperature to 3.4°C for the Baltic Sea surface temperature between the two model time slices (1960–1990 and 2070–2100). The projected warming was larger in the Baltic Sea than in the North Sea, and larger for the surface than for the volume mean. At the Drogden Station, the mean surface warming was 2.9°C, indicating that, according to this A2 scenario, the warming will continue at an average rate comparable to the observed in recent years.

The observed salinity in the transition zone showed decadal variability of up to 0.85, but no significant trends. The dense observational network also gives a detailed picture of the oceanographic conditions in the transition zone, especially in the 1930s, 1950s, and 1960s. This was used to produce a detailed climatology for the locations of the lightships and to give a detailed picture of the largest observed Baltic Sea inflow event in the 20th century, where salinity changes of up to 15 were recorded at several lightships.

The modeled changes in salinity are uncertain, because the transition zone sea surface salinity is too low in the model simulations, corresponding to a northward shift of the salinity gradient. The results depend on whether changes in the freshwater forcing were taken into account. When the freshwater forcing was kept at control run values, the Baltic Sea salinity did not change significantly from the control simulation, whereas the transition zone salinity rose 0.4 on average due to increased wind mixing. When the precipitation changes were included, corresponding to a 12.6% increase in the freshwater forcing, the Baltic Sea salinity decreased at a rate comparable to the observed in stagnation periods. However, the time slice modeling approach is not suitable for determining the final outcome of such a decrease, as the time scales in the Baltic Sea are too long. The salinity decrease in the transition zone, relative to the scenario without changed freshwater forcing, was of the same magnitude as that of the Baltic Sea, but with a larger interannual variability. In that scenario the transition zone salinity decreased 0.5 on average. The North Sea salinity changes were less than

0.05 in both scenarios, and the transition zone bottom salinity showed a small decrease in both scenarios.

The stratification in the Great Belt and the Kattegat is important for the bottom oxygen conditions, especially in the late summer and early fall. It is highly dependent on the salinity. The lightship climatology gives a detailed picture of the average conditions, where stratification is strongest and the average bottom salinity show a maximum in early summer. The daily measurements also show the large variability and how the stratification can be broken down and restored with a time scale of days or weeks.

The model results for stratification have to be used with care since the low surface salinities indicate that the model stratification is in general too strong. However, the pattern of short term stratification variations is also seen in the model. In the future scenarios, there is a tendency for weaker stratification in the winter due to increased wind mixing and stronger stratification in the spring. The scenario results for the late summer and fall are more uncertain, but do not indicate changes of more than 10%. Thus, with this range of salinity changes, other factors are likely to be equally or more important for the future oxygen conditions.

The lightship observational records have proven to be of sufficient quality for both long-term and detailed studies of the temperature and salinity in the transition zone. They thus provide a unique dataset with a relatively dense coverage of daily open water profile data. The Danish coastal sea level has also been well-monitored by a network of tide gauges with records of 110 years, which, unlike the lightship records, are continued to the present. Future work on the combination of these observations with satellite altimetry and GPS data open new possibilities for the detection of regional sea level patterns in the sea level rise.

The cmod model has proven to be stable for multi-year simulations and provide detailed information on the physical oceanography, especially in the nesting area. Ongoing reanalysis-based hindcast studies will provide the possibility for validation and analysis of specific historic events, and help determine the cause of the low salinity in the transition zone. However, cmod has already now proven to be a useful tool for high resolution regional ocean climate studies in an area with complex oceanographic conditions.

10 Dansk Resumé (Danish summary)

Klimaforandringer påvirker de fysiske forhold i Nordsøen og Østersøen. I denne afhandling kombineres lange tidsserier af direkte målinger af havtemperatur, salinitet og vandstand med regional oceanmodellering. Kombinationen viser nye detaljer omkring ændringerne i det 20. århundrede og giver et scenarie for det 21. århundrede. Der er fokuseret på de geografiske forskelle, specielt for de indre danske farvande (Kattegat, Øresund og Bælthavet) og Arkona Bassinet.

Den observerede overfladetemperatur ved målestationen ved Drogden i Øresund viste en 10-års løbende middelværdi der varierede mellem 8,2 og 9,1°C mellem 1904 og 1985. I 1992 var den steget til 9.8°C, og den er blevet på dette niveau siden. Den store temperaturstigning underbygges af andre observationer. Modelscenariet viser en større opvarmning i Østersøen end i Nordsøen, og større opvarmning af atmosfæren end af havet i det 21. århundrede. I det aktuelle A2 scenarie er opvarmningen ved Drogden 2,9°C fra 1960–1990 til 2070–2100. Dette indikerer at den opvarmning der er observeret siden 1980'erne vil fortsætte.

Salinitetsmålinger fra de indre danske farvande giver et detaljeret billede af saltvandsindstrømninger til Østersøen og den vertikale stratifikation. Kombinationen af temperatur- og salinitetsmålinger danner også basis for en detaljeret klimatologi for fyrskibenes målepunkter. Modelresultater indikerer at fremtidige salinitetsændringer i de indre danske farvande og Arkona Bassinet afhænger af ændringer i Østersøens salinitet og i vinden. Øget vind fører til øget opblanding og øget middelsalinitet, mens et fald i Østersøens salinitet fører til et tilsvarende fald i de indre danske farvandes salinitet. Derfor er det usikkert hvilken retning saliniteten vil bevæge sig i fremtiden, men i de indre danske farvande er størrelsen af de modellerede ændringer mindre end den naturlige variabilitet.

Modelresultaterne indikerer at de største bidrag til en stigende middelvandstand i studieområdet vil komme udefra. I Danmark vil ændringerne blive delvist kompenseret af isostatisk landhævning. Middelværdien af den observerede absolutte vandstandsstigning som målt af 8 danske vandstandsmålere fra 1901–2000 er 1,5 ± 0,5 mm/år (90% konfidensinterval), og størstedelen af usikkerheden skyldes en foreløbig bestemmelse af landhævningen. Modelscenariet indikerer øget vestenvind og øgede stormflodshøjder på den tyske, danske og norske nordsøkyst og i bunden af Botniske Bugt og Finske Bugt. Det modellerede nedre estimat for ændringerne i Esbjerg ved et A2 scenarie var 19–37 cm i tillæg til ændringerne i middelvandstanden. Modelresultaterne viste ingen signifikante vind-inducerede ændringer af stormflodshøjderne i de indre danske farvande eller Arkona Bassinet.

Observationerne fra fyrskibe og vandstandsmålere har vist sig at være af god kvalitet til klimastudier, og de digitaliserede data har givet mulighed for studier der inddrager mange stationer og lange tidsserier. Endeligt har disse første lange kørsler med DMI-BSHcmod vist at modellen er egnet til klimasimuleringer.

List of acronyms and abbreviations

BSH Bundesamt für Seeschifffart und Hydrographie

cmod DMI-BSHcmod, the regional ocean model used in this thesis

DMI Danish Meteorological Institute

DNN Dansk Normal Nul (old Danish reference system)

DVR90 Dansk Vertikal Reference 1990 (recent Danish reference system)

EUREF The IAG Reference Frame Sub-Commission for Europe

F12 The atmospheric forcing scenario for the control simulation

GCM Global circulation model (global model used for climate simulations)

GLOSS The Global Sea Level Observing System

GPS Global Positioning System

ICES The International Council for Exploration of the Sea, `www.ices.dk`

IPCC Intergovernmental Panel on Climate Change, `www.ipcc.ch`

ITRF2005 International Terrestrial Reference Frame, 2005

HadAM3H The GCM used for forcing in this thesis, see Chapter 5.2

HIRHAM The atmospheric RCM used for forcing in this thesis, see Chapter 5.2

HIRLAM The atmospheric model used for weather forecasts at DMI

KDI Danish Coastal Authorities

MOG2D The alternative ocean model for storm surge calculations, see Chapter 6.1

NAO index North Atlantic Oscillation Index

NERI Danish National Environmental Research Institute

NOAmod The 2D barotropic model used for sea level boundary conditions to cmod

PSMSL Permanent Service for Mean Sea Level

RCM Regional climate model

S12 The atmospheric forcing scenario for the future simulation

SMHI Swedish Meteorological and Hydrological Institute

SRES IPCC Special Report on Emissions Scenarios

v9 the cmod control simulation

v10 the cmod scenario simulation with changed precipitation

v12 the cmod scenario simulation without changed precipitation

References

Aas, E. (1986). *Metoder i fysisk oseanografi.* Institut for geofysikk, Universitetet i Oslo. (4. utgave, in Norwegian)

Ådlandsvik, B. (2008). Marine downscaling of a future climate scenario for the North Sea. *Tellus*, *60A*, 451–458.

Ærtebjerg, G. (2007). *Marine områder 2005–2006 – tilstand og udvikling i miljø- og naturkvaliteten* (Faglig rapport fra DMU No. 639). Danish National Environmental Reseach Institute. Available from `http://www.dmu.dk/Pub/FR639.pdf` (In Danish with English summary)

Andersen, I. (1994). *Salt- og vandtemperaturforhold i de indre danske farvande* (Technical report No. 94-4). DMI. (in Danish)

Andersson, H. C. (2002). Influence of long-term regional and large-scale atmospheric circulation on the Baltic sea level. *Tellus*, *54A*, 76–88.

Barbosa, S. M. (2008). Quantile trends in Baltic sea level. *Geophys. Res. Lett.*, *35*, L22704.

Belkin, I. M. (2009). Rapid warming of large marine ecosystems. *Progress In Oceanography*, *81*(1-4), 207–213.

Bendtsen, J., Gustafsson, K. E., Söderkvist, J., & Hansen, J. L. S. (2009). Ventilation of bottom water in the North Sea–Baltic Sea transition zone. *Journal of Marine Systems*, *75*(1–2), 138–149.

Bergström, S., & Carlsson, B. (1994). River runoff to the Baltic Sea: 1950–1990. *Ambio*, *23*(4–5), 280–287.

Binderup, M., & Frich, P. (1993). Sea-level variations, trends and cycles, Denmark 1890–1990 – proposal for a reinterpretation. *Annales Geophysicae-Atmospheres Hydrospheres And Space Sciences*, *11*(8), 753–760.

Bindoff, N., Willebrand, J., Artale, V., A, C., Gregory, J., Gulev, S., et al. (2007). Observations: Oceanic climate change and sea level. In S. Solomon et al. (Eds.), *Climate change 2007: The physical science basis. Contribution of working group I to the fourth assessment report of the Intergovernmental Panel on Climate Change.* Cambridge University Press, Cambridge, United Kingdom and New York, NY, USA.

Cazenave, A., Lombard, A., & Llovel, W. (2008). Present-day sea level rise: A synthesis. *Comptes Rendus Geosciences*, *340*(11), 761–770.

Christensen, J. H., Carter, T. R., Rummukainen, M., & Amanatidis, G. (2007). Evaluating the performance and utility of regional climate models: the PRUDENCE project. *Climatic Change*, *81, Supplement 1*.

Church, J. A., & White, N. J. (2006). A 20th century acceleration in global sea-level rise. *Geophys. Res. Lett.*, *33*, L01602.

Church, J. A., White, N. J., Coleman, R., Lambeck, K., & Mitrovica, J. X. (2004). Estimates of the regional distribution of sea level rise over the 1950–2000. *Journal of Climate*, *17*(13), 2609–2625.

Colding, A. (1881). *Nogle Undersøgelser over Stormen over Nord- og Mellem-Europa af 12te – 14de November 1872 og over den derved fremkaldte Vandflod i Østersøen* (Vidensk. Selsk. Skr. No. 6). Bianco Lunos Kgl. Hof-Bogtrykkeri, Copenhagen, Denmark. (in Danish with French resumé, available through the DMI library)

Conley, D. J., Carstensen, J., Ærtebjerg, G., Christensen, P. B., Dalsgaard, T., Hansen, J. L. S., et al. (2007). Long-term changes and impacts of hypoxia in Danish coastal waters. *Ecological Applications*, *17, Supplement: Eutrophication*, S165–S184.

Cushman-Roisin, B. (1994). *Introduction to geophysical fluid dynamics.* New Jersey, USA: Prentice-Hall, Inc.

Damm, P. (1997). *Die saisonale Salzgehalts- und Frischwasserverteilung in der Nordsee und ihre Bilanzierung.* Berichte aus dem Zentrum für Meeres- und Klimaforschung. (Reihe B: Ozeanographie, in German)

Danielssen, D., Svendsen, E., & Ostrowski, M. (1996). Long-term hydrographic variation in the Skagerrak based on the section Torungen-Hirtshals. *ICES J Mar. Sci.*, *53*, 917–925.

Debernard, J. B., & Røed, L. P. (2008). Future wind, wave and storm surge climate in the Northern Seas: a revisit. *Tellus*, *60A*, 427–438.

Dick, S., Kleine, E., Mueller-Navarra, S., Kleine, H., & Komo, H. (2001). *The operational circulation model of BSH (BSHcmod) – model description and validation* (Berichte des BSH No. 29/2001). Bundesamt fur Seeschifffart und Hydrographie. (48pp.)

Dietrich, G. (1950). Die natürlichen Regionen von Nord- und Ostsee auf hydrographischer Grundlage. *Kieler Meeresforschungen, Institut für Meereskunde an der Universität Kiel*, *VII*(2), 35–69. (in German)

Doscher, R., & Meier, H. E. M. (2004). Simulated sea surface temperature and heat fluxes in different climates of the Baltic Sea. *Ambio*, *33*(4–5), 242–248.

Duun-Christensen, J. T. (1990). Long-term variations in sea level at the Danish coast during the recent 100 years. *Journal of Coastal research*, *9*, 45–61. (Special issue: Proceedings of the Skagen Symposium 2–5 September 1990)

Duun-Christensen, J. T. (1992). Vandstandsændringer i Danmark. In J. Fenger & U. Torp (Eds.), *Drivhuseffekt og klimaændringer – hvad kan det betyde for Danmark* (pp. 93–104). Miljøministeriet, Denmark. (in Danish)

Ekman, M. (1999). Climate changes detected through the world's longest sea level series. *Global and Planetary Change*, *21*, 215–224.

Ekman, M., & Mäkinen, J. (1996). Mean sea surface topography in the Baltic Sea and its transition area to the North Sea: A geodetic solution and comparisons with oceanographic models. *J. Geophys. Res.*, *101*(C5), 11993–11999.

Farrell, W. E., & Clark, J. A. (1976). On postglacial sea level. *Geophys. J. R. astr. Soc.*, *46*, 647–667.

Feistel, R., Nausch, G., & Wasmund, N. (Eds.). (2008). *State and evolution of the Baltic Sea, 1952 – 2005: A detailed 50-year survey of meteorology and climate, physics, chemistry, biology, and marine environment.* Hoboken, USA: John Wiley & Sons, Inc.

Fenger, J. (2000). Implications of accelerated sea-level rise (ASLR) for Denmark. In *Proceedings of SURVAS expert workshop on European vulnerability and adaption to impacts of accelerated sea-level rise (ASLR).* Hamburg, Germany.

Fenger, J., Buch, E., Jakobsen, P. R., & Vestergaard, P. (2008). Danish attitudes and reactions to the threat of sea-level rise. *Journal of Coastal Research*, *24*(2), 394.

Flather, R. A., & Williams, J. A. (2000). Climate change effects on storm surges: methodologies and results. In J. J. Beersma, M. Agnew, D. Viner, & M. Hulme (Eds.), *Climate scenarios for water-related and coastal impacts* (p. 66-78).

Fonselius, S. (2001). History of hydrographic reseach in Sweden. *Proc. Estonian Acad. Sci. Biol. Ecol.*, *50*(2), 110–129. Available from `http://www.kirj.ee/esi-l-b/b50-2-5.pdf`

Franck, H., Matthäus, W., & Sammler, R. (1987). Major inflows of saline water into the Baltic Sea during the present century. *Gerlands Beiträge zur Geophysik*, *96*, 517–531.

Fu, L.-L., & Cazenave, A. (Eds.). (2001). *Satellite altimetry and earth sciences. A handbook of techniques and applications.* Academic Press. (International Geophysics Series vol. 69)

Gästgifvars, M., Müller-Navarra, S., Funkquist, L., & Huess, V. (2008). Performance of operational systems with respect to water level forecasts in the Gulf of Finland. *Ocean Dynamics*, *58*(2), 139–153.

Gierloff-Emden, H. G., Højerslev, N. K., Krause, G., Peters, H., Siedler, G., Weichart, G., et al. (1986). *Oceanography (Landolt-Börnstein V3A)* (J. Sündermann, Ed.). Springer-Verlag.

Gosnell, R., Fairall, C. W., & Webster, P. J. (1995). The sensible heat of rainfall in the tropical ocean. *Journal of Geophysical Reseach*, *100*(C9), 18437–18442.

Graham, L. P. (2004). Climate change effects on river flow to the Baltic Sea. *Ambio*, *33*(4–5), 235–241.

Graham, L. P., Hagemann, S., Jaun, S., & Beniston, M. (2007). On interpreting hydrological change from regional climate models. *Climatic Change*, *81, Supplement 1*.

Gram-Jensen, I. (1991). *Stormfloder* (Teknisk rapport No. 91-1). DMI. (in Danish)

Grinsted, A., Moore, J. C., & Jevrejeva, S. (2009). Reconstructing sea level from paleo and projected temperatures 200 to 2100 AD. *Clim. Dyn.*

Gustafsson, B. G., & Westman, P. (2002). On the causes for salinity variations in the Baltic Sea during the last 8500 years. *Paleoceanography*, *17*(3), 1040.

Gustafsson, E. O., & Omstedt, A. (2009). Sensitivity of Baltic Sea deep water salinity and oxygen concentration to variations in physical forcing. *Boreal Environment Research*, *14*, 18–30.

Hahn-Pedersen, M. (2003). Reports on Baltic lights – Denmark. In J. Litwin (Ed.), *Baltic Sea identity: Common sea – common culture?* (pp. 81–83). Centralne Muzeum Morskie w Gdansku, Gdansk, Poland. (ISBN 83-919514-0-5)

Hallegatte, S., Patmore, N., Mestre, O., Dumas, P., Morlot, J. C., Herweijer, C., et al. (2008). *Assessing climate change impacts, sea level rise and storm surge risk in port cities: A case study on Copenhagen* (OECD Environment Working Paper No. 3). OECD. (ENV/WKP(2008)2)

Hansen, L. (2007). *Hourly values of sea level observations from two stations in Denmark. Hornbæk 1890–2005 and Gedser 1891–2005* (Technical Report No. 07-09). Danish Meteorological Institute. Available from `www.dmi.dk` (with data supplement)

Heaps, N. S. (1967). Storm surges. *Oceanography and Marine Biology - an Annual Review*, *5*, 11–47.

Heaps, N. S. (1983). Storm surges, 1967–1982. *Geophys J. R. astr. Soc.*, *74*, 331–376.

Hjøllo, S. S., Skogen, M. D., & Svendsen, E. (2009). Exploring currents and heat within the North Sea using a numerical model. *Journal of Marine Systems*, *78*(1), 180–192.

Højerslev, N. K. (1989). *Vandbevægelser i kystnære områder (Systemet Østersøen – Nordsøen).* Københavns Universitet, afd. for Fysisk Oceanografi: HCØ Tryk, Denmark. (In Danish)

Holgate, S., Jevrejeva, S., Woodworth, P., & Brewer, S. (2007). Comment on "a semi-empirical approach to projecting future sea-level rise". *Science*, *317*, 1866.

Holgate, S. J., & Woodworth, P. L. (2004). Evidence for enhanced coastal sea level rise during the 1990s. *Geophys. Res. Lett.*, *31*, L07305.

Huess, V. (2001). *Sea level variations in the North Sea - from tide gauges, altimetry and modelling* (Scientific report No. 01-08). DMI. Available from `www.dmi.dk`

Hurrell, J. W., Kushnir, Y., Ottersen, G., & Visbeck, M. (Eds.). (2003). *The North Atlantic oscillation: Climate significance and environmental impact* (No. 134). American Geophysical Union.

Ivchenko, V. O., Danilov, S. D., Sidorenko, D. V., Schröter, J., M.Wenzel, & Aleynik, D. L. (2007). Comparing the steric height in the Northern Atlantic with satellite altimetry. *Ocean Sci.*, *3*, 485–490.

Jacob, D., & Omstedt, A. (2005). *BALTEX phase I, 1993–2002, State of the art report* (International BALTEX Secretariat Publication Series No. 31). (181 pp.)

Jakobsen, F. (1997). Hydrographic investigation of the northern Kattegat front. *Continental Shelf Research*, *17*(5), 533–554.

Janssen, F., Schrum, C., & Backhaus, J. O. (1999). A climatological data set of temperature and salinity for the Baltic Sea and North Sea. *German J. Hydrography*(suppl. 9), 1–245.

Janssen, F., Schrum, C., Hübner, U., & Backhaus, J. O. (2001). Uncertainty analysis of a decadal simulation with a regional ocean model for the North Sea and Baltic Sea. *Clim. Res.*, *18*, 55–62.

Jensen, M. H., Lassen, J., Lindeborgh, N. C., Marsbøll, S., Müller-Wohlfeil, D.-I., Hansen, J., et al. (2008). *IGLOO – indikatorer for globale klimaforandringer i overvågningen* (J. W. Hansen, M. Nedergaard, & F. Skov, Eds.). Agency for Spatial and Environmental Planning, Ministry of the Environment, Copenhagen, Denmark. (in Danish)

Jones, R., Murphy, J., Hassell, D., & Taylor, R. (2001). *Ensemble mean changes in a simulation of the European climate of 2071–2100 using the new Hadley Centre regional modelling system HadAM3H/HadRM3H* (Tech. Rep.). Bracknell, UK: Hadley Centre, Met Office. (Available at prudence.dmi.dk)

Katsman, C. A., Hazeleger, W., Drijfhout, S. S., Oldenborgh, G. J. van, & Burgers, G. J. H. (2007). *Climate scenarios of sea level rise for the northeast Atlantic Ocean: a study including the effects of ocean dynamics and gravity changes induced by ice melt* (Kluwer Academic Publishers). Netherlands: Royal Netherlands Meteorological Institute (KNMI).

Kjellström, E., Döscher, R., & Meier, H. E. M. (2005). Atmospheric response to different sea surface temperatures in the Baltic Sea: coupled versus uncoupled regional climate model experiments. *Nordic Hydrology*, *36*, 397–409.

Kjellström, E., & Lind, P. (2009). Changes in the water budget in the Baltic Sea drainage basin in future warmer climates as simulated by the regional climate model RCA3. *Boreal Env. Res.*, *14*, 114–124.

Kleine, E. (1994). *Das operationelle Modell des BSH für Nordsee und Ostsee, Konzeption und übersicht* (Technical Report No. 126S). Bundesamt für Seeschifffart und Hydrographie.

Knudsen, S. B., Sørensen, C., & Sørensen, P. (2008). *Analyse af middelvandstande i Vadehavet* (Tech. Rep.). Kystdirektoratet (Danish Coastal Authority), Denmark. Available from `www.kyst.dk` (in Danish)

Kullenberg, G. (1983). The Baltic Sea. In B. H. Ketchum (Ed.), *Estuaries and enclosed seas* (pp. 309–335). Elsevier.

Landerer, F., Jungclaus, J., & Marotzke, J. (2007). Regional dynamic and steric sea level change in response to the IPCC-A1B scenario. *J. Phys. Oceanogr.*, *37*, 296–312.

Leppäranta, M., & Myrberg, K. (2009). *Physical oceanography of the Baltic Sea*. Springer.

Levitus, S., Antonov, J. I., Boyer, T. P., Garcia, H. E., & Locarnini, R. A. (2005). Linear trends of zonally averaged thermosteric, halosteric, and total steric sea level for individual ocean basins and the world ocean, (1955–1959)–(1994–1998). *Geophysical Research Letters*, *32*(16), L16601.

Lynch, D., & Gray, W. (1979). A wave equation model for finite element tidal computation. *Computers and Fluids*, *7*, 207–228.

MacKenzie, B. R., Gislason, H., Möllmann, C., & Köster, F. W. (2007). Impact of 21st century climate change on the Baltic Sea fish community and fisheries. *Global Change Biology*, *13*, 1348–1367.

MacKenzie, B. R., & Schiedek, D. (2007a). Daily ocean monitoring since the 1860s shows record warming of northern European seas. *Global Change Biology*, *13*(7), 1335–1347.

MacKenzie, B. R., & Schiedek, D. (2007b). Long-term sea surface temperature baselines – time series, spatial covariation and implications for biological processes. *Journal of Marine Systems*, *68*(3–4), 405–420.

Madsen, K. S., & Højerslev, N. K. (2009). Long-term temperature and salinity records from the Baltic Sea transition zone. *Boreal Env. Res.*, *14*, 125–131.

Madsen, K. S., Høyer, J. L., & Tscherning, C. C. (2007). Near-coastal satellite altimetry: Sea surface height variability in the North Sea–Baltic Sea area. *Geophysical Research Letters*, *34*,

L14601.

Matthäus, W. (2006). *The history of investigation of salt water inflows into the Baltic Sea – from the early beginning to recent results* (Meereswissenschaftliche Berichte No. 65). IOW.

Matthäus, W., & Franck, H. (1992). Characteristics of major Baltic inflows – a statistical analysis. *Continental Shelf Research*, *12*(12), 1375–1400.

McGranahan, G., Balk, D., & Anderson, B. (2007). The rising tide: assessing the risks of climate change and human settlements in low elevation coastal zones. *Environment and Urbanization*, *19*(1), 17–37.

Meehl, G., Stocker, T., Collins, W., Friedlingstein, P., Gaye, A., Gregory, J., et al. (2007). Global climate projections. In S. Solomon et al. (Eds.), *Climate change 2007: The physical science basis. Contribution of working group I to the fourth assessment report of the Intergovernmental Panel on Climate Change.* Cambridge, United Kingdom and New York, NY, USA.: Cambridge University Press.

Meier, H. E. M. (2006). Baltic Sea climate in the late twenty-first century: a dynamical downscaling approach using two global models and two emission scenarios. *Climate Dynamics*, *27*(1), 39–68.

Meier, H. E. M., Kjellstrom, E., & Graham, L. P. (2006). Estimating uncertainties of projected Baltic Sea salinity in the late 21st century. *Geophysical Research Letters*, *33*, L15705.

Milne, G. A., Gehrels, W. R., Hughes, C. W., & Tamisiea, M. E. (2009). Identifying the causes of sea-level change. *Nature Geoscience*, *2*, 471–478.

Mitrovica, J. X., Tamisiea, M. E., Davis, J. L., & Milne, G. A. (2001). Recent mass balance of polar ice sheets inferred from patterns of global sea-level change. *Nature*, *409*, 1026–29.

Nakicenovic, N., Alcamo, J., Davis, G., Vries, B. de, Fenhann, J., Gaffin, S., et al. (2000). *Emission scenarios. A special report of working group III of the Intergovernmental Panel on Climate Change* (N. Nakicenovic & R. Swart, Eds.). Cambridge, UK: Cambridge University Press.

Nielsen, J. W. (2001). *DMIs operationelle stormflodsvarslingssystem, version 2.0 (in Danish)* (Tech. Rep. No. 01-02). Danish Meteorological Institute.

Nielsen, M. H. (2005). The baroclinic surface currents in the Kattegat. *Journal of Marine Systems*, *55*, 97–121.

Omstedt, A., Chen, Y., & Wesslander, K. (2005). A comparison between the ERA40 and the SMHI gridded meteorological databases as applied to Baltic Sea modelling. *Nordic Hydrology*, *36*, 369–380.

Omstedt, A., & Hansson, D. (2006). Erratum to: "the Baltic Sea ocean climate system memory and response to changes in the water and heat balance components" (vol 26, pg 236–251, 2006). *Continental Shelf Research*, *26*(14), Erratum: 1685–1687.

Omstedt, A., Meuller, L., & Nyberg, L. (1997). Interannual seasonal and regional variations of precipitation and evaporation over the Baltic Sea. *Ambio*, *26*(8), 484–492.

Osborn, T. J. (2004). Simulating the winter North Atlantic Oscillation: the roles of internal variability and greenhouse gas forcing. *Clim. Dyn.*, *22*, 605–623.

OSPAR Commission. (2000). *Quality status report 2000: Region II – Greater North Sea* (Tech. Rep. No. 136). OSPAR Commission. Available from `www.ospar.org` (ISBN 0 946956 48 0)

Otto, L., Zimmerman, J., Furnes, G., Mork, M., Saetre, R., & Becker, G. (1990). Review of the physical oceanography of the North Sea. *Netherlands Journal of Sea Research*, *26*(2–4), 161–238.

Pätsch, J., & Lenhart, H. (2004). *Daily loads of nutrients, total alkalinity, dissolved inorganic carbon and dissolved organic carbon of the European continental rivers for the years 1977–2002* (Berichte aus dem Zentrum für Meeres- und Klimaforschung, Reihe B: Ozeanographie No. 48). University of Hamburg.

Pawlowicz, R., Beardsley, B., & Lentz, S. (2002). Classical tidal harmonic analysis including error estimates in MATLAB using T_TIDE. *Computers and Geosciences*, *28*, 929–937.

Pedersen, F. B. (1993). Fronts in the Kattegat: The hydrodynamic regulating factor for biology. *Estuaries*, *16*(1), 104–112.

Pettersson, O. (1931). *Vattenutbytet mellan Skagerak och Östersjön.* Svenska Hydrografisk-Biologiska Kommissionens skrifter, Hydrografi series, volume 9.

Pfeffer, W. T., Harper, J. T., & O'Neel, S. (2008). Kinematic constraints on glacier contributions to 21st-century sea-level rise. *Science*, *321*(5894), 1340–1343.

Pugh, D. (1987). *Tides, surges and mean sea-level: a handbook for engineers and scientists.* Wiley, Chichester.

Rahmstorf, S. (2007a). Response to comments on "a semi-empirical approach to projecting future sea-level rise". *Science*, *317*, 1866.

Rahmstorf, S. (2007b). A semi-empirical approach to projecting future sea-level rise. *Science*, *315*, 368–370.

Rahmstorf, S., Cazenave, A., Church, J. A., Hansen, J. E., Keeling, R. F., Parker, D. E., et al. (2007). Recent climate observations compared to projections. *Science*, *316*(5825), 709.

Räisänen, J., Hansson, U., Ullerstig, A., Döscher, R., Graham, L., Jones, C., et al. (2004). European climate in the late twenty-first century: regional simulations with two driving global models and two forcing scenarios. *Climate Dynamics*, *22*(1), 13–31.

Rockel, B., & Woth, K. (2007). Extremes of near-surface wind speed over Europe and their future changes as estimated from an ensemble of RCM simulations. *Climatic Change*, *81, Supplement 1*, 267–280.

Rodhe, J. (1998). The Sea. In A. R. Robinson & K. H. Brink (Eds.), (Vol. 11, pp. 699–731; 24: The Baltic and North Seas: A process-oriented review of the physical oceanography). John Wiley & Sons, Inc., New York.

Rohling, E. J., Grant, K., Hemleben, C., Siddall, M., Hoogakker, B. A. A., Bolshaw, M., et al. (2008). High rates of sea-level rise during the last interglacial period. *Nature Geoscience*, *1*, 38–42.

Roode, N., Baarse, G., Ash, J., & Salado, R. (Eds.). (2008). *Coastal flood risk and trends for the future in the North Sea region, synthesis report.* The Hague, The Netherlands: Rijkswaterstaat – Centre for Water Management (RWS).

Rossiter, J. R. (1967). An analysis of annual sea level variations in European waters. *Geophys. J. R. astr. Soc.*, *12*, 259–299.

Schinke, H., & Matthäus, W. (1998). On the causes of major Baltic inflows – an analysis of long time series. *Continental Shelf Research*, *18*, 67–97.

Schmager, G. (2008). Climate atlas of the Baltic Sea. In R. Feistel, G. Nausch, & N. Wasmund (Eds.), *State and evolution of the Baltic Sea, 1952–2005: A detailed 50-year survey of meteorology and climate, physics, chemistry, biology, and marine environment.* Wiley. (electronic appendix)

Schmidt-Thomé, P., Kallio, H., Jarva, J., Tarvainen, T., Greiving, S., Fleischhauer, M., et al. (2006). *The spatial effects and management of natural and technological hazards in Europe – ESPON 1.3.1* (ESPON report No. 1.3.1). Geological Survey of Finland (GTK). Available from `www.espon.lu`

Schmith, T., Johansen, S., & Thejll, P. (2007). Comment on "A semi-empirical approach to projecting future sea-level rise". *Science*, *317*, 1866.

Schrum, C., Alekseeva, I., & John, M. S. (2006). Development of a coupled physical-biological ecosystem model ECOSMO: Part I: Model description and validation for the North Sea. *Journal of Marine Systems*, *61*(1–2), 79–99.

She, J., Berg, P., & Berg, J. (2007). Bathymetry impacts on water exchange modelling through the Danish Straits. *Journal of Marine Systems*, *65*(1–4), 450–459.

Skjoldal, H. R. (2007). *Update report on North Sea conditions – 2nd quarter 2007* (ICES/EuroGOOS North Sea Pilot Project – NORSEPP). ICES, EuroGOOS. Available from `www.ices.dk/marineworld/norsepp.asp`

Smith, R. L. (1986). Extreme value theory based on the r largest annual events. *Journal of Hydrology*, *86*, 27–43.

Solomon, S., et al. (Eds.). (2007). *Climate change 2007: The physical science basis. Contribution of working group I to the fourth assessment report of the Intergovernmental Panel on Climate Change*. Cambridge University Press, Cambridge, United Kingdom and New York, NY, USA. Available from `http://www.ipcc.ch/ipccreports/ar4-wg1.htm`

Søndergaard, M., Kronvang, B., Pejrup, M., & Sand-Nielsen, K. (Eds.). (2006). *Vand og vejr om 100 år: Klimaforandringer og det danske vandmiljø*. Hovedland, Denmark. (in Danish)

Sørensen, P., Sørensen, C., Ingvardsen, S. M., Andersen, I., & Kloster, B. B. (2007). *Højvandsstatistikker 2007 – Extreme sea level statistics for Denmark, 2007* (Danish Coastal Authority). Available from `www.kyst.dk` (In Danish with English summary)

Sparre, A. (1984). *The climate of Denmark – summaries of observations from light vessels III–IV* (Climatological Papers Nos. 10–12). Copenhagen: Danish Meteorological Institute.

Stigebrandt, A. (1980). Barotropic and baroclinic response of a semi-enclosed basin to barotropic forcing from the sea. In H. J. Freeland, D. M. Farmer, & C. D. Levings (Eds.), *Fjord oceanography* (pp. 151–164). Plenum.

Stigebrandt, A. (1984). Analysis of an 89-year-long sea-level record from the Kattegat with special reference to the barotropically driven water exchange between the Baltic and the Sea. *Tellus Series A*, *36*(4), 401–408.

Stigebrandt, A. (2001). Physical oceanography of the Baltic Sea. In F. Wulff et al. (Ed.), *A systems analysis of the Baltic Sea* (Vol. 148, pp. 19–73). Springer-Verlag.

Stigebrandt, A., & Gustafsson, B. G. (2003). Response of the Baltic Sea to climate change – theory and observations. *Journal of Sea Research*, *49*(4), 243–256.

Storch, H. von, & Woth, K. (2008). Storm surges: perspectives and options. *Sustain. Sci.*, *3*, 33–43.

Storch, H. von, Zorita, E., & González-Rouco, J. (2008). Relationship between global mean sea-level and global mean temperature and heat flux in a climate simulation of the past millennium. *Ocean Dynamics*, *58*(3–4), 227–236.

Suursaar, U., Jaagus, J., & Kullas, T. (2006). Past and future changes in sea level near the Estonian coast in relation to changes in wind climate. *Boreal Env. Res.*, *11*(2), 123–142.

Svansson, A. (1975). *Physical and chemical oceanography of the Skagerrak and the Kattegat. 1. Open sea conditions*. Fishery board of Sweden.

Sztobryn, M., Stigge, H.-J., Wielbińska, D., Weidig, B., Stanislawczyk, I., Kańska, A., et al. (2005). *Storm surges in the southern Baltic Sea (western and central parts)* (Berichte des Bundesamtes für Seeschifffahrt und Hydrographie No. 39). BSH, Germany.

Tawn, J. (1988). An extreme-value theory model for dependent observations. *Journal of Hydrology*, *101*, 227–250.

The BACC Author Team. (2008). *Assessment of climate change for the Baltic Sea Basin*. Springer. (ISBN: 978-3-540-72785-9)

Thodsen, H. (2007). The influence of climate change on stream flow in Danish rivers. *Journal of Hydrology*, *333*, 226–238.

Tsimplis, M., Shaw, A., Flather, R., & Woolf, D. (2006). The influence of the North Atlantic Oscillation on the sea-level around the northern European coasts reconsidered: the thermosteric effects. *Phil. Trans. R. Soc. A*, *364*(1841).

UNESCO. (1981). *The practical salinity scale 1978 and the international equation of state of seawater 1980* (Unesco technical paper in marine science No. 36). UNESCO. (Tenth report of the Joint Panel on Oceanographic Tables and standards, JPOTS)

UNESCO. (1988). *The acquisition, calibration, and analysis of CTD data* (Unesco technical papers in marine science No. 54). SCOR Working Group 51: UNESCO. Available from `unesdoc.unesco.org/images/0009/000969/096989EB.pdf` (ISSN 0503-4299)

Veerman, C. (2008). *Working together with water, a living land builds for its future.* Deltacommissie. Available from `www.deltacommissie.com/en/advies`

Wakelin, S. L., Woodworth, P. L., Flather, R. A., & Williams, J. A. (2003). Sea-level dependence on the NAO over the NW European Continental Shelf. *Geophysical Research Letters*, *30*(7), 1403.

Wilkin, J. L., Arango, H. G., Haidvogel, D. B., Lichtenwalner, C. S., Glenn, S. M., & Hedström, K. S. (2005). A regional ocean modeling system for the Long-term Ecosystem Observatory. *J. Geophys. Res.*, *110*, C06S91.

Wiltshire, K. H., & Manly, B. F. J. (2004). The warming trend at Helgoland Roads, North Sea: phytoplankton response. *Helgoland Marine Research*, *58*, 269–273.

Woth, K. (2005). North Sea storm surge statistics based on projections in a warmer climate: How important are the driving GCM and the chosen emission scenario? *Geophysical Research Letters*, *32*(22), L22708.

Woth, K., Weisse, R., & Storch, H. von. (2006). Climate change and North Sea storm surge extremes: an ensemble study of storm surge extremes expected in a changed climate projected by four different regional climate models. *Ocean Dynamics*, *56*(1), 3–15.

Wyrtki, K. (1954). Der grosse Salzeinbruch in die Ostsee im November und Dezember 1951. *Kieler Meeresforschungen*, *10*, 19–25. (in German)

Appendix A Other model output

Due to time limitations, the model velocity, transport, and sea ice fields have not been thoroughly analyzed, but are briefly described below.

Velocity

The three-dimensional water velocity field is a diagnostic variable of the model. The control run mean velocity at 4 m's depth (corresponding to the coarse grid surface layer) is seen in Figure 59. The Kattegat circulation, which was also noted in the mean sea surface height is clearly seen in the fine grid domain.

Transports

Volume-, salt-, and heat transports were calculated every 15 minutes and later averaged as a part of the online post processing, following the standards of the NOOS cooperation (Stephan Dick, pers. comm.). Transports were calculated along selected NOOS and ICES transects (Fig. 60 and Table 12).

The cmod control run showed an average counterclockwise circulation in the North Sea, with the largest volume transports in the northern parts and during wintertime. At the Hanstholm transect (NOOS transect 8), the transport was about 0.3 Sv on average (1 Sv= 10^6 m^3/s), and 0.5 Sv in December and January (Fig. 61). The magnitude and seasonal pattern agrees well with the long-term mean values as calculated with the NORWECOM model (Skjoldal et al. 2005, REGNS 2005 working paper, as reported in Skjoldal, 2007), when the different transect locations are taken into account. Both models showed a relatively small net northward transport, on average 0.03 Sv in NORWECOM and 0.05 Sv in cmod. The cmod control run interannual variability was on the order of 0.1 Sv for the North Sea circulation and 0.05 Sv for the net transport, with the highest net transport around model year 1978 and increased circulation in the mid 1960s, and around 1978 and 1983 (model years). The modeled interannual variability in the outflow from the Baltic Sea was an order of magnitude smaller.

The future scenario with changed precipitation showed the same general features as in the control run (Fig. 61), but an increased seasonality, with a mean transport at the Hanstholm transect of 0.7 Sv in December and January.

Sea ice

The sea ice extend and thickness was calculated by the simplified sea ice model. The ice extend was greatly reduced in the scenario simulations, but none of the simulated winters were completely ice free.

Table 12: List of transects with transport calculations, see also map in Figure 60.

Number	Starting point		End point		Name
	Lat	Lon	Lat	Lon	
1	58° 24.0N	3° 04.8W	58° 24.0N	5° 54.6E	Wick (south of NOOS 4 + 5)
2	57° 09.0N	5° 00.0E	58° 09.0N	6° 30.0E	Lista (NOOS 6)
3	57° 06.0N	1° 55.2W	57° 06.0N	4° 55.2E	Aberdeen (NOOS 7)
4	57° 06.0N	5° 04.8E	57° 06.0N	8° 25.2E	Hanstholm (NOOS 8)
5	54° 18.0N	0° 24.0W	54° 18.0N	4° 15.0E	England East (NOOS 10)
6	54° 15.0N	4° 18.0E	53° 18.0N	5° 24.0E	Dutch North (NOOS 11)
7	52° 24.0N	1° 45.0E	52° 24.0N	4° 25.2E	Noordwijk (NOOS 12)
8	51° 06.0N	1° 24.0E	51° 03.0N	1° 42.0E	English Channel (NOOS 13)
9	50° 33.0N	1° 19.8W	49° 45.0N	1° 19.8W	Cherbourgh (NOOS 14)
10	55° 03.0N	6° 19.8E	53° 27.0N	6° 19.8E	Rottumerplaat (NOOS 19)
11	55° 06.0N	6° 24.0E	55° 06.0N	8° 34.8E	Sylt (NOOS 20)
12	58° 03.0N	8° 10.2E	57° 09.0N	8° 40.2E	Skagerrak opening (NOOS 9)
13	58° 27.0N	9° 00.0E	57° 39.0N	10° 00.0E	Torungen-Hirtshals (NOOS 21)
14	58° 57.0N	10° 10.2E	57° 39.0N	10° 10.2E	Skagerrak (NOOS 22)
15	57° 42.0N	10° 34.8E	57° 42.0N	11° 45.0E	Kattegat (NOOS 23)
16	56° 10.0N	10° 44.2E	56° 01.0N	11° 15.8E	ICES Kattegat SW
17	56° 05.4N	12° 28.2E	56° 16.5N	12° 28.2E	ICES Oresund N
18	56° 00.9N	12° 36.0E	56° 00.9N	12° 40.8E	Oresund (NOOS 24)
19	55° 23.1N	12° 24.0E	55° 23.1N	12° 47.4E	ICES Oresund S
20	55° 28.8N	9° 39.0E	55° 28.8N	9° 43.2E	Little Belt (NOOS 25)
21	55° 21.0N	10° 48.0E	55° 21.0N	11° 06.0E	Great Belt (NOOS 26)
22	54° 43.8N	11° 10.2E	54° 31.2N	11° 10.2E	Fehmarn Belt (NOOS 27)
23	54° 10.8N	11° 58.2E	54° 34.2N	11° 58.2E	ICES Gedser
24	54° 57.0N	12° 33.0E	54° 28.8N	12° 33.0E	Darss Sill (NOOS 28)
25	55° 24.0N	14° 00.0E	54° 04.8N	14° 00.0E	Arkona Basin (NOOS 29)
26	54° 57.0N	15° 10.2E	54° 09.0N	15° 10.2E	Bornholm S (NOOS 30)
27	55° 23.0N	14° 12.5E	55° 18.0N	14° 39.2E	Bornholm N (NOOS 31)
28	54° 51.0N	18° 21.0E	56° 27.0N	18° 21.0E	Slupsk Sill (ICES 25-26)
29	56° 30.0N	18° 15.0E	56° 30.0N	16° 15.0E	Middlebank (ICES 25-27)
30	56° 30.0N	20° 54.0E	56° 30.0N	18° 24.0E	ICES 26-28
31	56° 33.0N	18° 21.0E	56° 51.0N	18° 21.0E	Gotland S (ICES 27-28 S)
32	57° 57.0N	18° 50.4E	58° 27.0N	18° 50.4E	ICES 27-28 N
33	58° 33.0N	18° 50.4E	59° 27.0N	18° 50.4E	ICES 27-29
34	58° 30.0N	22° 15.0E	58° 30.0N	18° 54.0E	ICES 28-29
35	59° 21.0N	23° 49.8E	59° 51.0N	23° 49.8E	Gulf Of Finland (ICES 29-32)
36	60° 30.0N	19° 55.2E	60° 30.0N	18° 15.0E	Aaland W (ICES 29-30 W)
37	60° 30.0N	21° 15.0E	60° 30.0N	20° 04.8E	Aaland E (ICES 29-30 E)
38	63° 30.0N	22° 15.0E	63° 30.0N	19° 55.2E	Kvarken (ICES 30-31)

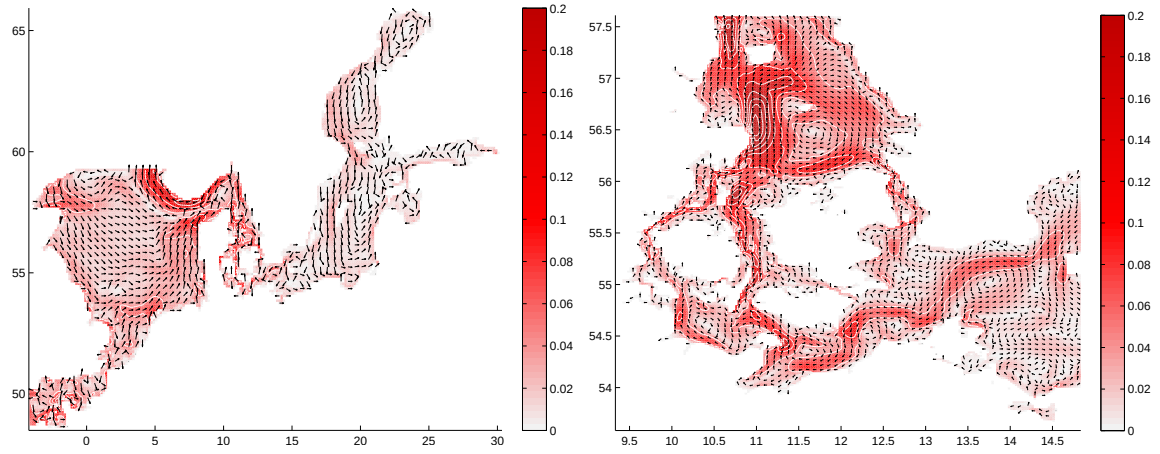

Figure 59: Mean 4 m currents in the model control run. Arrows indicate the direction, and the color scale indicates speed in m/s. Left: the coarse grid model domain, right: the fine grid domain.

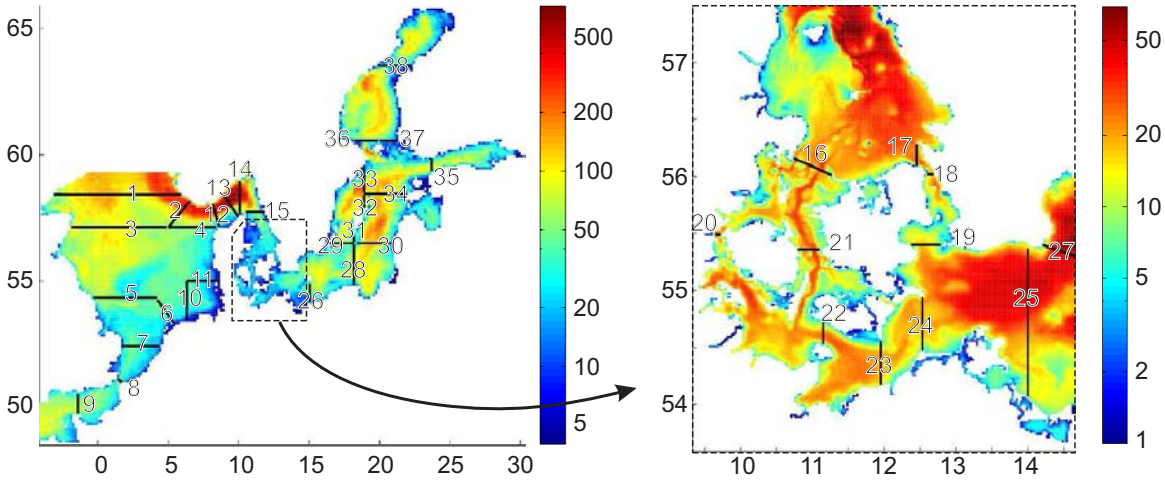

Figure 60: Transects with calculation of transports and 15 minutes resolution output, and model bathymetry (meters, logarithmic scale). Left: the coarse grid model domain, right: the fine grid domain. See Table 12 for names and end point locations.

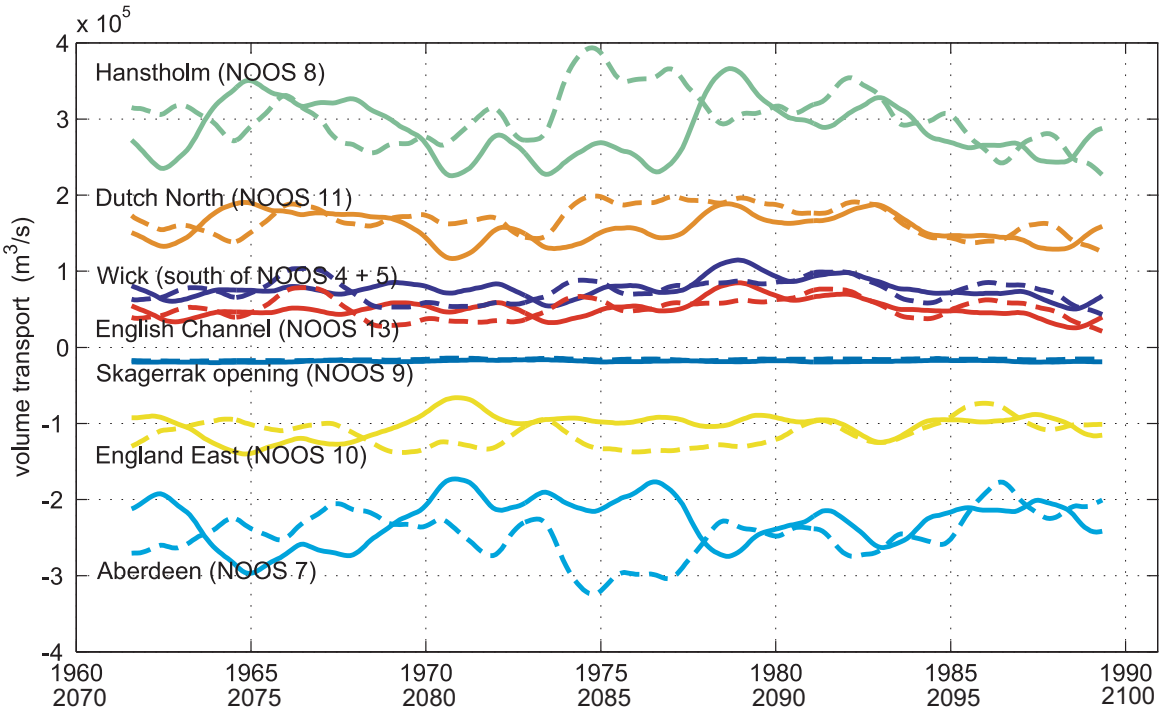

Figure 61: Interannual variations (3 year low pass filtered) in volume transport at selected NOOS transects in the North Sea. Solid line: cmod control run. Dashed line: cmod scenario run.

Appendix B Paper: Madsen and Højerslev 2009

BOREAL ENVIRONMENT RESEARCH 14: 125–131 © 2009
ISSN 1239-6095 (print) ISSN 1797-2469 (online) Helsinki 27 February 2009

Long-term temperature and salinity records from the Baltic Sea transition zone

Kristine S. Madsen[1) 2)] and Niels K. Højerslev[1)]

[1)] *Niels Bohr Institute, University of Copenhagen, Juliane Maries Vej 30, DK-2100 Copenhagen Ø, Denmark*
[2)] *Center for Ocean and Ice, Danish Meteorological Institute, Lyngbyvej 100, DK-2100 Copenhagen Ø, Denmark*

Received 18 Oct. 2007, accepted 29 June 2008 (Editor in charge of this article: Timo Huttula)

Madsen, K. S. & Højerslev, N. K. 2009: Long-term temperature and salinity records from the Baltic Sea transition zone. *Boreal Env. Res.* 14: 125–131.

The digitization of temperature and salinity data from lightships and coastal stations in the North Sea–Baltic Sea transition zone allows for multi-station and long-term studies of the oceanographic conditions of the last century. The salinity records, in combination with tide gauge records, are analyzed to demonstrate the development of a major inflow to the Baltic Sea, in terms of surface salinity, changes in stratification throughout the transition zone, and variations in the water level gradient in the zone. Also, temperature and salinity variations for years 1900–1998 are analyzed and show a 0.7 °C warming at the Drogden station towards the end of the 20th century, and no large change in salinity. The temperature change is largest in the winter and spring.

Introduction

The Baltic Sea is experiencing climate changes (The BACC Author Team 2008). To understand these changes, detailed measurements of previous hydrographic conditions are of high value. This study focuses on the temperature and salinity of the only open boundary to the Baltic Sea, the transition zone to the North Sea. Measurements of temperature and salinity have been conducted from a dense network of lightships and coastal stations since the year 1880 (Fig. 1). The data from individual stations have been investigated in numerous studies (e.g. Pettersson 1931, Svansson 1975, Stigebrandt 1984), while long-term multi-station studies have been limited, most likely by the amount of work required to analyze paper records of data. Many of these high quality data are available in digital form. This paper presents a set of available digital data and gives examples of how the data allow for description of the temporal and spatial details of salinity in a major inflow event to the Baltic Sea and analysis of the long-term variations in the transition zone. For a more general introduction to the transition zone, as well as information on other observations in the area, *see* e.g. Kullenberg (1983) and Rodhe (1998).

Study area and materials

The transition zone is the Baltic Sea's only open boundary to the world ocean and consists of Kattegat, the Great Belt, the Little Belt and the Sound. It is characterized by narrow straits and

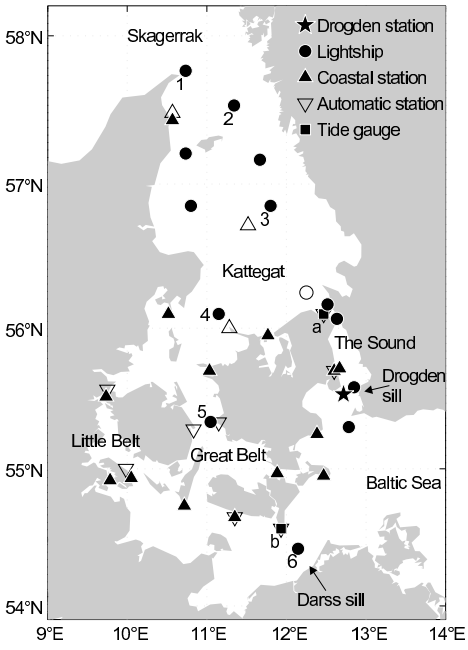

Fig. 1. The transition zone. Stations with data available during the 1951 inflow are marked with filled symbols, other stations with open symbols. The lightships are marked with numbers: (1) l/s *Skagens Rev*, (2) l/s *Læsø N*, (3) l/s *Anholt*, (4) l/s *Kattegat SW*, (5) l/s *Halsskov Rev*, (6) l/s *Gedser Rev*. The tide gauges are (a) Hornbæk and (b) Gedser. The Drogden station was a lightship until 1937, when it was replaced by a permanent station.

shallow sill depths (8 m at Drogden sill and 18 m at Darss sill, *see* Fig. 1), and the water exchange to the Baltic Sea is governed by fresh water forcing, sea level differences, and the topography in this zone. On average a two layer system is seen, stratified with brackish water from the Baltic Sea flowing out in the surface and a compensating, high salinity bottom current. The inflow of high saline water is limited by the topography, and only during special events will large amounts of high saline water cross the sills and flow into the Baltic Sea. The inflow event of 1951 was the largest observed in the 20th century. It lasted for 25 days, from 25 November to 19 December 1951, with a precursory period of 12 days, and was caused by a combination of preceding low sea levels in the Baltic Sea and three weeks of strong westerly winds (Wyrtki 1954, Matthäus and Franck 1992, Schinke and Matthäus 1998). Detailed salinity observations from this inflow event are presented in this paper.

On long time scales, the Baltic Sea is in balance with the world ocean and the atmospheric forcing. The time scale is about one year for heat, and thus temperature, and 30 times longer for salinity (Stigebrandt and Gustafsson 2003).

The study area is heavily loaded with ship traffic, and the systematic use of light towers for navigational purposes was initiated in 1560. From 1829, this system was supplemented by semi-stationary lightships in places where light towers could not be established, and most of these anchored ships have made oceanographic observations from 1875 onwards. The ships were withdrawn in the 1970s and 1980s (Hahn-Pedersen 2003).

The Danish lightship data (at the Danish Meteorological Institute (DMI)), have been digitized since the year 1931 (Sparre 1984), and are available for scientific use. Earlier data can be found in nautical-meteorological annuals of the Danish Meteorological Institute. The digital data include vertical profiles of temperature and salinity, waves, surface currents, and meteorological observations, all with daily resolution (measured at 7 or 8 a.m. local time). The data from Swedish ships are currently being digitized by the Swedish Meteorological and Hydrological Institute (SMHI) (J. Szaron (SMHI) pers. comm.), and vertical profiles of temperature and salinity, as well as currents at the surface and at one deep level, are available at variable temporal resolution (sub-daily to monthly), with some time series going back to 1924.

Besides the lightships, temperature and salinity have also been measured daily at Danish coastal stations, but only at one depth (surface). DMI has paper records of these data in the nautical-meteorological annuals back to 1873, and digitized data going back to 1931. Before 2000, the stations were regularly maintained and both temperature and salinity measurements are of high quality, hereafter the stations were replaced by automatic stations where only the temperature measurement is reliable.

The observation network is dense in the transition zone (Fig. 1), with much fewer stations in

Skagerrak and the surrounding seas. The number of observing lightships with digitized data was at its maximum (12–14) in the 1930s, 1950s and 1960s, whereas the number of coastal stations remained between 9 and 14 from 1931 to 1999 (Fig. 2). Note that the Drogden station started as a lightship, but was replaced by a permanent station in 1937. This record is digitized from 1900 to 1998, thus marking the longest digitally available high resolution sea temperature and salinity record in the area.

The measurements are generally expected to have accuracies of 0.2 °C and 0.1‰* for temperature and salinity, respectively (Andersen 1994). However, errors and complications are introduced, most importantly because of uncertainties in the depth determination for below-surface data (especially in case of strong currents), changes in instrumentation and personnel, and re-deployment of the lightships at new sites. Also, the coastal stations have mostly been placed in harbors. We have compared the monthly mean surface temperature and salinity records with the data from neighboring stations and with the data available from ICES (www.ices.dk/ocean), and found that the salinity values agreed very well, while some of the coastal data showed a larger seasonal cycle in temperature as compared with off-coast measurements.

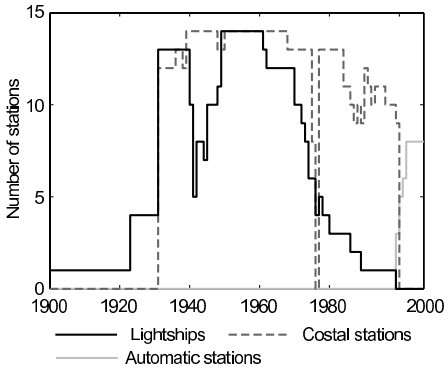

Fig. 2. Number of lightships, coastal stations, and automatic stations per year. Note that Drogden station is counted as a lightship.

Methods

To illustrate the possibilities for analyzing specific events offered by the digital data set, we focus on the daily salinity measurements at selected depths from 6 lightships for the period from 1 October 1951 to 1 March 1952 (Fig. 3), and on all available surface salinity measurements at three selected dates, chosen to show the buildup of the inflow (Fig. 4). A two-dimensional linear interpolation between available data has been calculated and is shown with contour curves.

The inflow is also reflected in the water level difference between the two tide gauges in Hornbæk and Gedser (Fig. 5). The two stations are selected to give the best possible estimate of the water level gradient of the narrow parts of the transition zone. Starting from hourly observations (Hansen 2007), we removed tidal effects by making a 25 hour running mean, and subtracted the 1900–2000 mean to remove differences in the reference level.

To investigate the long-term temperature and salinity development, we calculated the 10-year centered running mean surface temperature and salinity for the Drogden station (Fig. 6). The 10-year average length is chosen to filter out short-term variability while maintaining as narrow filtering window as possible; a 15-year filter has been tested with much the same results but less information at the ends of the time series. To support the analysis of the observations from the Drogden station, similar calculations were made for all other stations (Figs. 6a and b), and for air temperature measurements at the Landbohøjskolen station, Copenhagen, Denmark (55.6°N, 12.7°E, Fig. 6a).

The Drogden station measurements constitute one continuous series at a fixed position, the only major change being the shift from a lightship to a permanent station in 1937. Many of the other stations experienced movements of a few kilometers. To compensate for this effect, and allow for comparison between stations, we subtracted the climatological mean value (Janssen *et al.* 1999) from the salinity data, but not from the temperature data, where the spatial variation in this area is much smaller. Temperature data from coastal stations and the modern automatic stations were merged into one record when the stations were located close to each other.

*Since historic salinity observations were measured in a variety of units without defined conversion to psu, the salinities in this study are left dimensionless.

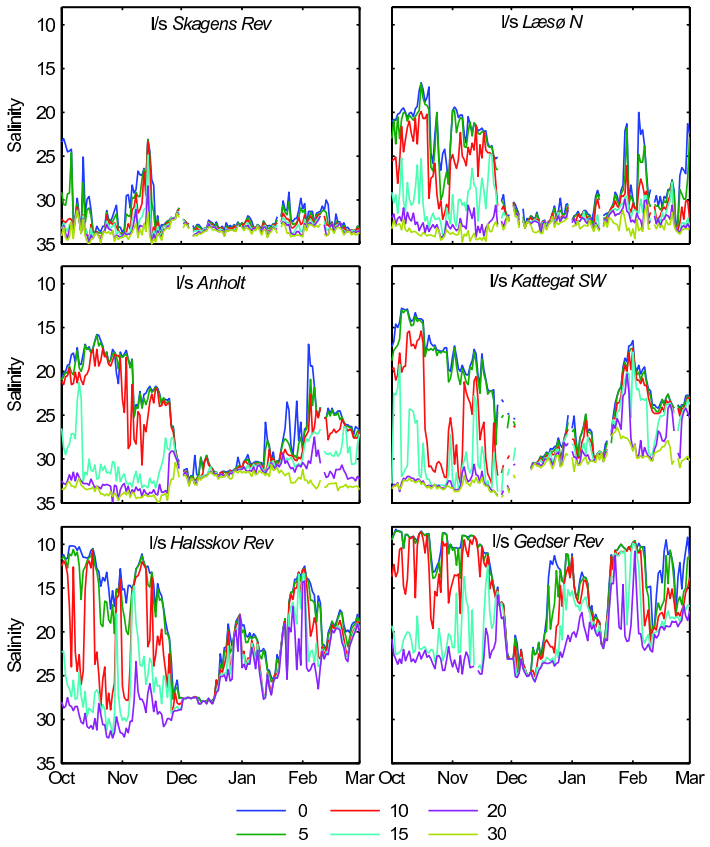

Fig. 3. The salinity at six lightships throughout the transition zone at selected depths and for the period from 1 October 1951 to 1 March 1952. Note that the *y*-axis is reversed.

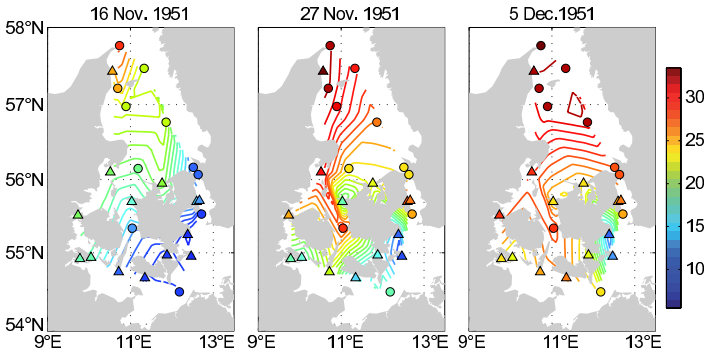

Fig. 4. Surface maps of the salinity on three selected dates during the precursory and inflow periods with contour curves of interpolated salinities (one salinity unit per curve).

In all calculations, 250 measurements per year or 60 measurements per season were required, and one missing year per 10 year mean was accepted.

Results and discussion

The daily salinity data show that the water in the transition zone was stratified before the 1951

inflow event (Fig. 3), with bottom salinities of 33‰ in Kattegat, falling to 23‰ at l/s *Gedser Rev* and surface salinities rising from 10‰ at l/s *Gedser Rev* to 22‰ at l/s *Læsø N*. The thickness of the surface layer was not constant, but was in most cases between 10 and 15 meters. At l/s *Skagens Rev*, the water was less stratified, and had a higher salinity.

The inflow event is clearly seen as a collapse of the stratification, with salinities above 30‰ in the whole water column in Kattegat, 27.5‰ at l/s *Halsskov Rev* and about 23‰ at l/s *Gedser Rev*. These numbers correspond well to the findings of Wyrtki (1954). The salinity at l/s *Gedser Rev* was approximately the same as that of the water that enters the Baltic Sea, as the station is close to the Darss Sill.

After the inflow, the water was again stratified at l/s *Gedser Rev*, while it remained mixed in Kattegat for another month. This made way for a smaller inflow in the middle of January 1952, and then the stratification was re-established all the way to l/s *Anholt*.

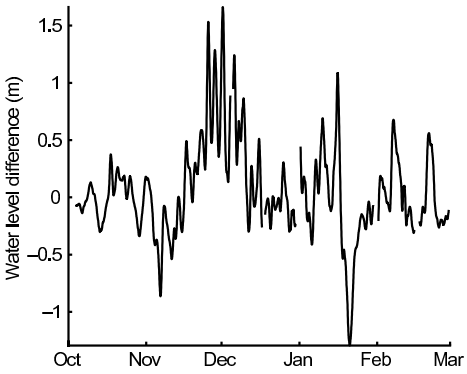

Fig. 5. The 25-hour running mean water level difference between the Hornbæk and Gedser tide gauges for the period from 1 October 1951 to 1 March 1952. Positive values indicate higher water level at Hornbæk than at Gedser, and thus possibilities for inflow.

This salinity pattern was supported by the surface maps (Fig. 4). On 16 November, in the

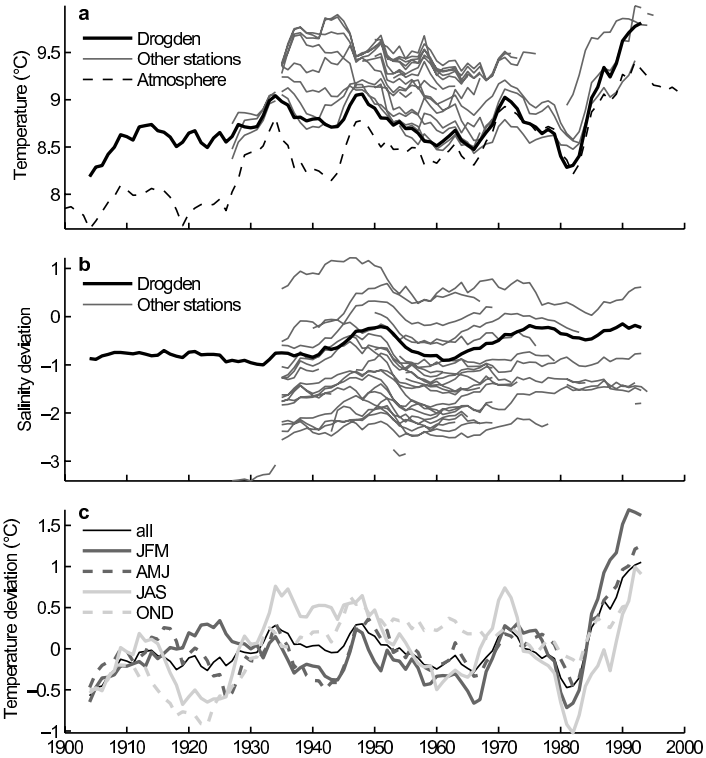

Fig. 6. 10 year running mean surface data. — **a**: temperature. — **b**: salinity deviations from climatology. — **c**: seasonal temperatures (January–March, April–June, July–September, and October–December), deviations from seasonal mean.

beginning of the precursory period, a normal situation with an increase in salinity from 10 at l/s *Gedser Rev* to 25 at l/s *Skagens Rev* was seen. On November 27, the inflow event was in its initial phase, and high salinity water was pressed through the Great Belt and the Sound. On 5 December, the inflow was fully developed, with high salinity water all the way to l/s *Gedser Rev*.

The inflow signal was also clearly seen in the water level measurements, with a water level up to 1.66 m higher at Hornbæk than at Gedser and a mean water level difference of 0.50 m during the 25-day inflow period. This is a large deviation as compared ith the 30-cm mean sea surface topography difference between the central Baltic Sea and Skagerrak (Ekman and Mäkinen 1996) and with the standard deviation of the year 1900–2000 time series of 0.34 m. A simple estimate of the resulting current velocities can be made based on the assumption of a one layer channel flow with friction (Stigebrandt 1980). According to this, the velocity is

$$u = \sqrt{\frac{2g}{1+\frac{2kL}{H}}\Delta\eta} \qquad (1)$$

where g is gravity acceleration, k is a drag coefficient, L and H are the channel length and depth, and $\Delta\eta$ is the water level difference between the ends of the channel. Stigebrandt uses g = 9.8 m s^{-2}, k = 0.003, L = 40 km, and H = 20 m, resembling the Great Belt system. With this, the mean and maximum inflow speeds in our case are estimated to be 0.9 m s^{-1} and 1.6 m s^{-1}, respectively.

The 1905–1985 running mean temperature at the Drogden station varied between 8.2 and 9.1 °C, rising to 9.8 °C in 1992 (Fig. 6a). This is generally supported by the data from the other stations when these data are available, and is thus assumed representative for the transition zone. The running mean air temperature shows a trend of 1.0 °C/century for the period 1904–1985, while only 0.1 °C/century for the Drogden station record. Despite of this, the correlation coefficient between the two records is 0.80, and the extra years of the air record, therefore, indicate that the high temperature towards the end of the century is persistent. Omstedt *et al.* (2004) noticed similar trends in records from Stockholm, and the BACC Author Team (2008) showed rising of the air temperature over the entire Baltic Sea.

The change in temperature towards the end of the century was largest in winter and spring, whereas the summer and autumn temperatures were only slightly higher than earlier in the century (Fig. 6c).

The Drogden station running mean salinity record varied within 0.85 throughout the century (Fig. 6b). The salinity was generally high around 1950 and from 1975 onwards, but with no large change towards the end of the period. Again, the data from the other stations support this. The relatively large variations in the mean value between the stations indicate that the climatology for the area possibly could be improved by including these data.

Concluding remarks

The North Sea–Baltic Sea transition zone water temperature and salinity were monitored on a daily basis by a network of lightships and coastal stations in the 20th century, and the major part of these unique time series is available in digital form.

The data allow for detailed studies of past events, here exemplified by the Baltic Sea inflow event of 1951. The horizontal and vertical details of the daily salinity observations enable us to follow the event during the precursory, inflow, and recovery periods, and we see the breakdown of stratification in the transition zone, salinities of up to 23‰ at the entrance to the Baltic Sea, and a water level gradient through the transition zone of up to 1.66 m.

The 10-year running mean surface temperature at the Drogden station showed no significant trend from 1904 to 1985, with running mean values ranging between 8.2 and 9.1 °C, but then a noticeable strong climatic signal at the end of the time series was seen: a 10-year mean value, centered in 1992, of 9.8 °C, 0.7 °C higher than earlier running mean values. Available data from the other stations generally support the observations from the Drogden station, and the signal was strongest in winter and spring. No similar change in salinity was seen.

Acknowledgements: The authors would like to thank SMHI's Swedish Ocean Archive (SHARK) for providing the Swedish lightship data. The air temperature data were provided by the National Climatic Data Center, NESDIS, NOAA, U.S. Department of Commerce, through the Data Support Section of the Computational and Information Systems Laboratory at the National Center for Atmospheric Research. NCAR is supported by grants from the National Science Foundation.

References

Andersen I. 1994. *Salt- og vandtemperaturforhold i de indre danske farvande*. Danish Meteorological Institute technical report 94–4.

The BACC Author Team 2008. *Assessment of climate change for the Baltic Sea basin*. Springer, Berlin.

Ekman M. & Mäkinen J. 1996. Mean sea surface topography in the Baltic Sea and its transition area to the North Sea: A geodetic solution and comparisons with oceanographic models. *J. Geophys. Res.* 101: 11993–11999.

Hahn-Pedersen M. 2003. Reports on Baltic lights — Denmark. In: Litwin J. (ed.), *Baltic Sea identity: common sea — common culture?*, Centralne Muzeum Morskie w Gdańsku, Gdańsk, Poland, pp. 81–83.

Hansen L. 2007. *Hourly values of sea level observations from two stations in Denmark. Hornbæk 1890–2005 and Gedser 1891–2005*. Danish Meteorological Institute technical report 07-9.

Janssen F., Schrum C. & Backhaus J.O. 1999. A climatological data set of temperature and salinity for the Baltic Sea and North Sea. *German J. Hydrography*, suppl. 9: 1–245.

Kullenberg G. 1983. The Baltic Sea. In: Ketchum B.H. (ed.), *Estuaries and enclosed seas*, Elsevier, Amsterdam, pp. 309–335.

Matthäus W. & Franck H. 1992. Characteristics of major Baltic inflows — a statistical analysis. *Cont. Shelf Res.* 12: 1375–1400.

Omstedt A., Pettersen C., Rodhe J. & Winsor P. 2004. Baltic Sea climate: 200 yr of data on air temperature, sea level variation, ice cover, and atmospheric circulation. *Climate Research* 25: 205–216.

Pettersson O. 1931. *Vattenutbytet mellan Skagerak och Ostersjön*. Svenska Hydrografisk- Biologiska Kommissionen Skrifter, Ny serie: Hydrorafi IX, Wald, Zachrissons Boktryckeri AB, Göteborg.

Rodhe J. 1998. The Baltic and North Seas: a process-oriented review of the physical oceanography. In: Robinson A.R. & Brink K.H. (eds.), *The sea*, John Wiley & Sons Inc., New York, pp. 699–731.

Schinke H. & Matthäus W. 1998. On the causes of major Baltic inflows — an analysis of long time series. *Cont. Shelf Res.* 18: 67–97.

Sparre A. 1984. *The climate of Denmark — summaries of observations from light vessels*. Danish Meteorological Institute climatological papers no. 10–12.

Stigebrandt A. 1980. Barotropic and baroclinic response of a semi-enclosed basin to barotropic forcing from the sea. In: Freeland H.J., Farmer D.M. & Levings C.D. (eds.), *Fjord oceanography*, Plenum Press, New York, pp. 141–164.

Stigebrandt A. 1984. Analysis of an 89-year long sea level record from the Kattegat with special reference to the barotropically driven water exchange between the Baltic and the sea. *Tellus* 36A: 401–408.

Stigebrandt A. & Gustafsson B.G. 2003. Response of the Baltic Sea to climate change — theory and observations. *J. Sea Res.* 49: 243–256.

Svansson A. 1975. *Physical and chemical oceanography of the Skagerrak and the Kattegat*. Report no. 1, Institute of Marine Research, Sweden.

Wyrtki K. 1954. Der Große Salzeinbruch in die Ostsee im November und Dezember 1951. *Kieler Meeresforschungen* 10: 19–25.